APPLICATION OF CHEMICAL MECHANICAL POLISHING PROCESS ON TITANIUM BASED MEDICAL IMPLANTS

A Dissertation

by

Zeynep Özdemir

Submitted to the

Graduate School of Sciences and Engineering
In Partial Fulfillment of the Requirements for
the Degree of

Doctor of Philosophy

in the
Department of Mechanical Engineering

Özyegin University
May 2017

Copyright © 2017 by Zeynep Ozdemir

APPLICATION OF CHEMICAL MECHANICAL POLISHING PROCESS ON TITANIUM BASED MEDICAL IMPLANTS

Approved by:

Associate Professor Bahar Başım,
Advisor,
Department of Mechanical Engineering
Özyeğin University

Professor Güray Erkol,
Department of Physics
Özyeğin University

Associate Professor Göksenin Yaralıoğlu
Department of Electrical and
Electronics Engineering
Özyeğin University

Associate Professor Rana Sanyal,
Department of Chemistry
Boğaziçi University

Date Approved: 30 May 2017

Assistant Professor Sedat Nizamoğlu
Department of Electrical and
Electronics Engineering
Koç University

To my family and my husband Senol Guler…

ABSTRACT

Biomaterials are commonly used as implant materials in the body for dental prostheses, orthopedic applications, heart valves and catheters. Based on the research studies conducted up to date, titanium and its alloys are known to be the most biocompatible materials due to their surface properties as well as extraordinary mechanical properties. Processing methods for the implant materials also affect the surface properties and may lead to contamination that can lessen the biocompatibility and after implantation may cause infection on patients which can be up to 4% in numbers. Changing the surface roughness and forming a surface oxide film have been implemented through various methods in the literature to increase of the biocompatibility and to ensure bio-inertness to the implant material. Sand blasting and chemical etching methods are commonly used for patterning the titanium surfaces to alter the surface roughness which can cause surface contamination. However, the other alternative methods such as high temperature plasma coating and laser patterning are costly.

In this dissertation, Chemical Mechanical Polishing (CMP) process is established as an alternative technique to the existing methods in the literature in order to change the implant material surface properties. CMP process is one of the methods used in the semiconductor industry to ensure surface planarization through simultaneous mechanical and chemical actions. The abrasive particles in the polishing slurries provide the mechanical effect during the process enabling nanometer level erosion and cleaning the implant from any potential contamination during its machining. The

chemical components of the slurry including the stabilizers, pH adjusters and oxidizers, on the other hand, help form a passive oxide film coating the surface. Generally, CMP is used to form very smooth surfaces but it has been demonstrated that by changing the slurry particle size and the pad material properties, it is possible to generated controlled roughness on the polished surface as well. The protective nature of the generated oxide film enables planarization in semiconductor applications. In implant applications of CMP, it is believed to help reduce the contamination on the surface of the bio-implants in the body environment and reducing the infection risk by stopping the chemical reactions in-vivo. It has been shown in the literature that the application of CMP on Ti films has been successful in terms of creating a smooth surface and a TiO_2 oxide film. However, its native oxide film after CMP has not been characterized fully for its protective nature other than the passivating properties of the Ti/TiN films in semiconductor CMP applications. Titanium oxide film is known to promote the biocompatibility, cell adhesion, formation of hydroxyapatite layers. Yet, the oxide films obtained by artificial oxidation methods result in thick films and have porous structures. Therefore, in this study, CMP process has been applied to the Ti plates synergistically to remove the potentially contaminated surface layers and induce controlled roughness on the implant surfaces. In addition, the treated surface oxide layers have been characterized for the nature of the metal oxide layers in terms of their self-protective properties. Furthermore, biocompatibility of the CMP implemented surfaces have been evaluated through cell growth and infection resistance capabilities through biofilm analyses and optimal surface parameters were determined according to the desirability of the surface responses which help promote the cell behavior.

In terms of carrying the results of this dissertation to the future studies, development of a 3 dimensional CMP process considering the 3-D nature of the implants is the most important necessity. The application of the 3-D CMP process on the implant surfaces is believed to be both an economical and more effective method on structuring the surface of the titanium based bio-implants. It is aimed to further develop a CMP driven surface nano-structuring methodology to create engineered surfaces on the Ti based bio-implants with self-protective surfaces to minimize chemical and bacterial reactivity, while promoting their biocompatibility through simultaneous surface patterning.

ÖZET

Biyomalzemeler vücutta implant malzemesi olarak diş protezlerinde, ortopedik uygulamalarda, kalp kapakçığı ve kataterlerde yaygın olarak kullanılmaktadırlar. Günümüze kadar yapılan araştırmalar sonucunda titanyum ve alaşımları sahip oldukları yüzey özelliklerinin yanı sıra olağanüstü mekanik özellikleri ile de en biyouyumlu malzemeler arasında yer almaktadırlar. İmplant malzemesinin işlenme prosesi de yüzey özelliklerini etkilemekte ve kontaminasyona neden olabilmektedir bu da biyouyumluluğu azaltmakta ve hastalarda implante edildikten sonraki süreçte bulgulanan ve %4 oranlarına ulaşabilen enfeksiyonlara neden olmaktadır. İmplant malzemelerin biyouyumluluğu ve biyoinertliğini arttırmaya yönelik malzemenin yüzey pürüzlülüğünün değiştirilmesi ve yüzeyde oksit film oluşturulması çeşitli yöntemler ile literatüre kazandırılmıştır. Yüzey pürüzlülüğünü değiştirmek amaçlı desenlemede genellikle kullanılan kumlama ve kimyasal aşındırma yöntemleri implant malzemesi yüzeyinde kontaminasyona neden olmaktadır. Ayrıca kullanılan diğer alternatif yöntemler olan yüksek sıcaklıkta plasma kaplama ve lazer ile desenlendirme yöntemleri ise yüksek maliyetlere neden olmaktadırlar.

Bu proje kapsamında implant malzeme yüzeylerinin işlenmesi için literatürde var olan yöntemlere alternatif olarak Kimyasal Mekanik Cilalama/Düzlemleme (CMP) prosesi getirilmiştir. CMP prosesi yarıiletkenler endüstrisinde kullanılan yöntemlerden biri olup aynı anda yüzeyi hem mekanik hem de kimyasal olarak düzlemleyebilmektedir. Proses sırasında kullanılan slurry içerisindeki aşındırıcı kimyasallar mekanik etki sağlayarak yüzeyde nanometre seviyelerinde aşınım sağlanarak üretim sırasında oluşan potansiyel kontaminasyondan arındırılmış yüzeyler

oluşturulmaktadır. Diğer taraftan slurrynin kimyasal bileşenlerini oluşturan stabilizatörler, pH ayarlayıcı ajanlar ve oksitleyiciler yüzeyde pasif oksit film kaplaması oluşturmaktadırlar. CMP genel olarak pürüzsüz yüzeyler oluşturmak amaçlı kullanılsa da cilalanan yüzeylerde kullanılan süspansiyonların tane boyutu ve cilalama pedinin dokusu değiştirilerek kotrollü bir pürüzlülük oluşturmak amaçlı kullanılabileceği de daha önceki çalışmalarda gösterilmiştir. Kimyasal olarak değiştirilmiş bu filmin reaksiyonu durduran koruyucu bir oksit tabakası olması yarıiletken uygulamalarında düzlemlemeyi sağlamaktadır. CMP'nin implantlara uygulanması sonucunda ise kimyasal reaksiyonları durdurarak yüzeyde oluşabilecek kontaminasyon ve enfeksiyon riskini azaltacağı düşünülmektedir. Literatürdeki sınırlı çalışmada implant malzemesi olarak kullanılan Ti filmler üzerindeki CMP uygulamalarının pürüzsüz bir yüzey ve TiO_2 oksit filmleri oluşturduğu belirtilmiştir. Ancak CMP prosesi sonucu biyoimplantlar üzerinde oluşan titanyum oksit filmin koruyucu özellikleri karakterize edilmemiş olmakla beraber, yarıiletkenler teknolojisinde kullanılan Ti/TiN filmlerin CMP sırasında pasif edici özellikleri bilinmektedir. Oluşturulan titanyum oksit filmlerin hücre tutunmasını, biyouyumluluğu ve hidroksiapatit tutunmasını arttırdığı bilinmektedir fakat oluşturulan oksit filmlerin çoğu yapay oksidasyon yöntemleri ile elde edildiklerinden kalın ve gözenekli bir yapıya sahiptirler. Bu filmler gözenekli yapıları nedeniyle alt katmanda bulunan ana metal malzemenin inertliğini sağlayamamakta ve kontaminasyonu engelleyememektedir Bu nedenle bu çalışmada, CMP prosesi uygulanarak implant malzemesi olarak kullanılan Ti plakalar üzerinde kontaminasyona maruz kalmış olabilecek üst tabakanın aşınımını ve aynı zamanda yüzeyde kontrollü nano/mikro boyutta pürüzlülük oluşumu sağlanmıştır. Ayrıca CMP ile metal yüzeylerde oluşan korunumlu metal oksit tabakaların yapısı yüzeydeki

kimyasal reaksiyonu sınırlamak açısından karakterize edilmiştir. CMP ile işlenen yüzeyleri biyouyumluluk ve biyofilm oluşumuna direnç açısından da karakterize edilmiş ve hücrelerin uyumluluklarına bağlı olarak hücre tutunmasını artmaya yönelik optimal yüzey özellikleri belirlenmeye çalışılmıştır.

Tez çalışmasının sonuçlarını ileriki aşaması düşünüldüğünde, implant malzemelerin üç boyutlu yapısı gözönüne alınarak 3-D çalışabilecek bir CMP prosesi geliştirmektir en önemli gereksinimdir. CMP tekniğinin titaniyum bazlı biyo-implantlar üzerinde üç boyutlu uygulamalarının diğer alternatiflere göre hem çok daha ekonomik hem de çok daha etkili bir yöntem olacağı düşünülmektedir. Titanyum ve titanyum alaşımlı biyolojik implantlar üzerinde CMP ile oluşturulacak nano-desenli yüzeylerin kendinden korunumlu oksit tabaka ile kimyasal ve bakteriyel reaksiyonları önlemesi ve aynı zamanda yüzey desenlemesi ile de biyouyumluluğu arttırması amaçlanmaktadır.

ACKNOWLEDGMENTS

I would like to express my deepest gratitude to my advisor, Associate Professor Dr. G. Bahar Basim, for her endless encouragement, inspiration and support. She always supported me in bad times and good times with her invaluable contributions and guidance to my life.

I would also like to acknowledge the other members of my dissertation committee for their valuable contributions to this dissertation.

I gratefully acknowledge the Marie Curie International Reintegration Grant (IRG) for supporting NANO-PROX "Nano-Scale Protective Oxide Films for Semiconductor Applications & Beyond" project to conduct this research.

I would like to thank Assoc. Prof. Dr. Berrin Erdag and Dr. Aylin Ozdemir at TUBITAK MAM-GEBI and Mr. Ozal Mutlu from Marmara University for their contribution to the cell growth and bacteria zone growth analyses.

I would like to extend a special gratitude to MODE Medikal Company for providing the dental implants used for this study.

I am grateful to my colleagues who have contributed to my Ph.D. lifespan by their wonderful friendship. Thank you for all of the meetings, chats and coffees over the years.

Finally, I would like to dedicate this dissertation to my family and my husband Senol Guler. It is their unreserved love and support that keeps me moving forward. This dissertation could not have been completed without their encouragement.

Thank you,

Zeynep

TABLE OF CONTENTS

LIST OF TABLES

LIST OF FIGURES

CHAPTER I

INTRODUCTION

Surface treatment methods are implemented to implantable materials to provide desired properties for accelerating the in-vivo healing performance in order to obtain an advanced implantation routine. Success of a medical implantation operation is influenced by many factors, which mostly depend on the response of the surrounding host tissue cells towards the presence of the implant. Biocompatibility, bio-stability and material surface properties such as chemical composition, wettability and surface energy are the main factors that play an important role on tissue-implant interaction and osseo-integration. Recent studies in the literature show that increased surface roughness simultaneously increases the total surface area and improve the cell adhesion to the implant material [LeG07, Sam05, Zha06]. Many properties beyond the implant surface and its composition contribute to the implant performance on the healing process, including the type of selected bulk material. As a hard tissue replacement, commercially pure titanium (cp Ti) and its Ti-6Al-4V alloy are widely preferred as replacement biomaterials instead of stainless steel and Cr-Co alloy. This is due to the superior mechanical properties (strength to density ratio) and biocompatibility of Ti owing to the stable passive oxide layer formation that serves as a passivation layer on Ti when it's placed in a physiological environment [Bud04, Jún11, Eli08, Sch08]. Titanium tends to form an amorphous and stoichiometrically imperfect oxide layer in the air, which is referred as a protective oxide layer. This native titanium oxide is defined as an inert ceramic biomaterial and it tends to form a direct chemical bond with the bone tissue

naturally [Sul03, Gem07, Var08]. The quality and properties of the titanium oxide film such as thickness, porosity, and crystal structure are also directly affected by the surface treatment method selected [Var08, Gul04, Cho11].

Figure 1.1 shows the classification of the implant surface treatment methods including additive and subtractive processes performed by mechanical, chemical and physical methods. These techniques are employed to the implant materials to alter their surface chemistry, chemical structure, bio-mechanical properties and morphology [Ani11]. The mechanical methods including the machining and blasting processes generally result in either smooth or rough surface finish to manipulate the tissue response. Machined or as generally termed as "turned implants" are the antecedent of the dental implant industry, however, the resulted surface topography generally has the marks and traces of the used manufacturing tools [Pat16]. On the other hand, blasting is one of the most commonly applied techniques to increase surface roughness by using various size particles mainly including alumina (Al_2O_3) and titania (TiO_2) as the hard grains [Li99, Kim08]. The constituted surface roughness depends on the application technique of the blasting process and the used particle type and size. However, some of the particles are usually left on the material surface after blasting process, which may impair bone formation by a possible competitive action on the calcium ions [Wen96]. Novel methods were tried to solve these problems by using more biocompatible particles such as Hydroxyapatite (HA) and Biphasic calcium phosphate (BCP) to reduce the effect of particle contamination on the tissue response, which perform better in terms of their integration in-vivo.

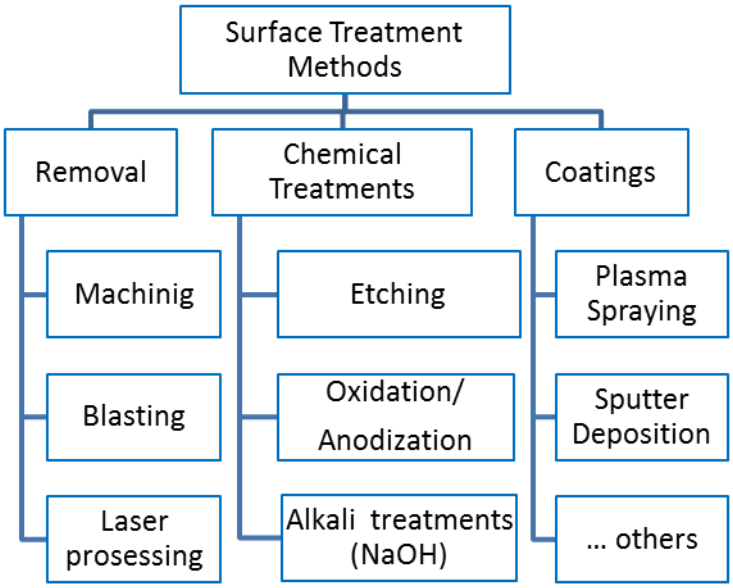

Figure 1.1 Classification of the surface treatment methods according to the type of implemented process.

Beyond the mechanical treatments, chemical methods were also used to improve surface characteristic in combination with the mechanical methods. Sand blasting and acid etching (SLA) surface treatment method is an example of this type of methods, which includes sand blasting process followed by acid etching treatment on the implant. Chemical dipping application on an implant using an acidic solution changes the surface structure and assists in removing the particles embedded onto the implant during blasting operation from the implant surface. Different acid solutions and combinations are commonly applied for chemical surface treatments as a function of acid type, concentration and exposure duration. Etching process is typically conducted as a separate procedure following sand-blasting or other mechanical treatments. It has been observed to improve osseo-integration but after the etching operation a blurry looking film is formed on the implant surface [Sin12, Oka09]. Other than these chemical methods, coating applications are other alternatives for the improvement of the surface properties of the implant materials. For coating process, plasma spraying, laser ablation, pulsed laser deposition, sputtering and simply dip coating are typically

practiced with HA as the coating material on the implant surface as a good coating substance and it was also observed to enhance the osseointegration [Cho11, Mob09]. All of these surface treatment methods tend to produce a biocampatability promoting surface structure on the implant material with controlled surface chemistry and topography which help attachment of the cell layers [Cho11, Lum01]. The most recent studies on the clinical oral implants focused more on the surface topographical alterations rather than the chemical surface properties of implant due to the mechanical interlocking mechanism between the tissue and the implant material [Sul03]. The homogeneity of the surface structure also influences the interaction of the tissue with the implant surface. Isotropic structures create more random response of the cells to the implant material surface. On the other hand, laser surface treatments introduced for anisotropic surface roughness are also available that can simply orient the cell growth in a specific direction [Kur05, Mir07, Ken13, Obe13]. Furthermore, the key factor on the reaction of the live tissue relies on the surface irregularities at the nano scale to the micron level. Literature has shown that response of the osteoblast cells is more promoted by the micro scale roughness. Yet, the soft tissue fibroblast cells are more compatible with the nanometer scale roughness on the surface [Var08, Ken13, Obe13]. Therefore, the degree of surface roughness scaling from nano to micro level is critical for the control of tissue response by selective promotion or demotion of the cell attachment process as it shown in Figure 1.2. While the complete bone formation can take up to 3 weeks, the preliminary integration that takes place in the first week of implantation is critical and should promote the cell attachment while demoting any bacteria attachment and cytotoxic side-effects.

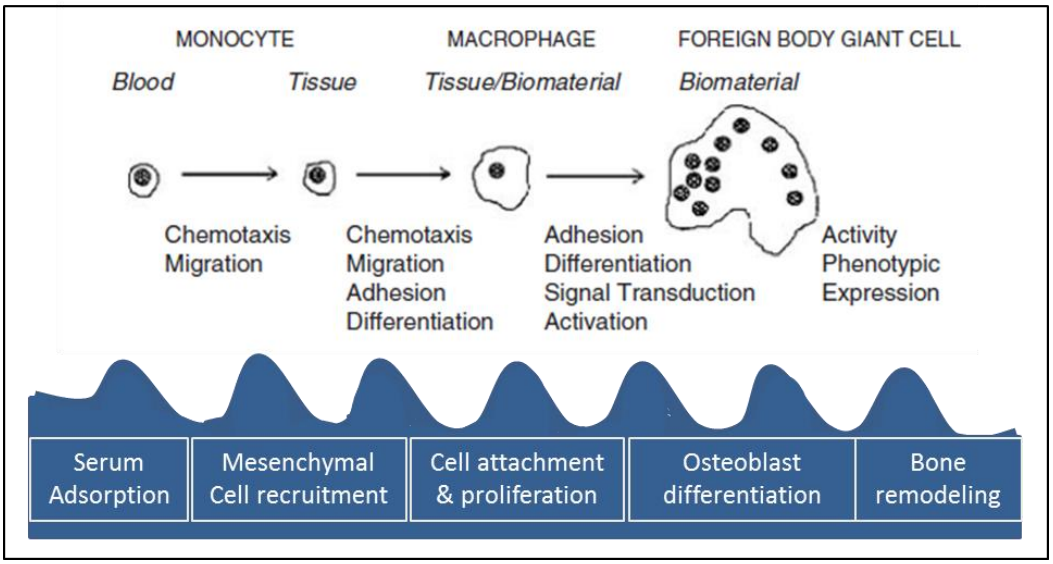

Figure 1.2 Initial processes on the interface between a biomaterial and bio-fluid immediately after implantation [Bud04].

In the present work Chemical Mechanical Polishing (CMP) process is introduced as an alternative technique to alter the surface nature of the biomedical implants [Bas14]. The CMP process has initially been introduced for glass polishing and later on implemented on the planarization of the interlayer metal connectors and dielectrics in microelectronics manufacturing [Bas11]. In CMP process, the top layer of the material surface is exposed to the chemicals in the polishing slurry which includes nano-size particles and chemicals. Interaction between the slurry chemicals and the metal forms a chemically altered top film which is removed by the mechanical abrasion of the nano particles. Chemo-mechanical abrasion makes the difference as compared to the pure mechanical polishing techniques that are used for the implant surface finishing [Sit99]. The chemically modified top layer has to be a protective oxide; i.e.; continuous and pore free oxide layer to enable planarization by stopping chemical corrosion on the recessed metal surfaces while the elevated structures are polished [Kau91]. Previously, titanium CMP was utilized to planarize Ti/TiN layers used as barriers to aluminum interconnect diffusion into the dielectric layers in microelectronics applications

[Cha03]. Moreover, CMP implementation application on the Ti surface has also been demonstrated by an earlier study where the surface layer was shown to be created as a titanium oxide film which might also help promote biocompatibility in addition to helping removal of the reacted and contaminated surface layers by mechanical abrasion [Oka09, Tan07].

Application of the CMP process on titanium based bio-implants brings out a synergistic effect which includes (i) cleaning the surface of the material which is potentially contaminated during processing by mechanically removing a nano-scale top layer during the process, (ii) creating a continuous, pore free and nano-scale oxide layer on the material surface in order to limit any additional contamination and hence decrease the risk of infection and inhibit corrosion and (iii) inducing controlled surface smoothness/roughness by designing the CMP process variables such as slurry particle size, solids loading as well as the type and concentration of the oxidizer and other slurry chemicals.

In this dissertation, following the introduction in Chapter 1, Chapter 2 gives a brief summary about the properties of the titanium as an implant material and covers the literature on the topic of general surface structuring methods for implant surface treatment. The main purpose of the surface modification is to maintain the bulk properties of the material while altering the top layer surface to promote biocompatibility. General modification methods can either alter the atoms, compounds or the layers of the existing surface by using different coating materials. These methods can be classified into different categories according to their processing steps. They can be categorized under three main topics as illustrated in Figure 1.1, which are; (i) mechanical treatments, (ii) chemical treatments and (iii) coatings. Literature has more than ten different surface texturing processes which can be counted as subcategories and

all of them have some advantages and disadvantages. Yet so far, the ideal surface texturing method has not been established. In this context CMP process is suggested as an alternative method to induce controlled smoothness or roughness to the implant material surfaces.

In chapter 3, application of the CMP process on the titanium implant material surface is examined with respect to the role of slurry particles, pad materials and oxidizer concentration. Their impact on the surface quality and modification is quantified in terms of the material removal rate response, surface roughness and wettability performances. Evaluations were conducted initially on the titanium plates in addition to the 3D dental implants made of titanium.

Chapter 4 focuses on the surface oxide film formation and characterization after the CMP treatment of the implant materials. The necessary conditions to satisfy the formation of a protective oxide film were evaluated through different oxidizer concentrations and the protective nature of the oxide films were evaluated through Pilling-Bedworth (PB) ratio calculations. Additionally, surface energy values of the samples were examined under conditions enhancing the P-B ratio as the passivation of the surface oxide layer contributes to the protective nature of the formed oxide layer.

Chapter 5 details the biological in vitro evaluations of the treated titanium surfaces. This study aims to obtain a better biocompatibility after CMP treatment via cell viability and cytotoxicity as initial steps to examine the altered samples. Furthermore, surface cell attachment behavior was evaluated in both short term and long term periods under in vitro conditions. Cell viability including the in vitro life span was quantified with respect to surface characteristics of the implants. The analyses

were utilized to predict the in-vivo trends based on the fundamentals of the biological activity promotion.

Chapter 6 focused on the design criteria for the selection of the best performing implants processed by CMP based treatment on the responses promoting biological performance of the implants. Especially, surface treatment conditions such as particle size, oxidizer concentration were investigated as a function of applied downforce during CMP to control the surface topographical structure as well as the wettability and material removal rate responses.

Finally in chapter 7 the findings of this dissertation are summarized and the suggestions are outlined for the future work to make CMP a commercial application in the implant industry.

CHAPTER II

SURFACE STRUCTURING METHODS FOR TITANIUM BASED IMPLANT MATERIALS

In this chapter, a brief description of the conventional surface texturing processes are presented starting by explaining the reasons for using titanium as the main bio-implant material for hard tissue replacement. Material based properties are discussed on the basis of biocompatibility, stability and mechanical durability through the lifetime of the implant materials. Eventually, the potential surface treatment methods are evaluated depending on their application procedures and the resulting surface properties on the implant. Furthermore, advantages and deficiencies of each method are also compared in terms of materials performance. The requirements of developing more precise methodologies for the surface structuring of titanium based implant material surfaces are also discussed. Most importantly, CMP process is introduced as an alternative process for the controlled surface structuring of the titanium implants with a focus on the necessary process adaptations.

2.1 Conventional Medical Implant Materials

Biomedical implants and devices have long been introduced to medical applications. Even though composites and polymers are also used as implants, metallic materials are primarily employed for the manufacturing of biomedical implants for hard tissue replacement [Her11]. The selection of the most competitive materials for in vivo applications, in the body, depends on the prime functions of the implant. For the

replacement of the bone tissue, the main targets are to optimize the mechanical properties to ensure good durability against high loads as well as providing mechanical stiffness representative of the natural bone tissue [Lam09].

Metals and metallic alloys have been commonly used as bone replacements implants in various parts of the body as can be seen in Table 2.1, for more than a century [Lan95]. Corrosion resistance is one of the main prerequisites for metallic implants to prevent degradation [Lam09]. Many different types of metallic materials and alloys with different chemical composition and microstructures are being commonly used which can be classified in three main groups as given in the following;

- stainless steel [Rec01, Kur14, Dad07],
- cobalt- chrome (Co-Cr) based alloys [Caw03, Esp10, Kum05],
- titanium and titanium based alloys [Gee09, Ma12, Mis13, Bha03].

There are many types of stainless steels available with different corrosion resistance values and mechanical properties. AISI 316L is the most favorable steel for the biomedical implant applications [Rat04, Dav03], which contains 17-19% Cr and 12-14% Ni making it stronger than the regular steel. 2-3% of Mo increases the corrosion resistance in the aggressive environments. Yet, the modulus of the elasticity value of the stainless steel is around 200 GPa, which is much higher than a cortical bone and that should be taken into account for the load bearing implants. Over the years, Co-Cr alloys have also been introduced in biomedical implant engineering in place of the stainless steel due to their excellent wear resistance. The corrosion resistance of the metallic biomaterials in aggressive environments (chloride ions are present in the physiological media) relies on their passivation capability which is related to the thin protective surface oxide layer formation, like in the case of Cr_2O_3 and TiO_2 [Pan96, Arc01, Mat11,

Yan06]. Although alloying of stainless steels is commonly practiced, the use of elements such as Ni, Cr and Co were observed to release ions in the body environment and the dissolved metal ions create toxic effects causing adverse tissue reactions locally [Yan14]. Despite the release problem of the Mo and W ions in vivo, these alloys improve the mechanical properties and abrasion resistance of the metals [Wil81]. The forged Co-Ni-Cr-Mo alloys show improved mechanical properties and they are used for making heavily loaded joint implants such as the ankle replacements. Fabrication process of the Co-Cr based implants crates the main difference in the mechanical properties of the implants.

Table 2.1 Three major biocompatible metal and their biomedical applications [Man17].

Alloys/Materials	Applications	Implants
Stainless steel	Orthopaedic Dentistry Cardiovascular	• Femoral prosthesis, orthopaedic implants, acetabular cup applications, noble metal ion implantation, reconstructive surgery, rovascular implants (aneurysm clips), monobloc hip stems. • Dental implants, orthodontic wire leads • Cardiovascular stents, heart valve parts, coronary stents.
Cobalt-chromium alloys	Orthopaedic Dentistry Cardiovascular	• Total hip arthoplasty, reciprocating pin-on-disk testing, bone in-growth structure, orthopaedic implants, total hip implant, endothelial cells, vascular smooth muscle cells, osteoblasts (bone-forming cells), reconstructive surgery, rovascular implants (aneurysm clips), total knee substitution joint, medical implants, femoral stems, bone implant applications, load-bearing implants, bearing surface implant, • Dental implants, removable partial dentures, orthodontic wire leads. • Vascular stents, heart valve parts.
Titanium and its alloys	Orthopaedic Dentistry Cardiovascular	• Reciprocating pin-on-disk testing, joints, hip stems, orthopaedic prostheses, total hip implant, endothelial cells, vascular smooth muscle cells, osteoblasts (bone-forming cells), acetabular cup, reconstruction of craniofacial defects, channel implants, hard tissue substitutions, bone substitution implants, reconstructive surgery, rovascular implants (aneurysm clips), human mesenchymal stem cells (hMSC), self-assembled monolayers (SAMs), skeletal prostheses, load-bearing implants. • Dental implants, orthodontic wire leads. • Cardiovascular vascular stents, heart valve parts.

Fabrication through the casting is not a preferred method due to the formation of large dendritic grains and micro-pores, decreasing the yield strength and fatigue strength of the alloyed material [Zhu89, Dob83, VSa76]. The wrought Co-Cr based alloys show better mechanical properties in comparison to the cast alloy. Therefore, they are preferred for the applications where strong tribological loads are encountered. Moreover, both stainless steel and Cr-Co alloys have higher modulus values as compared to the natural bone, which cause insufficient stress transfer to the bone resulting in bone desorption and disintegration by the implant after some years of operation. Elastic modulus of most commonly used biomedical implant materials are given in Figure 2.1. As can be seen from the figure, Ti and it's alloys have lower modulus of elasticity as compared to the stainless steel and Co-Cr alloys. Additionally, Table 2.2 compares some mechanical properties of the stainless steel, Co-Cr alloy and Ti and its alloys in relation to the selected processing method. The process control, design and thermo mechanical properties of Ti makes it an ideal implant material for the orthopedic prosthetic devices.

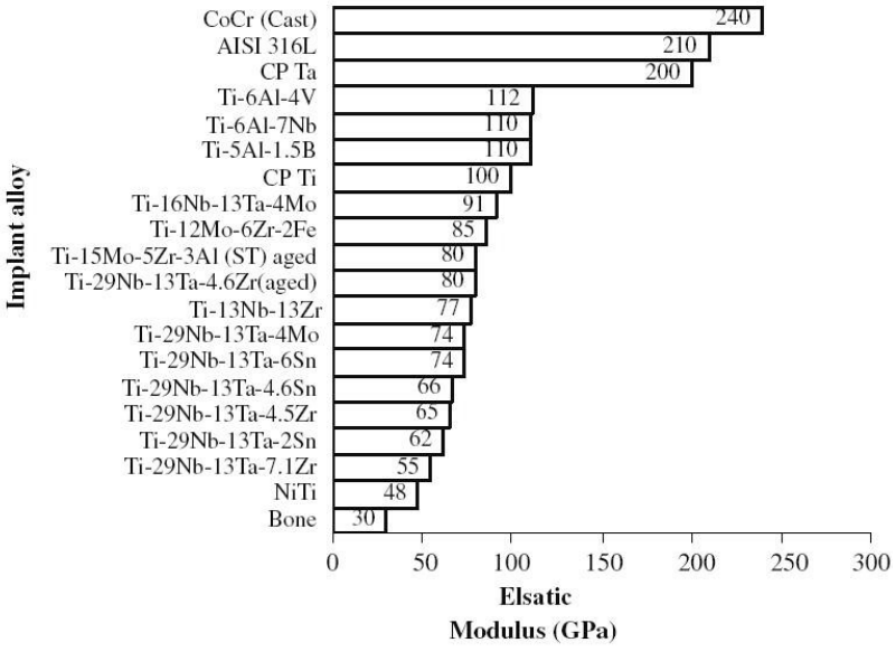

Figure 2.1 Medical alloys modulus elasticity [Gee09].

Titanium can be alloyed with different elements to change the mechanical properties such as higher stiffness and lower weight (density) according to the desired application. Table 2.3 shows some of the Ti and Ti alloy properties which can be employed as implant materials.

Table 2.2 Typical Mechanical Property of Implant Materials [Rat04].

Material	ASTM designation	Condition	Young's modulus (GPa)	Yield strength (MPa)	Tensile strength (MPa)	Fatigue endurance limit (at 10^7 cycles, $R = -1$[c]) (MPa)
Stainless steel	F745	Annealed	190	221	483	221–280
	F55, F56, F138, F139	Annealed	190	331	586	241–276
		30% Cold worked	190	792	930	310–448
		Cold forged	190	1213	1351	820
Co–Cr alloys	F75	As-cast/annealed	210	448–517	655–889	207–310
		P/M HIP[b]	253	841	1277	725–950
	F799	Hot forged	210	896–1200	1399–1586	600–896
	F90	Annealed	210	448–648	951–1220	Not available
		44% Cold worked	210	1606	1896	586
	F562	Hot forged	232	965–1000	1206	500
		Cold worked, aged	232	1500	1795	689–793 (axial tension $R = 0.05$, 30 Hz)
Ti alloys	F67	30% Cold-worked Grade 4	110	485	760	300
	F136	Forged annealed	116	896	965	620
		Forged, heat treated	116	1034	1103	620–689

Table 2.3 Mechanical properties of biomedical titanium and its alloys [Gee09].

Material	Standard	Modulus (GPa)	Tensile strength (MPa)	Alloy type
cp Ti (grade 1-4)	ASTM* 1341	100	240-550	α
Ti-6Al-4V ELI	ASTM F1472	112	895-930	α+β
Ti-6Al-7Nb	ASTM F1295	110	900-1050	α+β
Ti-5Al-2.5Fe	—	110	1020	α+β
Ti-13Nb-13Zr	ASTM F1713	79-84	973-1037	Metastabe β
Ti-12Mo-6Zr-2Fe	ASTM F1813	74-85	1060-1100	β
Ti-35Nb-7Zr-5Ta		55	596	β
Ti-29Nb-13Ta-4.6Zr	—	65	911	β
Ti-35Nb-5Ta-7Zr-0.4O		66	1010	β
Ti-15Mo-5Zr-3Al		82		β
Ti-Mo	ASTM F2066			

2.1.1 Titanium Based Medical Implants

Titanium was introduced to implant production in 1930s, since its lightweight and superior chemo-mechanical features exceeded the properties of stainless steel and cobalt alloys and presented it as a convenient material for the implant applications. The first use of titanium as dental implants began with Branemark's prosthesis design in 1960s. Simultaneously, orthopedic devices for the hip-joint replacements were developed by using titanium based materials. Figure 2.2 gives examples of commercially used titanium implants [Bra69, Ade81]. Beyond the desirable mechanical properties, Ti and its alloys have superior corrosion resistance and biocompatibility properties and these features allow them to be used as adequate implant materials in the body environment [Sch03, Pan96, Lon98]. Until today, commercially pure Ti and Ti6Al4V are the most used titanium based materials as hard tissue replacements in artificial bones, joints and dental implants [Rat04]. On the other hand, recent research studies have shown that titanium alloys can release aluminum and vanadium ions in the host tissue creating toxic effects and inflammation of the surrounding body parts [Hoe94, Ger05]. Consequently, commercially pure titanium is the mostly preferred material due to its excellent corrosion resistance properties where inertness is more important as compared to the mechanical performance such as in dental applications. Although, the bio-inertness of the titanium may cause a long osseointegration period, titanium is still the only metallic material that has a capability to osseointagrate [Noo87, Hoe94, Vas11].

Figure 2.2 Commonly used titanium based medical implants as a) artificial joint b) dental implant c) hip joint and d) knee joint [Bra69, Ade81].

In addition to mechanical properties, titanium and its alloys tend to form an adherent and protective oxide film spontaneously during the passivation/re-passivation reaction. Formation of this titanium oxide film on the surface contributes to the bioactivity, which leads to the interfacial bond formation between the implant material and the surrounding tissues [Li94]. Beyond the listed advantages of titanium, such as mechanical advantages, bio-adaptability may still limit the usage of titanium and its alloys as biomedical implant materials. Therefore, to improve the osseointegration, bioinerty and wear resistance of the titanium based implants additional treatment methods are generally implemented to the titanium based implant materials.

2.1.1.1 Titanium based dental implants

Many diseases and trauma may lead to tooth loose. Therefore, the use of the dental replacements is needed to ensure a support in place of the missing teeth. The dental implant is inserted into the jaw bone and it emerges with the bone which is called as the osseointegartion. In the recent years, there is a growing concern on the dental industry due to the increasing life expectancy of the general public leading to an increase in the elderly population [Gbi13]. The American Association of Oral and Maxillofacial Surgeons's statistics showed that 69% of adults (ages between 35-44) have lost at least one tooth and 26 % of the elderly people have lost all of their permanent teeth [Gav14]. The statistical numbers also showed that approximately 100,000-450,000 dental implants are placed every year and titanium based implants have the majority as can be seen in Figure 2.3 [Gup10]. Typically, dental implants are made by using Grade IV commercially pure Ti due to its excellent biocompatibility and high resistance to corrosion in aggressive body media.

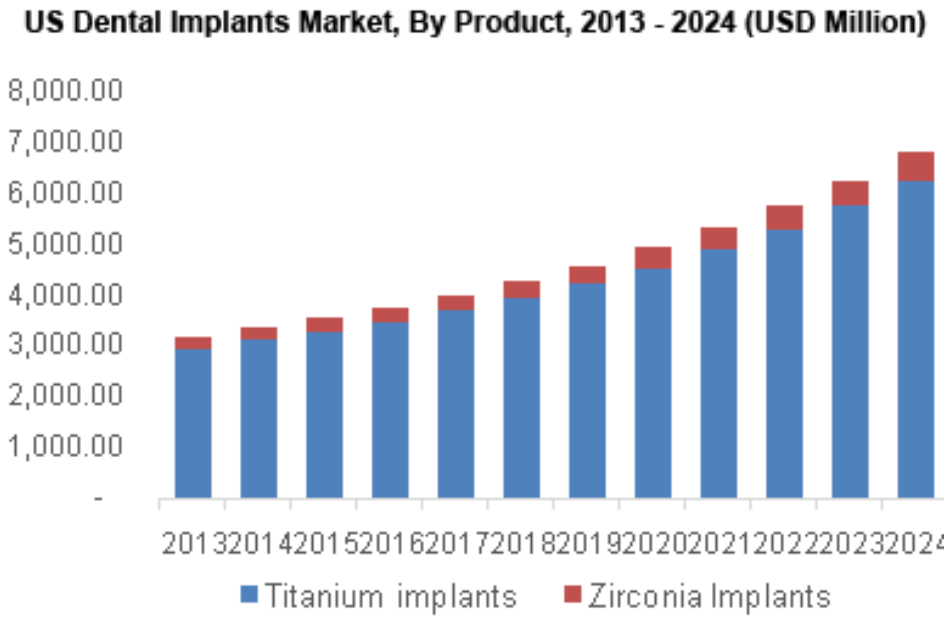

Figure 2.3 Global Titanium dental implant market.

Today, the expected success rate of the implantation process is around 95% in the single tooth replacement cases. However, in a healthy person, the success rate ranges between the 90-95% although this ratio mostly depends on the personal health conditions (such as bone quality and age) beyond the design factors [Paq06]. Today there are more than 40 manufacturers in the dental implant market in order to achieve the improvement on the success rate through new techniques developed [Dud12]. Yet, it is still required to advance these techniques more and further evaluations are conducted to be able to improve the long term success of the dental implants.

2.2 Overview of the Conventional Chemical, Mechanical and Physical Processes for Biomaterial Surface Modification

Implant ability depends on the chemical, mechanical and topographical features of the materials which directly influence the tissue healing process and integration of the implant into the bone tissue. As mentioned earlier, titanium and Ti alloys are preferred as implants due to their excellent properties such as high strength, low density, good corrosion resistance and inertness in the body environment. However, relatively low elastic modulus and poor wear resistance of the titanium may be the prime reason for loosening of the implants in a long term period. Scientist and engineers are still working for further modification of the implant materials to promote these poor properties. Several basic methods are summarized in this section which are utilized to enhance the implant material surface properties. These suggested methods, include additive and subtractive techniques to create physically and chemically altered implant surfaces.

2.2.1 Machined Surface

Machining is one of the primary methods to alter the implant surface to improve the tissue response towards the implant. The machining process simply involves the production of material by using a cutting tool to remove unwanted parts from the sample to produce the desired shape. This process enables relatively smooth surfaces and it is also called as the turning or milling process. After machining, manufactured implants are submitted to cleaning procedures for decontamination. These techniques generally produce a surface with defects as can be seen in Figure 2.3, containing grooves, ridges and trace of the tool that is used for manufacturing. The presence of defects can cause elevated surface roughness that creates mechanical resistance through bone interlocking. Furthermore, these grooves may demote the cell growth and can result in longer healing times after the implantation process [Ani11].

Implant material surface finish is qualified through surface roughness value as a factor as it affects the rate of osseointegration. Various roughness scales have been published with different measurement procedures for machined surfaces and optimal roughness for hard tissue implants is proposed to be in the range of 1-10 μm [Bau13]. Literature showed that a turned surface roughness is around 0.96 μm with 8.6 μm average peak spacing [Gar12]. Besides these investigations, experimental results have demonstrated that for a better bone fixation of the implants an average surface roughness (Ra) around 1.5μm can be identified as a rough surface according to Wennerberg and coworkers. Machined titanium implants have been widely used for a long time and they perform successfully in clinical applications in the long-term. Nevertheless, this surface finishing method has not resulted in a good osteointegration for all the samples. Due to their lower resistance to removal torque, machined dental implants are becoming less preferable and unavailable [Ani11].

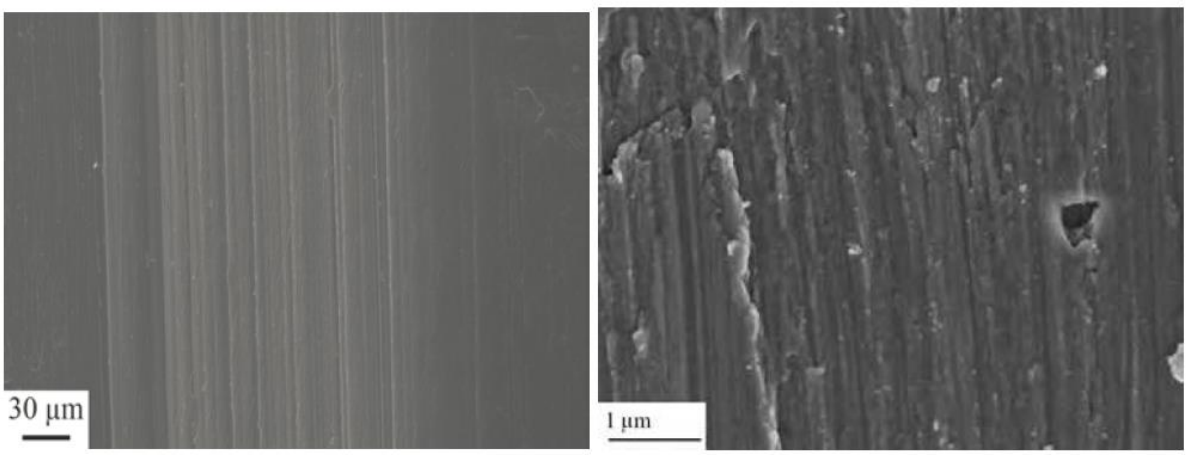

Figure 2.4 Machined surface Scanning electron microscopy images [Bal11].

These results have provided guidance to new surface development methods where topographical based changes are tried to ensure the mechanical interlocking between the tissue and the implant surface more successfully [Sul03].

2.2.2 Blasting

Blasting is one of the frequently used methods for alteration of the implant surface via using different size hard ceramic particles. It is generally called as sandblasting or girt-blasting. The process consists of exposing the particles through a nozzle with compressed air towards the implant material surface. The particles hitting the surface form a crater texture. The resultant surface morphology depends on the utilized particle properties such as shape, hardness and size, in addition to the duration of the process, speed of the particles and distance from the source of the particle to the implant. Mainly, silica (SiO_2), corundum/alumina (Al_2O_3), titania (TiO_2), and calcium phosphate ($CaPO_3$) particles are used with size ranges from nano to micro scale. Particle diameter directly affects the surface isotropy. Previous studies have shown that blasting with alumina particle size between 25-75 µm resulted in an isotropic surface, which has a roughness value in between 1.1-1.5 µm.

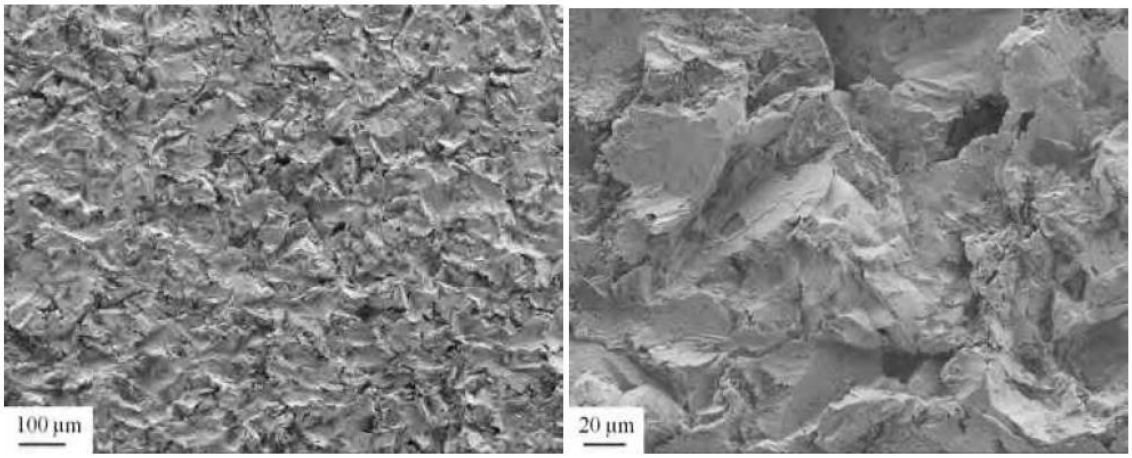

Figure 2.5 Sandblasted surface Scanning Electron Microscopy (SEM) images [Bal11].

Nevertheless, increased particle size formed a relatively anisotropic surface with average roughness deviating around 2.0 µm [Gar12]. On the other hand, using titanium dioxide particles with particle size around 25 µm generated rather rougher surfaces in the 1-2 µm range [Gar12]. In vivo studies of the these blasted samples showed that surface roughness around 1.5 µm have a better bone response in both short and long term periods in a rabbit bone. [Gar12, Wen95, Wen97]. Yet, post blasting research showed that particles maybe left on the implant material surface even after the cleaning and sterilization steps. It has been demonstrated that when implant material is inserted into the body environment, these embedded particles can be released into the surrounding tissue and disrupt bone formation through competitive ion activity on calcium ions [Syk04, Bla92, Par12, Man10].

2.2.3 Acid Etching

Another alternative to the surface treatment methods is the chemical etching process that implies the immersion of the metallic implant into an acidic solution. Chemical solution corrodes the material surface and forms micro pits and craters with a

specific shape and diameter sizes ranging between 0.5 to 2 μm [Gup08, Ors00, Mas02]. Acid etching can be performed by using various strong acidic chemicals such as HCl, HF, HNO_3 and H_2SO_4 and combinations of them [Mdo04]. The created surface structure depends on the concentration of the acidic solution, exposure time and the temperature. Etching process allows selective removal of the oxide layers and parts of the base material depending on the resolution kinetics of the oxide film. In addition, removal rate is also effected from the materials crystallography and grain size nature. The chemical dissolution does not cause any mechanical stresses on the material, which is an advantage as compared to the other surface roughening methods [Has04, Poh02].

Dual acid etching technique has been recommended to produce a micro texture by using acidic chemicals in a sequence [Ans00, Van04, San05, Tak03]. The advantage of this method is that it can ensure higher adhesion of fibrin and osteogenic cells on the implant material [Ori00]. Micro-roughness induced titanium surfaces have been shown to improve rapid osseointegration in long term periods [Won95, Cho03, Bra09]. In addition to creating homogeneous roughness, etching increases the surface activity and bio-adhesion properties of the metallic implants [Ors00, Bra09].

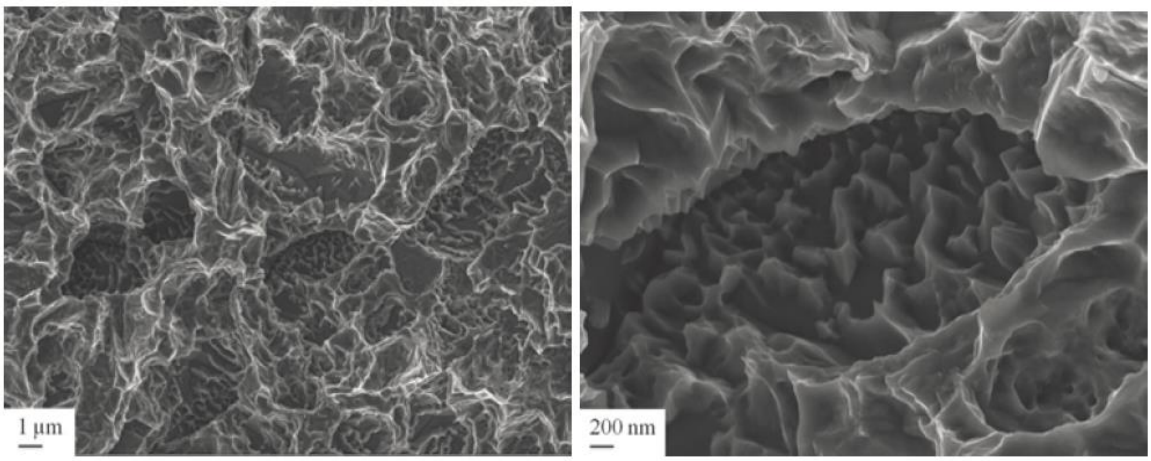

Figure 2.6 Acid etched Ti surface Scanning electron microscopy (SEM) images [Bal11].

On the other hand, alkaline etching can also be performed by using strong base chemicals similar to the acidic etching [Poh02]. Despite these enhancements, etching can cause hydrogen embrittlement of the titanium and decrease fatigue resistance through forming micro cracks on the material surface.

2.2.4 Sand blasting and acid etching

Commercially available dental implants are usually produced by blasting and acid etching (SLA). In this technique, surface is produced by a large grit sand blasting process (250-500 μm) followed by an acid etch to obtain macro roughness and micro pits simultaneously [Kim08]. When compared to the regular blasting processes, acid etching ensures cleaning of the residual particles and induces micro texture and hence increasing the total surface area of the implant material [Gal05, Bus98, Coc98].

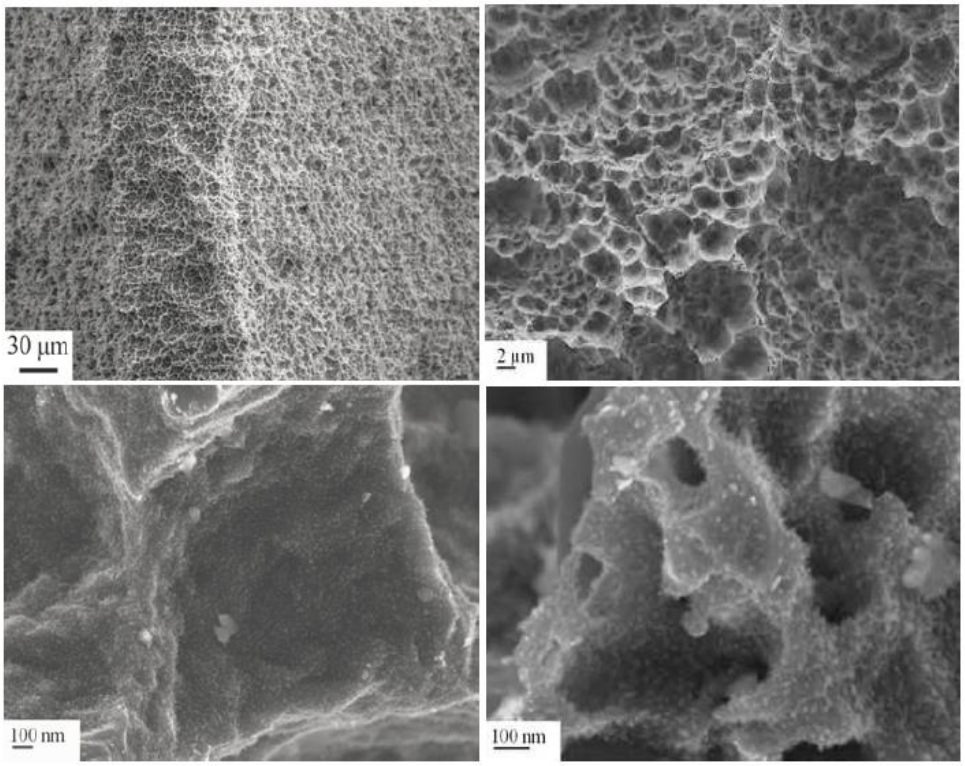

Figure 2.7 Sand blasted and acid etched Ti surface scanning electron microscopy (SEM) images [Bal11].

Consequently, these SLA surfaces were found to have better cell and bone integration as compared to the other conventional methods [Born08, Kim08, Hal03, He09]. Regular grit blasted and etched surfaces show a hydrophobic surface nature, however, surfaces treated through SLA process have a hydrophilic surface that results in stronger bone interaction with the implant material [Gup08, Bal11].

2.2.5 Oxidized/Anodized Implant Surfaces

Anodic oxide formation process can be used to change the properties of the surface oxide layer of the implant to make it more biocompatible through anodization [Gup10]. This method is an electrochemical process and performed by applying a voltage on the implant material, which is immersed in a gentle electrolyte to be passivated. These electrolytes are mainly diluted acid solutions or buffered solutions. When the potential is applied to the material, electrolytic reaction occurs at the anode resulting in the growth an oxide film on the implant surface. The substrate to be anodized is usually covered by a thin native oxide film (which is generally porous) in the range of nano to micro scale due to the interaction with air or electrolyte [Sch03]. When strong acids are used, the oxide film will be cleared off along the current lines and thickened in the other zones [Sul05]. This technique results in an increased thickness and altered crystalline structure of the surface oxide film. The effectiveness of the process depends on the anodic potential, current density, temperature, electrolyte concentration and selected material combination. It has been documented that this process resulted in micro-pores and improved cell attachment and proliferation performance as well as enhancing the biomechanical removal torque values [Zhu04, Gup10, Gur08, Alb81, Her08, Eli10].

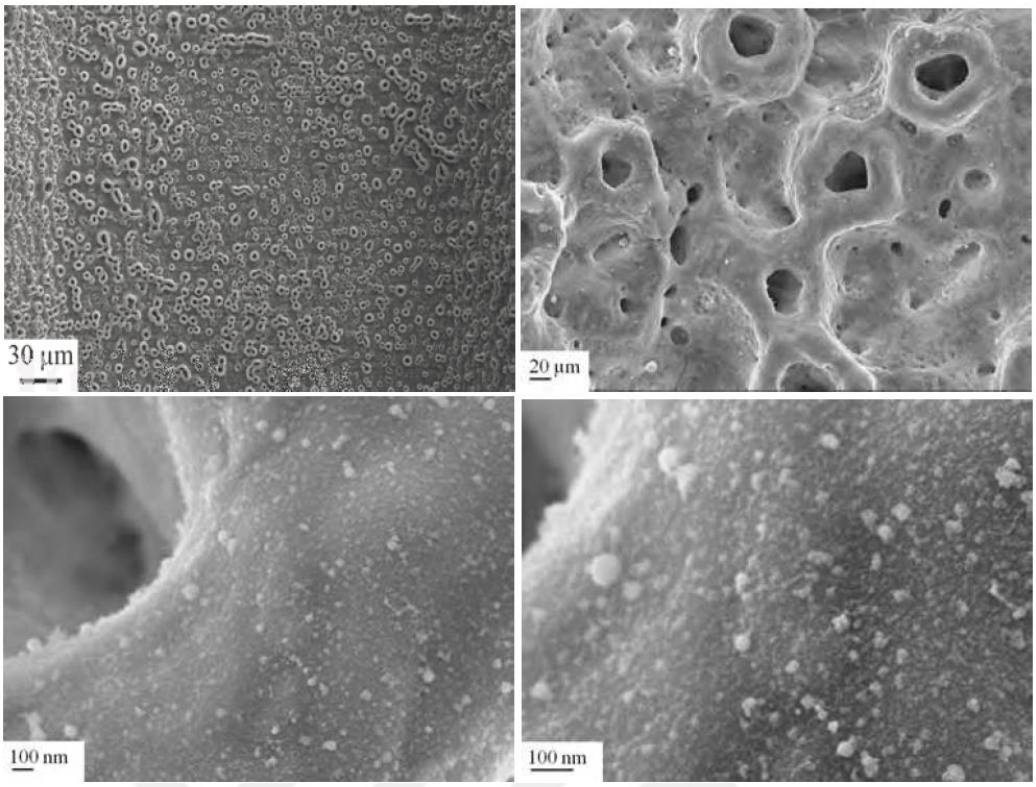

Figure 2.8 Oxidized Ti surface Scanning electron microscopy (SEM) images [Bal11].

2.2.6 Laser processing

Laser patterning method is a micromachining process that can structure a 3D implant surface at micro and nano meter levels. This technique can produce complex surface morphologies with desired roughness for better osseointegration. Laser processing involves generating short pulses of single wavelength light and supplying this energy focused on one dot. Increased energy results in increased roughness, pore size and thicker oxide film formation [Sul02].

Laser treated Ti implant materials showed relatively reduced surface contamination with carbon and oxygen elements and increased removal torque when placed in rabbit tibia bone [Li04, Gag00, Dep05]. Furthermore, this method ensures controllable pore structure formation with specific depth, diameter and spacing without using extra chemicals [Hem12].

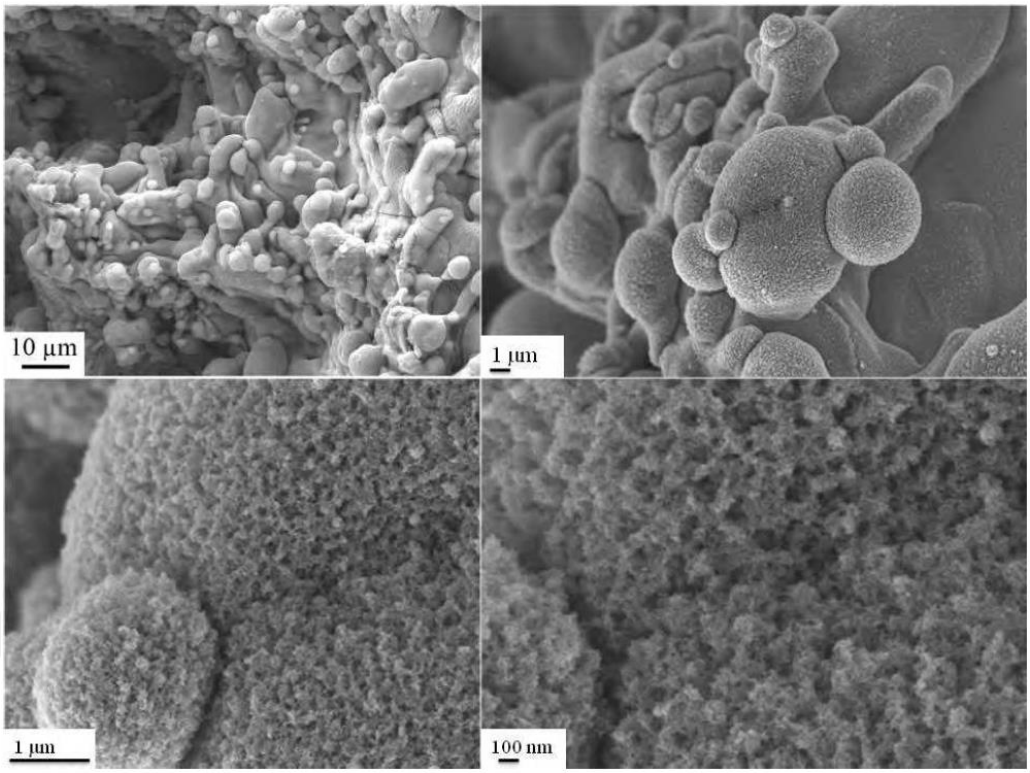

Figure 2.9 Laser treated Ti surface Scanning electron microscopy (SEM) images [Bal11].

2.2.7 Coatings

Beyond the chemical and physical methods, coating is an alternative technique implemented on the implant surfaces to increase the material's biocompatibility. Some reactive materials have a capability to form an interfacial chemical bonding with the surrounding tissue cells and provide a better fixation to the implant material in the body environment. Because of this reason, the surface reactive chemicals are usually applied to the metallic implants as coating materials. The coating elements must have a sufficient adhesion to the implant material surface and must be mechanically stable. Different types of coating methods have been introduced in the literature such as plasma spraying, physical vapor deposition, magnetron sputtering deposition, ion beam assisted deposition, pulsed laser deposition, sol-gel method, electrochemical deposition and micro-arc oxidation.

2.2.7.1 Plasma spraying

Plasma spraying involves heating the hydroxyapatite, calcium phosphate or titanium particles by a plasma torch at high temperatures (15000-20000K) and spraying them on to the subtract material in an inert media [Hah70, Got97]. This method increases surface area of the material up to a nearly six fold higher than the initial surface and forms a film of 100 to 300μm in thickness [Wil97, Ani11]. This increase in thickness depends on the implant geometry, particle size, temperature and distance between the nozzle and the implant material [Lac98, Ros91, Ver93]. Yet, while this increased surface area ensures a better interaction with the bone tissue, it can also become a risk for the oral microbial infection [Mom12].

On the other hand, coatings applied through plasma spraying may possibly undergo delamination and split apart from the surface due to the poor longer term adherence. This can result in failure at the interface of the implant and the coating during the implant insertion or after osseointegration [Coe09].

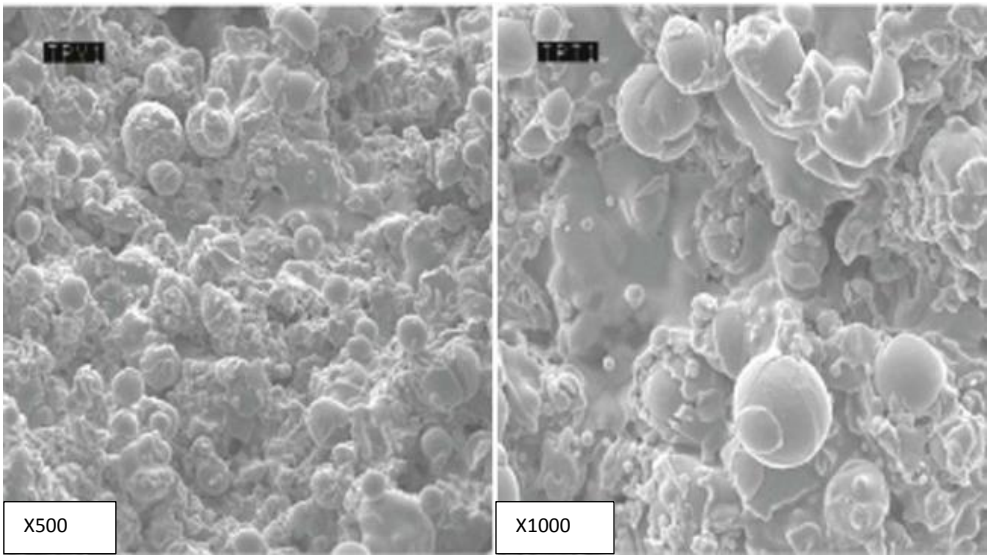

Figure 2.10 Plasma treated Ti surface scanning electron microscopy (SEM) images at 500 and 1000X magnification [Fio15].

2.2.7.2 Sputter deposition

Sputtering process has been introduced as a useful method for the bio-ceramic deposition. It has many variations such as ion sputtering, magnetron sputtering and radio frequency sputtering. Mainly, all of them are based on the same technique where the molecules or atoms of a material are taken out of an object are bombardment at high energy via ions in a vacuum chamber. The removed particles are entrenched on a substrate material in the vacuum chamber.

This technique has a lot of advantages such as high deposition rates and high purity of the final films, film uniformity, dense structure and being suitable for most of the materials. However, deposition rate is low and process itself is extremely slow and also may produce amorphous coatings on the implant surfaces [Jas93, Por04, Yan05, Jan93].

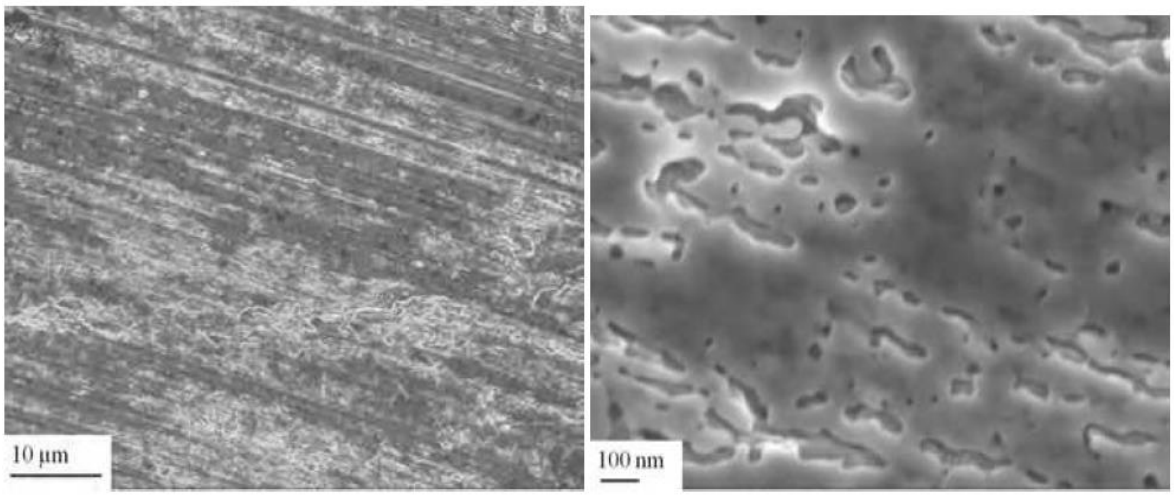

Figure 2.11 Sputtering applied Ti surface scanning electron microscopy (SEM) images [Bal11].

2.3 Chemical Mechanical Polishing as an alternative method for implant surface modification

Chemical Mechanical Polishing (CMP) process is a complicated technique that includes the effects of contact mechanics, fluid dynamics and slurry chemical interactions simultaneously. The process of CMP was initially developed for the glass polishing then it has been implemented to microelectronics manufacturing in semiconductor industry for the polishing/planarization of SiO_2 dielectric oxide layers [Att94]. CMP technique is a simple process that can supply both local and global planarization on the wafer surface through chemical and mechanical actions, where a chemical reaction promotes the mechanical removal of the selected substrate. Basic schematic of the CMP process is shown in Figure 2.11, where the material to be polished is held against a rotating polymeric pad with an applied down-force. Simultaneously, a polishing slurry flows in between the substrate and the polishing pad in a constant flow rate. Therefore, the CMP technique has dual action; first, planarization of the surface layer and second, material removal. Literature extends in that the CMP process can be utilized for polishing of various metallic materials, insulators, polysilicon, ceramic materials and also packaging elements [Zan04]. The efficiency of the CMP process depends on the components of the process namely, surface to be polished, polishing slurry and the polishing pad material.

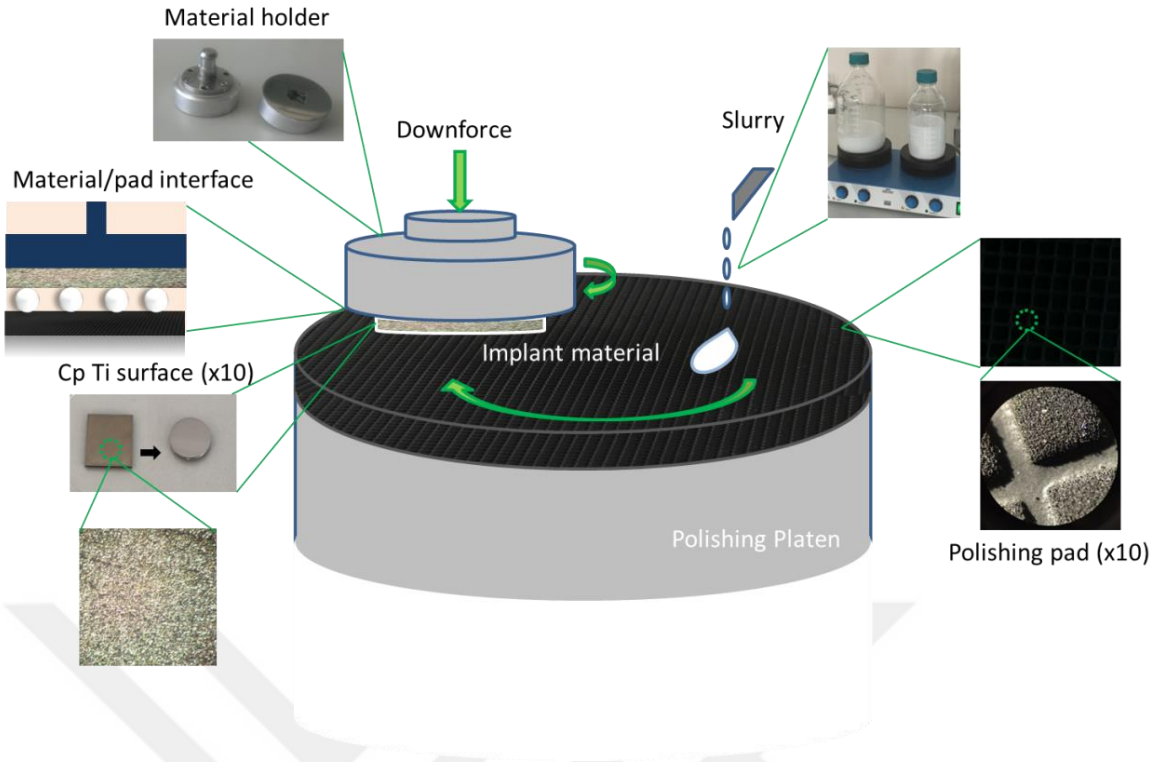

Figure 2.12 Schematic of the general CMP process and components of the technique.

2.3.1 Surface to be polished

CMP process has been implemented for silicon dioxide planarization, other dielectrics, metals and interconnects and polymeric layers to ensure planarized surface finish. The process chemistry starts a reversible reaction driving the formation of a chemically modified thin surface film formation which can decomposed or mechanically abraded through the nano-scale abrasive particles in the slurry to enable material removal from the surface [Ste97, Pau03]. Within the metallic materials CMP has been fist used for tungsten vias and later expanded to different metallic materials including Al, Cu, Ta, Ti, TiN and TaN. Furthermore, high and low-k dielectrics such as SiO_2 doped glasses, Si_3N_4, polymers and polysilicon have also been adopted with Cu integration [Utt91, Kau91]. In semiconductor technology, aluminum and its alloys were the primarily used metals due to good conductivity yet Cu took over for its better

electro-migration resistance, followed by gold and silver for their low resistivity properties. Polymeric materials are the suitable candidates for tuning the dielectric constants in the circuitry [Ste97]. However, the polymeric materials are prone to high temperatures and high stresses induced during CMP and naturally complicated to polish because of that. Copper technology has already replaced the aluminum metallization in the new-generation microprocessors with the reducing sizes of the transistors, It also becomes necessary to find alternative barrier materials to be utilized for Cu integration which are better performing than the standard Ta/TaN integration [Pan82, Koh03].

2.3.2 Polishing Pad

Following the type of the material to be planarized, CMP performance is also influenced by the selection of the polishing pads and the correctly formulated slurries including the slurry abrasive types and compatible chemistries [Bou12, Ali05]. Polishing pad is responsible to transfer the mechanical force over to the surface to be polished, carrying the slurry chemicals and also removing the materials dissolved from the polished surface [Kal07]. Surface characteristics and the type of the pad material are important in controlling the material removal rates and provide planarization selectively on the wafer surface.

Generally, polishing pads are fabricated from polyurethane which has a high strength, modulus and elongation properties [Hep82]. Additionally, porosity and hardness characteristics of the pad materials are tunable to adapt the specific conditions based on selected material during CMP [Jai94]. In order to induce planarization, a robust and durable pad material is preferable to induce consistent properties through the pad life. Furthermore, pad materials must be inert with respect to the slurry chemicals. However, a relatively flexible pad is necessary to prevent possible breakage of the wafer during the CMP process. These variable requirements led to the production of

advanced pad materials as can be seen in Figure 2.12. A conventional polishing pad consists of two different layers. The IC 1000/Suba IV stacked pad is made of attaching an IC 1000 layer to the Suba IV subpad to ensure that the pad conforms with the wafer shape, while the top IC-1000 pad is tougher to provide global planarization while preventing dishing and erosion.

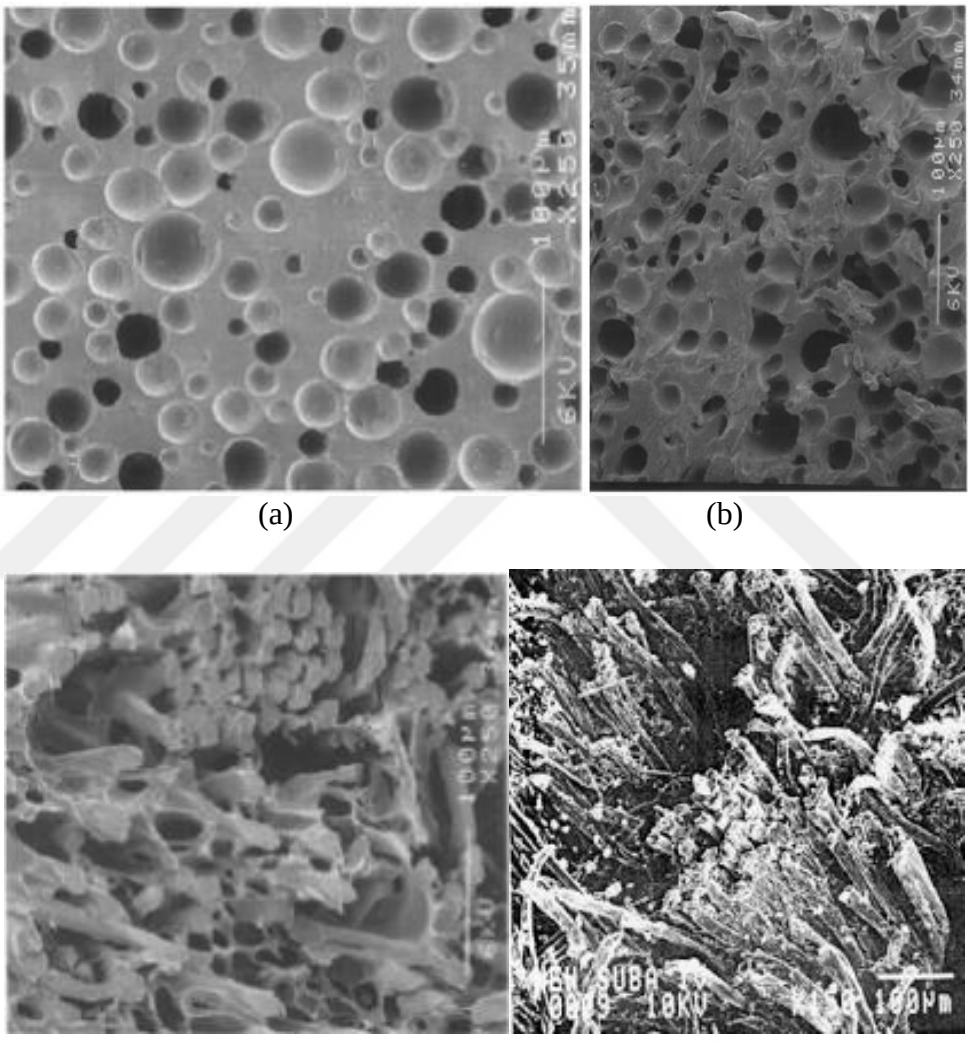

Figure 2.13 Cross section and top surface SEM images of an IC1000 (a&b) a Suba IV (c&d) pad [Lua02, Ste97].

The surface macro structure of the pad is important for the homogenous distribution of the slurry chemicals to the wafer surface. Pores with a size ranging in between micro to macro scale help transportation of the slurry within various patterned groves to transfer slurry at over the wafer interface. During the polishing process, the properties of the pad can change due to deformation, which can reduce polishing rates and planarization efficiency. The plastic deformation of the pad can induce local glazing that can reduce pad performance. Fixed abrasive pads were tried as an alternative, which enabled controlled particle distribution but resulted in major surface defectivity [Ngu01, Ve100]. Therefore, the conventional polymeric pads and free slurry particles are continued to be used for the CMP process [Tri99, Bra00].

2.3.3 Polishing Slurry

The chemical component of the CMP process is provided by the slurries which are highly engineered. Performance of the CMP process is mostly dependent on the slurry formulations, which can control the chemical action through formulation chemistry and the mechanical action by the nano size abrasive particles. Most commonly used abrasive particles are SiO_2, Al_2O_3 and CeO_2 for the CMP formulations. These abrasive particles are suitable candidates due to their mono-dispersed and narrow size distributions [Zha10]. To optimize the slurry performance, polishing rates, material selectivity, uniformity, post cleaning efficiency, planarity, dispersion behavior and shelflife should be considered [Ste97].

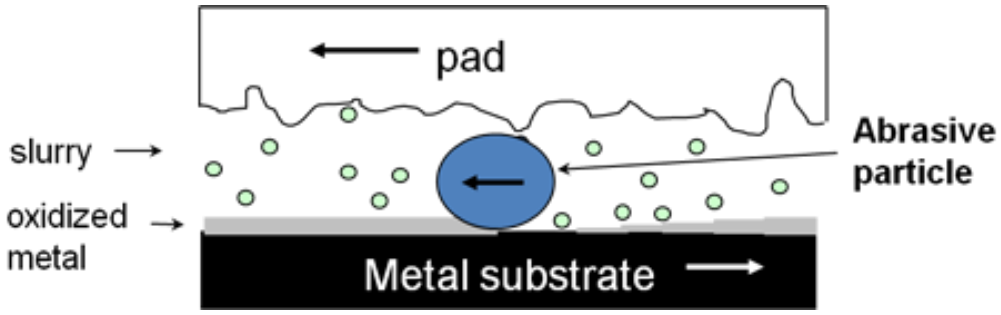

Figure 2.14 Schematics of the slurry interactions during the CMP process [Gli16]

In CMP process, components of the slurry chemicals affect the properties of the chemically modified surface layer formation on the substrate. The compatibility between the formation of this chemically altered layer and its removal by the nanometer size abrasive particles control the material removal rate and the defectivity performance as can be seen in Figure 2.14.

2.3.4 Advantages and disadvantages of the CMP process

CMP process is a complex method, which includes chemical and mechanical actions simultaneously through the three main components as explained previously. In addition, each of the components may vary depending on the temperature, pressure and relative velocity of the surface. Therefore, it is really challenging to be able to control the CMP parameters for the optimization. Nevertheless, the CMP process is one of the most precise methods to achieve the controlled surface treatment due to this multi-agent assembly. The CMP process is a universal method, which is applicable for all types of surfaces acquiring global planarization. In semiconductor fabrication, the CMP process provides a reduced topography, which enables precise photolithography and hence tighter design rules and interconnection levels. On the other hand, chemical components of the CMP process provide an alternative to patterning of the metal surfaces, which

makes it a candidate by eliminating the use of more difficult methods such as ion/plasma etching. In addition, while the CMP is implemented on the implant surface, no hazardous chemicals are used as in the etching process. Furthermore, multi-functional variables of the CMP process help in increasing reliability, speed and yield within a low cost operation.

However, the CMP process is designed for the planarization of the 2-dimensional materials. In order to utilize CMP in the implant industry, the current CMP process should be adapted to a 3-dimesional (3D) design. Regular polishing methods are applied for the large bone replacements in 3D manner as can see in Figure 2.15. A robotic arm holds each implant towards the polishing fabric and the polisher fabric reaches the each curve on the implant through robotic arm movements. Nevertheless, the general polishing method is not effective based on the surface finish quality and composition, and also speed and time spend during the operation.

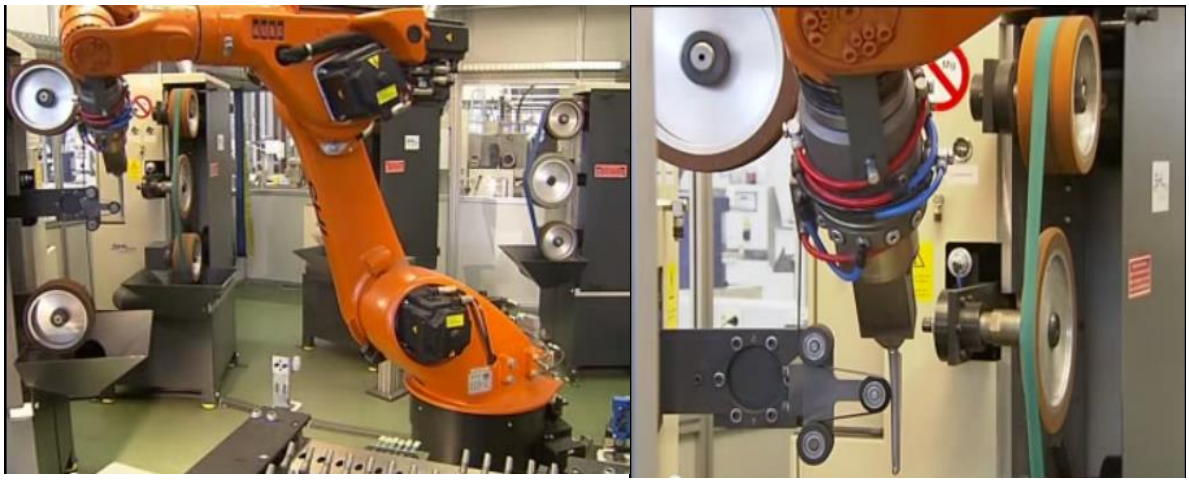

Figure 2.15 Industrial robotic arms are commercially being used for surface polishing of larger scale bone implants [https://www.youtube.com/watch?v=gO_8spCu29M]

2.4 Scope of the Dissertation

Surface treatment of medical implants is still a developing field for the identification of most optimal material surface treatment methodology. Studies in the literature have indicated that most of the surface processing methods has disadvantages based on the in vivo implant evaluation. Based on the detailed review of the variable surface treatment methods, this study investigates CMP process as an alternative technique to induce controlled surface texture to the titanium based implant materials. Therefore, CMP conditions for processing the titanium based material surfaces were examined to achieve controlled surface structuring, material removal and optimal surface quality performances. Furthermore, optimization of the CMP process was investigated by changing slurry chemicals and pad type. Additionally, biocompatibility of the CMP induced titanium implants were evaluated through cytotoxicity, cell viability and bacteria growth analyses. Although this dissertation primarily focused on the dental implants, it is expected that the outcomes of this study can be applied to the other types of implant to enhance the surface properties.

CHAPTER III

APPLICATION OF CHEMICAL MECHANICAL POLISHING ON TITANIUM IMPLANT SURFACES

3.1 Introduction

Chemical Mechanical Polishing (CMP) process has been introduced initially for glass polishing for telescopes and large lenses and extended into the planarization of wafer surfaces in the microelectronics manufacturing based on initial developments conducted by IBM in 1980's [Bas11]. In CMP process, the top film of the material to be polished is exposed to the polishing slurry chemicals, which consist of submicron size particles, pH adjusters, stabilizers and corrosives. Interaction of these chemicals with the substrate materials result in a chemically altered top film formation that is removed by the mechanical abrasion of the slurry abrasive particles. Hence, it is a novel method as compared to the general mechanical treatment techniques used for implant surface treatments [Sit99]. The success of CMP process is measured by the material removal rate and the surface quality of the substrate material. Preferable material removal rate and surface finish are achieved in the CMP process by the synergistic effects of the chemical and mechanical forces. It has been demonstrated that in the CMP process, chemical content of the polishing slurry is responsible for facilitating abrasion through chemically modified film formation, whereas mechanical forces help achieve the required surface topography [Run96]. The mechanical action in the CMP process is mainly provided by the nano-size abrasive particles as they move in between the pad and the substrate surface under the applied load.

In microelectronics, titanium CMP process is performed to planarize Ti and TiN layers, which are used as interconnect diffusion barriers in between aluminum and the dielectric layers

for the first level of metallization [Cha03]. Recently, it has been experimented that the application of CMP on titanium films has been more successful in terms of forming an oxide film on the titanium surface as compared to etched films, which also contributes to the biocompatibility [Oka09, Tan07]. Furthermore, CMP application on titanium has shown that the titanium surfaces treated by CMP using colloidal SiO_2 slurries with oxidizer concentration of 3wt% were much clear and compositionally continuous as compared to the electrochemical etching. Electrochemical etch has formed a yellowish and blurry titanium oxide layer on the titanium during the process. In this study, CMP has been utilized to induce nano-scale smoothness or nano/micro scale roughness on the bio-implant surface in addition to helping removal of the contaminated surface layers. Particularly, we focus on the dental implants to change the surface roughness in a control manner. Implementation of the CMP process on titanium based bio-implants inducing controlled surface smoothness or roughness by designing the CMP process variables such as slurry particle size and type, solids loading as well as the oxidizer type and concentration are the primary factors evaluated.

In this chapter, the results of the CMP process conducted by using Al_2O_3, TiO_2 and SiO_2 slurry particles and H_2O_2 as an oxidizer on commercially pure (cp) Ti samples with different polishing pads are presented. Simultaneously, CMP responses of the titanium plates with different slurries, pad materials and oxidizer concentrations are discussed in terms of material removal rate responses and surface topography changes in correlation to the surface roughness values measured by using atomic force microscope (AFM) and wettability analysis conducted through the contact angle measurements. In order to demonstrate the utilization of CMP on dental implants, both titanium plates and dental implants were processed in this study with the results discussed in detail.

3.2 Experimental

3.2.1 Chemical mechanical polishing treatment of the titanium surface

CMP analyses were conducted on titanium foils with 1 mm thickness and 99.6% purity (TI000430) obtained from Goodfellow Cambridge Limited. The original foil which was 300 x 300 mm in size was cut to 14 x 14 mm pieces to fit to the holder of the CMP tool. The original titanium foil sample surface, which is considered as baseline in this experimental study, was annealed. Figure 3.1a illustrates the optical micrograph of the anodized titanium plate surface (200X) as well as the SEM cross sectional image illustrating the thick and porous oxide layer with 30–40 μm thickness. Figure 3.1b shows the titanium based dental implant used to implement the optimized CMP conditions through hand polishing on a 3-D sample. The dental implants were provided by MODE Medical Company and they were only shaped by machining prior to their exposure to the CMP testing. Figure 3.1.d shows the machined surface structure of the dental implant itself (200X).

CMP experiments were conducted on a tabletop Tegrapol-31 polisher. Figure 3.2.a shows the 2-dimensional standard CMP set up as it is developed for the polishing and planarization of the 2-D structures. CMP slurries were prepared by using three different oxide compounds which are generally used in CMP slurry formulation. Two of the polishing slurries were prepared in house by using alumina (Al_2O_3) and titania (TiO_2) particles with the size of 50 nm, 25 nm, respectively. Additionally, a commercial silica based slurry (SiO_2) was used as alternative slurry obtained from BASF, SE company in Germany. All the slurries prepared at the same slurry solids concentration as weight percentage (5 wt. %). The pH values were adjusted according to the selected nanoparticle's isoelectric point (iep) to ensure the stability during the polishing process. In order to provide a long term stability, the prepared slurry suspensions were ultrasonicated long enough by repeated pH adjustments until the slurry was fully stabilized which was confirmed by slurry particle size distribution analyzed by Coulter LS 13 320 particle size analyzer. CMP tests were conducted at 70 N down force which is equivalent to a 7.88 psi pressure on the used sample size.

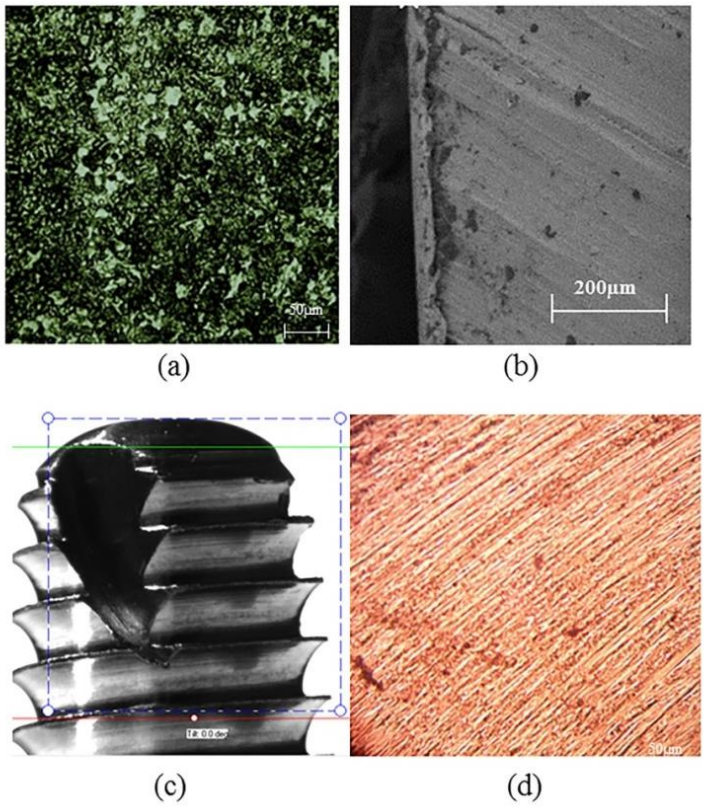

Figure 3.1 Surface structures of (a) baseline anodized titanium plate sample (200X magnification) (b) SEM X-section illustrating thick surface oxide, on the baseline titanium plate (c) baseline machined dental implant sample with no additional surface treatment (4X) and (d) machined dental implant magnification at 200X

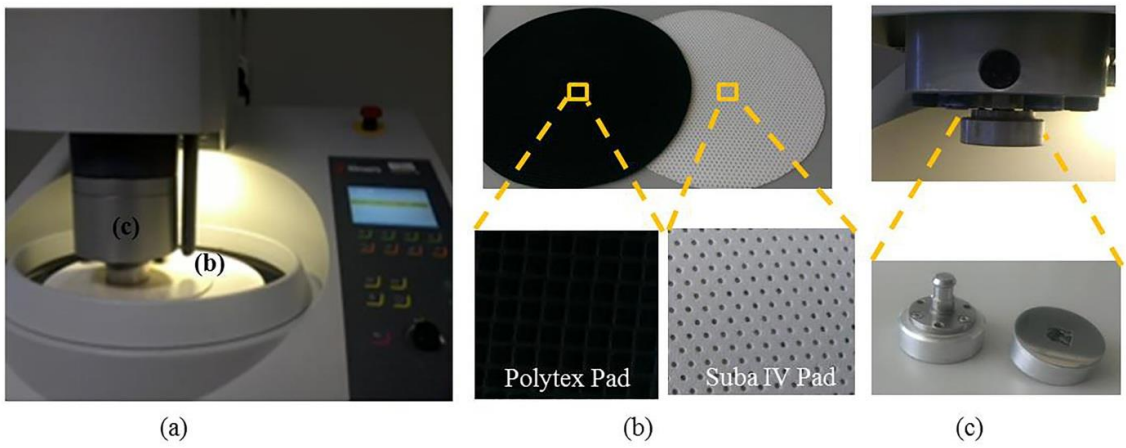

Figure 3.2 CMP configuration for polishing 2-D titanium plates (a) tabletop CMP tool (Struers, Tengramin) (b) polytex and Suba IV polishing pads and (c) CMP sample holder.

The titanium plates were polished by using a SubaIV subpad stacked under a polytex buff pad to smoothen the surface while protecting the macro-scale shape of the plates. This soft-pad configuration enables a gentle interaction between the pad and the implant surface providing local smoothening while maintaining the physical shape of the surface that is required for the screw pitch of the dental implants. Furthermore, IC1000 polyurethane pad was also used to enable the planarization of the samples to induce nano size roughness or smoothness on the titanium plates. In addition, Figure 3.3 illustrates two sizes of sand papers (silicon carbide, SiC, 150C and P320) that were used in place of the polishing pad to create the micro structures through CMP process. Figure 3.2.b and 3.2.c illustrate the CMP pads and the sample holder, respectively. In Figure 3.2 b, the picture with dark colored square surface structure belongs to the Polytex pad used as the prime pad and the lighter colored pad with the circular holes belongs to the Suba IV sub-pad. Hydrogen peroxide (H_2O_2 obtained from Sigma Aldrich at %34.5–36.5 concentration) was used as an oxidizer in the CMP experiments except for the baseline sample, which received no additional treatment. Furthermore, one of the samples was polished without the oxidizer to expose the underlying titanium metal in order to understand the effect of formation of an oxide layer during CMP implementation on bio-compatibility of the sample. Samples tested with the polymeric CMP pads and abrasive papers were polished for 2 minutes at different oxidizer addition. Material removal rates were calculated through weight loss of the samples before and after polishing by Swiss Made ES125SM model precise scientific balance (five digits after the decimal point, 0.01 mg accuracy). All samples were cleaned in ultrasonic bath with pH adjusted (pH 9) water for 5 minutes and dried with nitrogen gas before they were characterized. Same experimental procedure was implemented on the 3-D dental implant samples obtained from Mode Medical Limited, by using a polymeric brush and flowing slurry on the samples as they were hand polished.

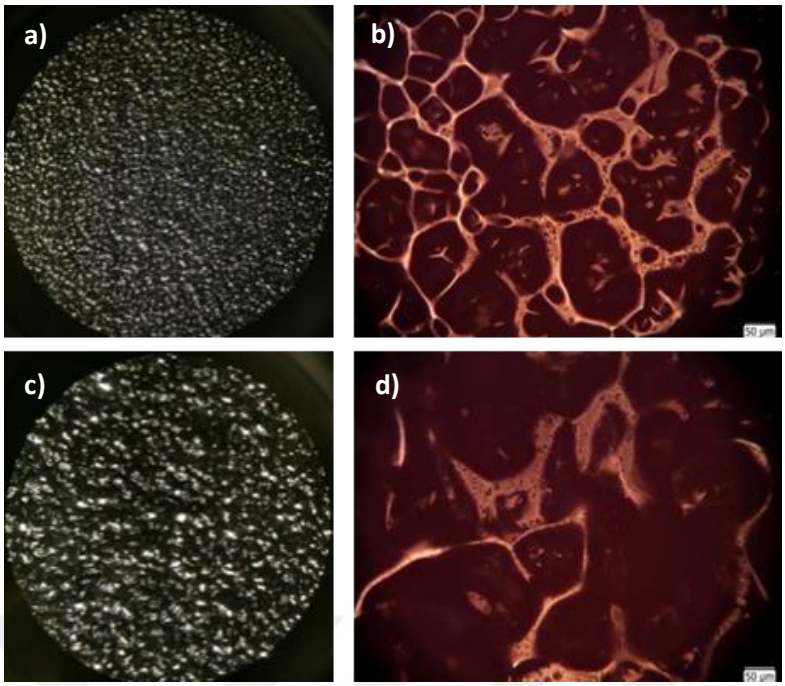

Figure 3.3 SiC based abrasive papers (a) 45µm particle size (10X) (b) 45µm particle size (200X), (c) 90µm particle size (10X) and (d) 90µm particle size (200X magnification).

3.2.2 Slurry characterization

Aqueous slurry suspensions were prepared at constant pH to minimize the agglomeration risk for a reproducible and scratch free CMP process. Since all particles in water have a surface charge due to interaction of neutral OH (hydroxyl) surface functional sites (H^+ or OH^-) with the surface, material may be negatively or positively charged depending on the solution pH. Hydrogen ion concentration at a pH where the total negative and positive charges are equal to each other is called the point of zero charge or the isoelectric point. On the other hand, counter ions surrounding each particle form an opposite charge cloud around the particle which is called the zeta potential. When the particles are close to each other, this charged clouds overlap and tend to form repulsive interactions amoung the same type particles ensuring stability of the suspension [Mat01].

Selected CMP slurry particles used in this study have a wide range of iep values due to their chemical nature. Since it is know that metallic oxides are basic oxides, as can be seen in

the Table 3.1, when they are prepared in aqueous media, pH values are higher. Alumina (Al_2O_3) and Titania (TiO_2) particles have iep values at pH ~8-9 and ~5-6, respectively that are higher than silica. This means that using these pH values will screen the surface charge and results is unstable colloidal system for the particles in aqueous media. Hence Al_2O_3 slurry pH was adjusted to pH 4 to increase surface charge as positive zeta potential and TiO_2 slurry pH was adjusted to pH 11 as a negative zeta potential. The other abrasive SiO_2, is an acidic oxide and gives a value of 2.8-3 when it is in a water suspension. Therefore, the silica based slurry pH was adjusted to 9 for stability giving a negative zeta potential. In order to evaluate the stability response of these slurries, the slurry particle size distributions were analyzed by Static Light Scattering particle size measurement instrument, Coulter LS-13 320, at their own pH value by adjusting the pH of the background water in the universal liquid module during the measurements.

The slurry particle size analyses by Coulter LS 13 320, are reported in Figure 3.4, Figure 3.5 and Figure 3.6 for Al_2O_3, TiO_2 and SiO_2 abrasives, respectively. Through the volume percent and number percent distributions it can be clearly seen that Al_2O_3 and TiO_2 based slurries possess two peaks on the percent volume distribution, which means there are soft agglomerates (coagulation) in the slurries as observed by the secondary peak at the larger sizes. While the percent number distributions of the Al_2O_3 and TiO_2 slurries have shown 116 and 92 nm mean size of the particles, volume based measurements resulted in larger sizes due to stability issues with the slurries made in the laboratory. On the other hand, commercial SiO_2 slurry has shown a single peak on both percent volume and number based measurements indicating uniform sized particles under selected slurry conditions. The average size of the SiO_2 based slurry was measured as 90nm with a tight standard deviation value.

Table 3.1 Properties of the slurry abrasive particles

Oxide type of slurry	Moh's Hardness	Isoelectric point (iep)	pH	
			In DI-water	In CMP slurry
Alumina (Al_2O_3)	8-9	8-9 [Tar98]	6.5	4.0
Titania (TiO_2)	5.5-6.5	5-6 [Fin07]	6.4	11.0
Silica (SiO_2)	7	2-3 [Die01]	3.4	9.0

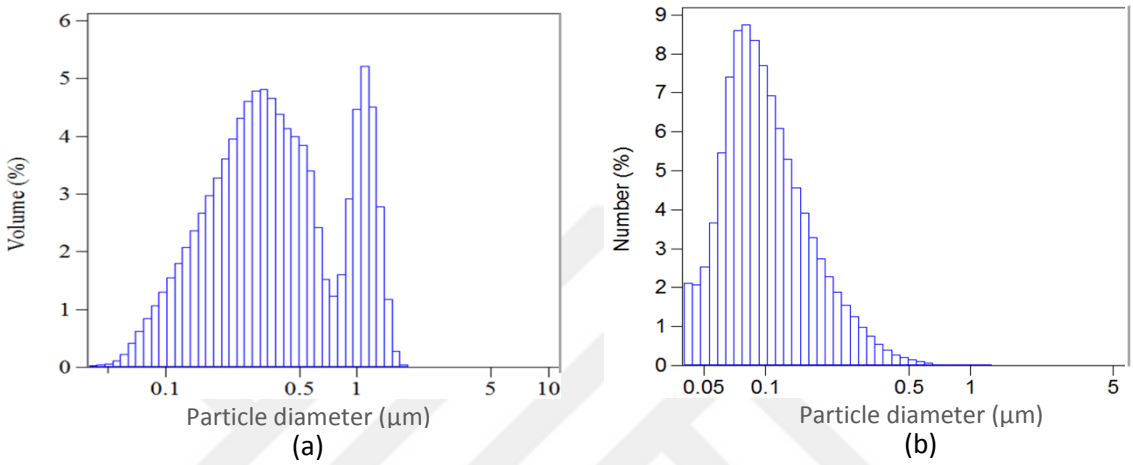

Figure 3.4 Particle size distributions of Al_2O_3 particles at pH 4 (a) Volume % based and (b) Number % based distribution.

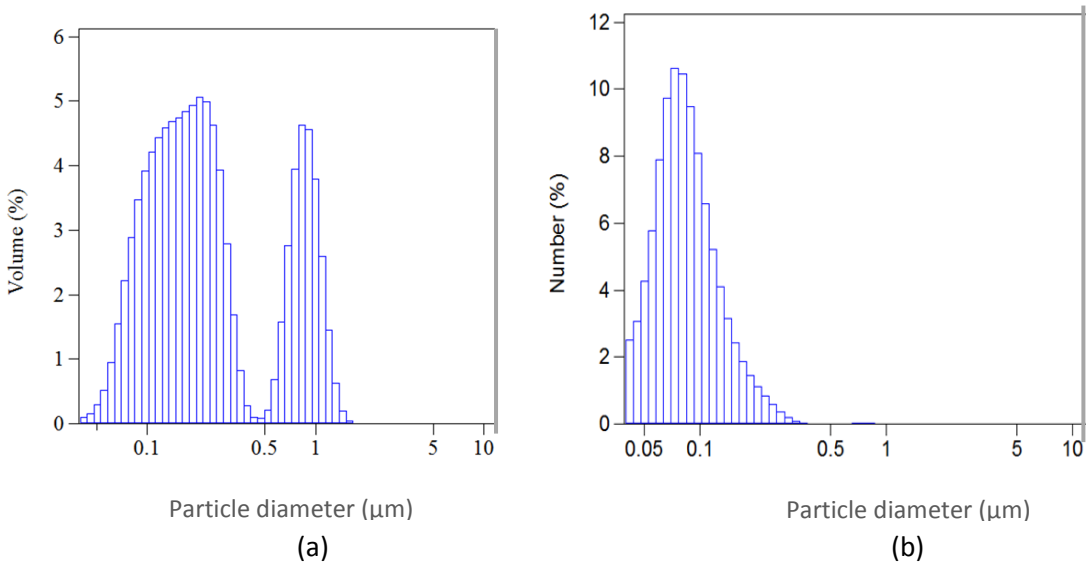

Figure 3.5 Particle size distributions of TiO_2 particles at pH 11 (a) Volume % based and (b) Number % based distribution

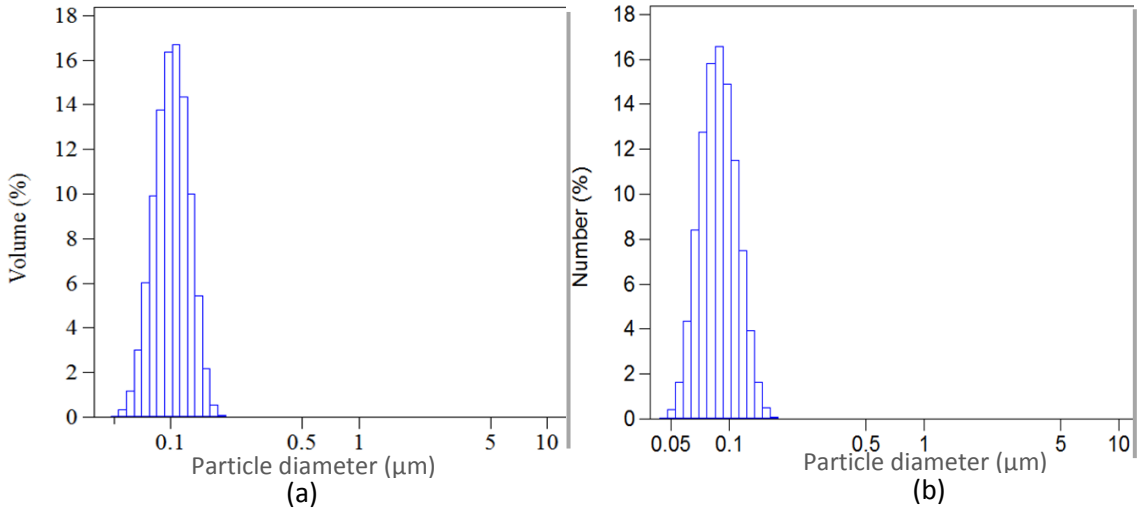

Figure 3.6 Particle size distributions of SiO_2 slurry at pH 9 (a) Volume % based and (b) Number % based distribution

3.2.3 Surface characterization

3.2.3.1 Wettability characterization

All the 2-D and 3-D titanium substrates were characterized for wettability response through contact angle measurements with simulated body fluid (SBF) which is prepared according to Kokubo et al. method [Kok90], by using a KSV ATTENSION Theta Lite Optic Contact Angle Goniometer using the sessile drop method. Five drops were measured on each sample. The drop images were stored by a camera and an image analysis system calculated the contact angle (Θ) from the shape of the drops.

Preparation of simulated body fluid;

Simulated body fluid ion concentrations are nearly equal to human blood plasma. The reagents dissolved in 500 ml of distilled water one by one in the order as given; NaCl (7.996 g), $NaHCO_3$ (0.350g), KCl (0.224 g), K_2HPO_4.3H2O (0.228g), $MgCl_2 \cdot 6H_2O$ (0.305 g), 40ml 1N HCl, $CaCl_2$ (0.278 g), Na_2SO_4 (0.071 g) and $(CH_2OH)_3CNH_2$ (6.057g). The temperature was raised to 37 °C and the pH was adjusted to 7.4 using 1 N HCl and the final volume to 1000 mL using DI-water.

3.2.3.2 Surface topography and roughness characterization

The surface topographies of the 2-D specimens were examined by Nanomagnetics Atomic Force Microscope (AFM) using contact mode. Surface roughness values were recorded on 10×10 μm scan area and reported as an average of minimum three measurements taken on the samples. CMP generated metal oxide thin films are verified to be in nanometer scales (1–10 nm) [Kar15] and high energy beams of the Scanning Electron Microscopy (SEM) results in damage on these ultra-thin films, or require a coating to be applied (which changes the nature of the thin oxide layer). Therefore, AFM technique was preferred for characterization of the CMP induced titanium surfaces (AFM does not require a coating application on the surface) [Kau91]. SEM analyses were conducted to obtain the cross sectional analyses on the original titanium plate by JEOL JIB- 4501SEM to analyze the thickness of the anodized titanium oxide layer. Furthermore, profilometry analyses were performed to measure the roughness values of the titanium plates at a micron scale in 3-dimension and in mm scale in X-Y dimension by using a Mitutoyo SJ-400 profilometer. 4mm lengths were scanned on the samples on three different locations and averaged to report the average roughness (Ra) and average roughness height (Rz) values.

3.2.3.3 Characterization of mechanical properties

In order to evaluate to surface mechanical properties Vickers hardness tests and tensile tests were conducted on the titanium samples. The hardness values were evaluated through Vickers Hardness (HV) test protocol on the baseline sample and CMP implemented titanium samples with ARS9000 Full-Automatic Microhardness Testing System and the data was processed through its software (after 3 measurements on each sample surface).Tensile strength evaluations were conducted with a hydraulic type Instron Tensile Testing Machine. Specimens were prepared in the desired orientation by following the test standards. The central portion (gage portion) of the sample length is usually smaller in cross section than the end portions.

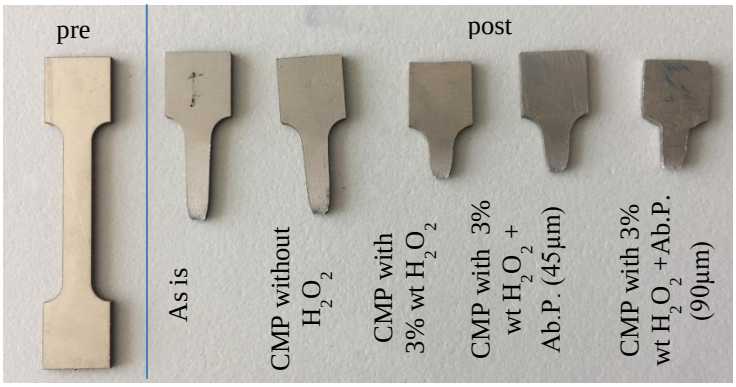

Figure 3.7 Tensile test specimens before and after the tensile test application.

This ensures the failure to occur at a section where the stresses are not affected by the device grip as can be seen in Figure 3.7.

3.3 Results and Discussion

3.3.1 Material Removal Rate Response for 2D Samples

3.3.1.1 Effect of slurry chemicals (abrasive particles)

CMP is a process that combines both mechanical and chemical actions where the mechanical polishing is provided by the action of the abrasive particles. Therefore, the interaction of the slurry particles with the material surface is one of the major components driving the metal surface removal mechanisms. The mechanism depends on two actions i) corrosive wet etching of metal and ii) metal oxidation & passivation. Different metal oxides have different degrees of water solubility and if the oxide is insoluble adherent and continuous, it can prevent the oxygen diffusion until the slurry particles mechanically abrade the surface layer. This enables topographic selectivity.

In the preliminary CMP evaluations, a hard pad (IC1000 polyurethane) wad used to provide smooth surface finish by using three different slurry abrasives, Al_2O_3, TiO_2 and SiO_2. CMP experiments were conducted by; (i) without oxidizer and (ii) in the

presence of 3 wt % H_2O_2. Figure 3.8.a shows the removal rate values for the CMP without addition of an oxidizer, which are close to each other for all the three slurry formulations. TiO_2 has slightly higher material removal rate (MRR) as compared to SiO_2 and Al_2O_3 yet it is not statistically significant. Additionally, wettability performances of the polished samples have a correlation with the material removal rate values as can be seen from the Figure 3.8.b. Contact angle values increased with the increasing removal rates. The highest contact angle value was obtained as 61.34° with the TiO_2 slurry treatment. On the other hand, samples processed with the 3wt% H_2O_2, have shown different results due to the surface oxide formation during the CMP. Figure 3.9.a and 3.9.b give the material removal rates and contact angle values by using 5% wt Al_2O_3, SiO_2 and TiO_2 slurry abrasives, where the lowest material removal rate was obtained with the TiO_2 slurry. In addition, contact angle values showed a reverse correlation with the removal rate in the presence of the H_2O_2 in the slurries. Al_2O_3 slurry resulted in the highest removal rate value of 133.16 nm/min with the lowest contact angle value of 52.10°. Removal rate mechanism of the slurry in CMP treatment was observed to be affected by the hardness of the selected particles as they affect the mechanical abrasion. As it is given in Table 3.1 the Moh's hardness values of the selected particles and the removal rates observed were also found to be correlated and the lowest MRR value was obtained with the softest TiO_2 particles.

In addition to the CMP process, the post CMP cleaning performance has also been observed to be affected by the type of the slurry abrasives. TiO_2 particles tend to attack titanium surface during the oxide layer formation due to both being titanium oxide in composition. Hence, the applied cleaning procedure was not strong enough to remove the TiO_2 particles form the surface as can be seen in Figure 3.10. Additional cleaning steps had to be applied to these samples by using acetone in an ultrasonic bath

for 10 minutes. However, cleaning was still not satisfactory for the elimination of the particles from the surface. Therefore, TiO_2 slurry was not used to polish the 3D titanium samples for the further evaluations.

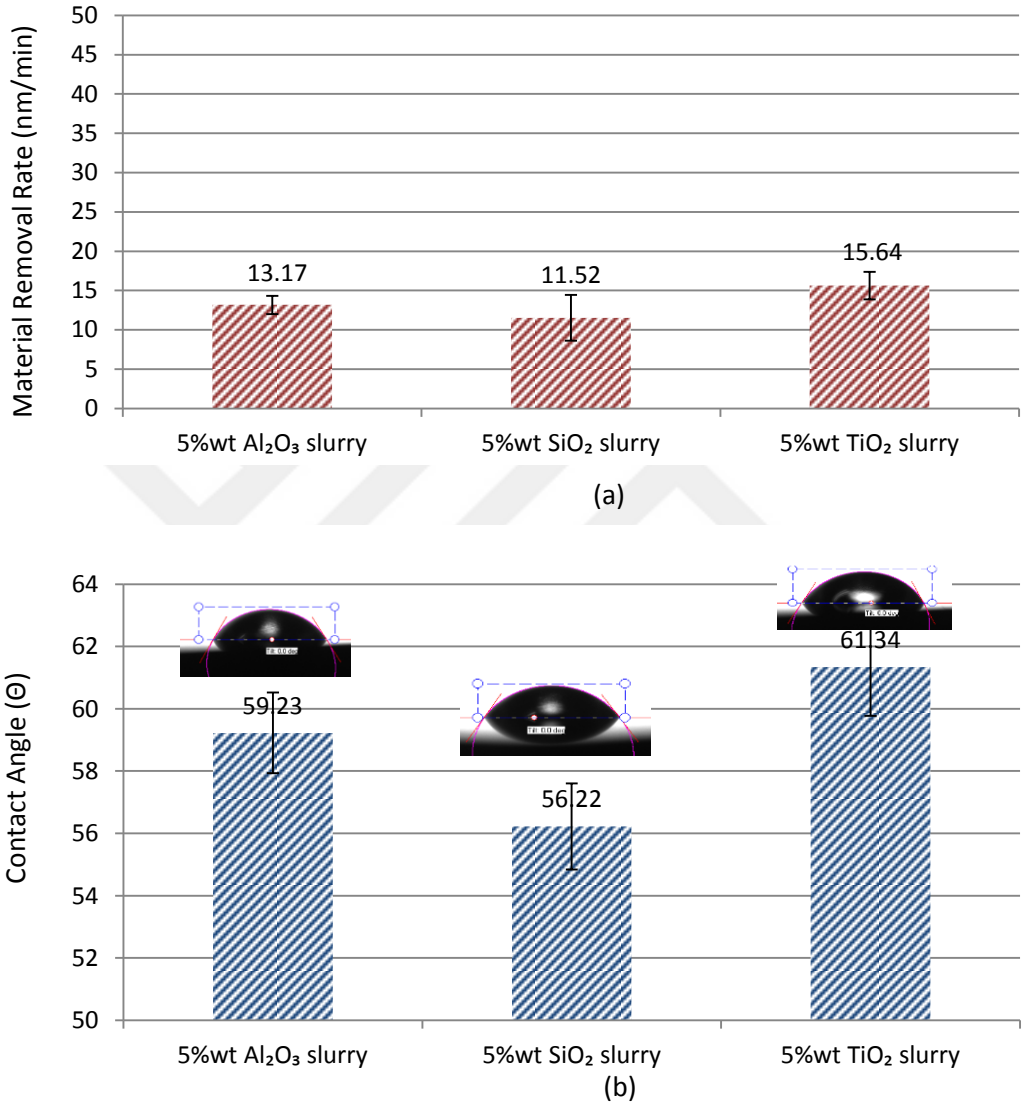

Figure 3.8 CMP performance of the Ti samples without H_2O_2 using

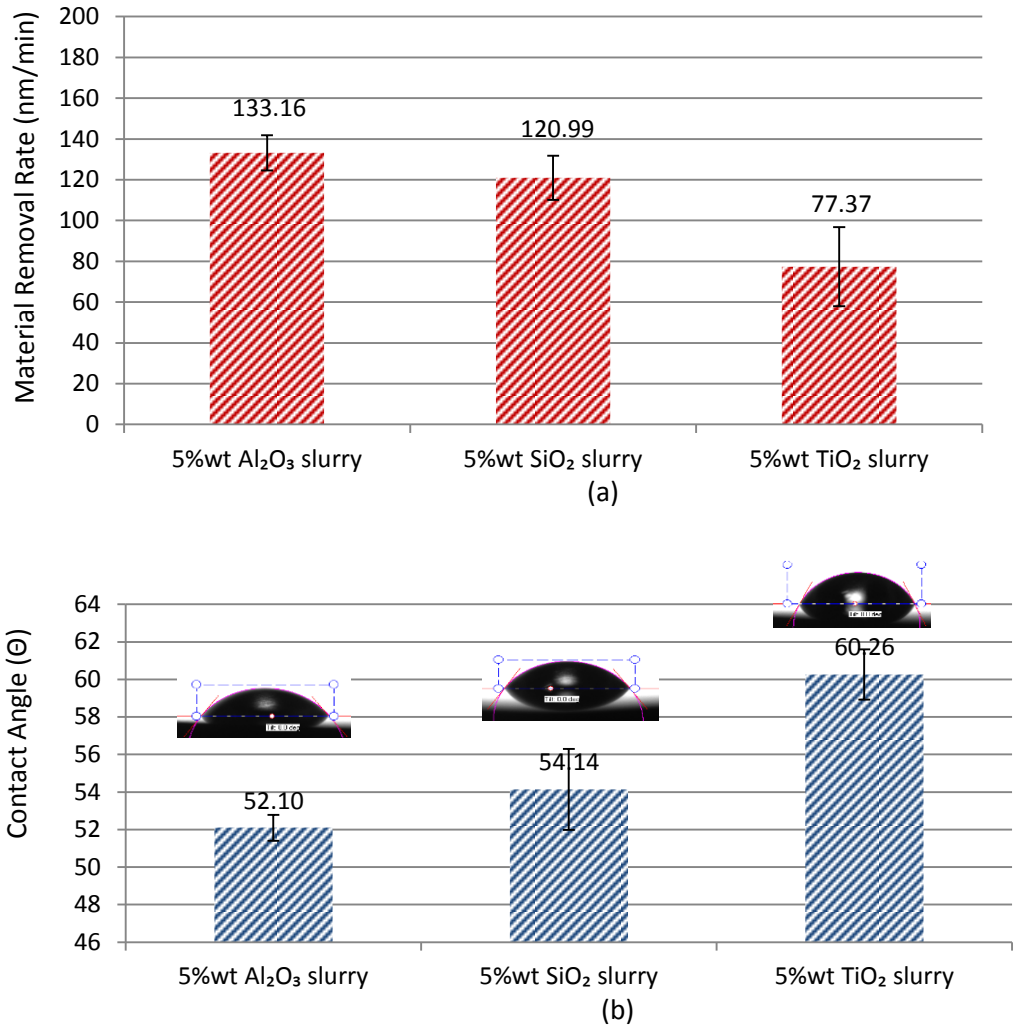

Figure 3.9 CMP performance of the Ti samples in the presence of 3 wt % H_2O_2 in the slurry

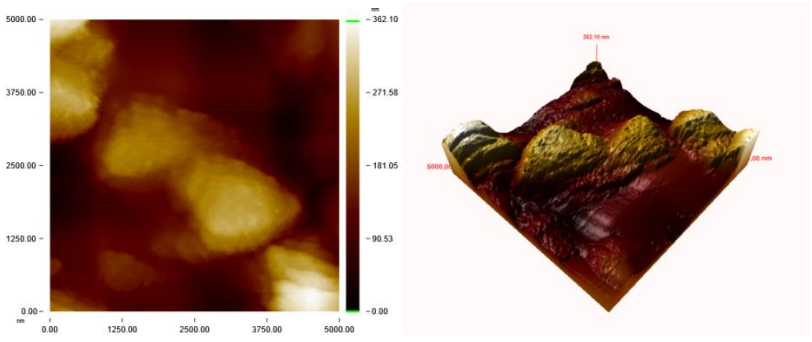

Figure 3.10 Atomic force microscopy (AFM) images of the polished titanium sample through 5wt% TiO_2 slurry illustrating the titania particles stuck on the surface.

3.3.1.2 Effect of oxidizer concentration

The oxidizer concentration is another important parameter for a desirable CMP performance. Therefore, various H_2O_2 concentrations were examined with three different slurry chemicals and results were evaluated through removal mechanisms and wettability behavior. Figures 3.11, 3.12 and 3.13 compare the material removal and contact angle responses as a function of slurry oxidizer concentration for 5% wt Al_2O_3 (Figure 3.11), SiO_2 (Figure 3.12) and TiO_2 (Figure 3.13) slurries, respectivelly.

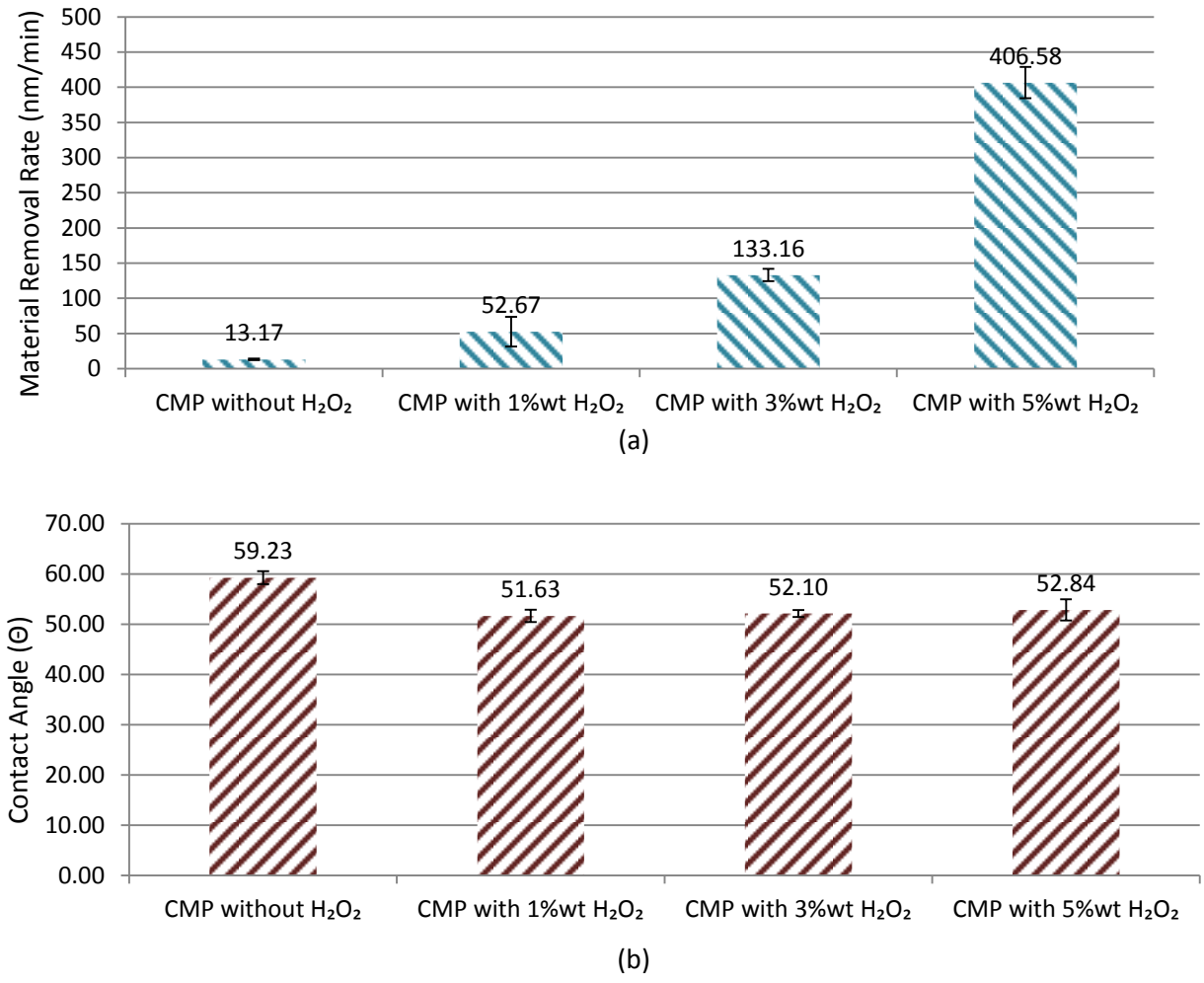

Figure 3.11 CMP performance of the Ti plates as a function of the oxidizer concentration with Al_2O_3 abrasive containing slurry.

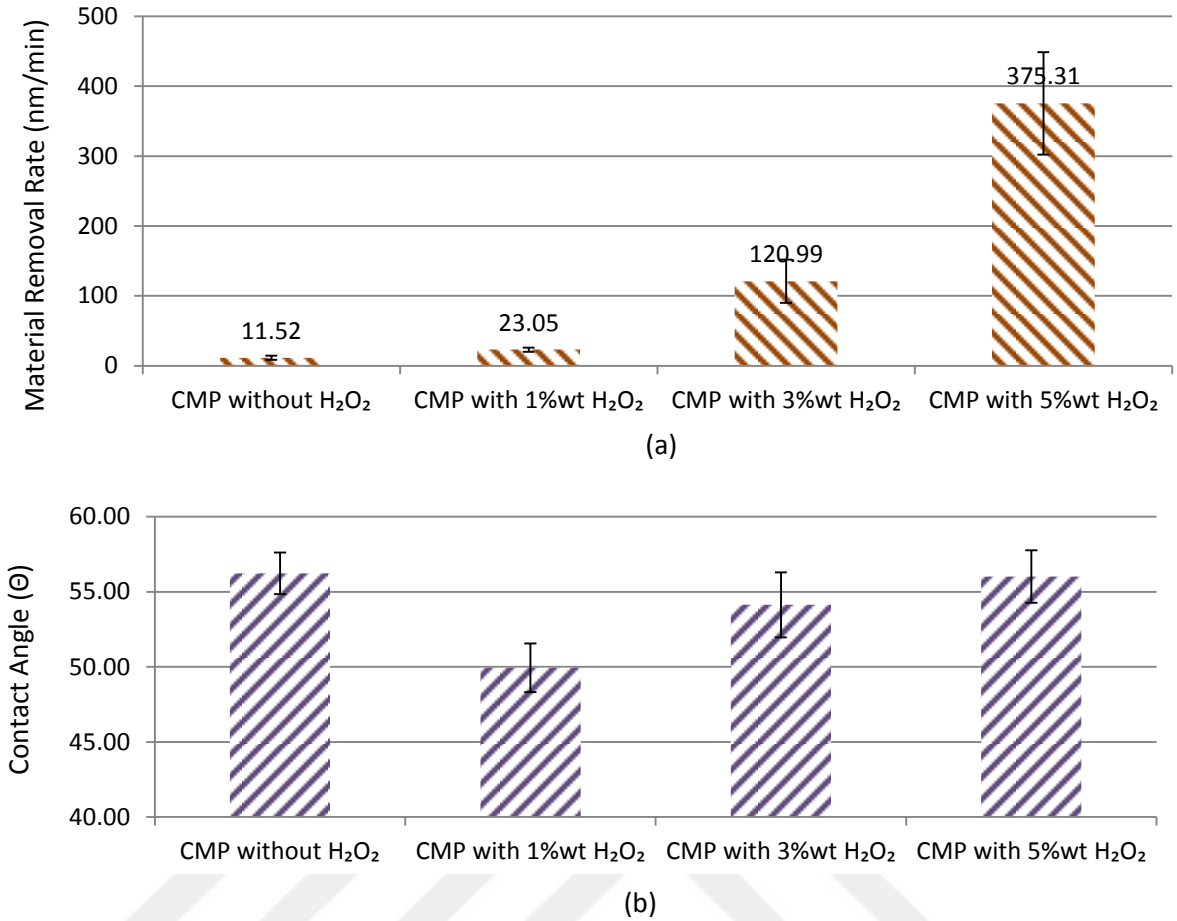

Figure 3.12 CMP performance of the Ti plates as a function of the oxidizer concentration with SiO_2 abrasive containing slurry.

The removal rate of Ti via different slurry solutions in the absence and presence of 1wt%, 3wt% and 5wt% H_2O_2 addition is shown in Figure 3.11, Figure 3.12 and Figure 3.13 for Al_2O_3 , SiO_2 and TiO_2, respectively. Very low material removal rates were observed in the absence of the oxidizer during the CMP treatment and actual rates were below 15nm/min for all three slurry types. Ti surface tends to form a TiO_2 layer when exposed to an oxidizer. Hardness value of this film is nearly close or in some case lower than the titanium. Therefore, much higher removal rates were observed with an oxidizer in the slurry [Cha03]. It can be seen clearly from the Figure 3.11, Figure 3.12 and Figure 3.13 that increased oxidizer concentration resulted in increased material removal rate responses.

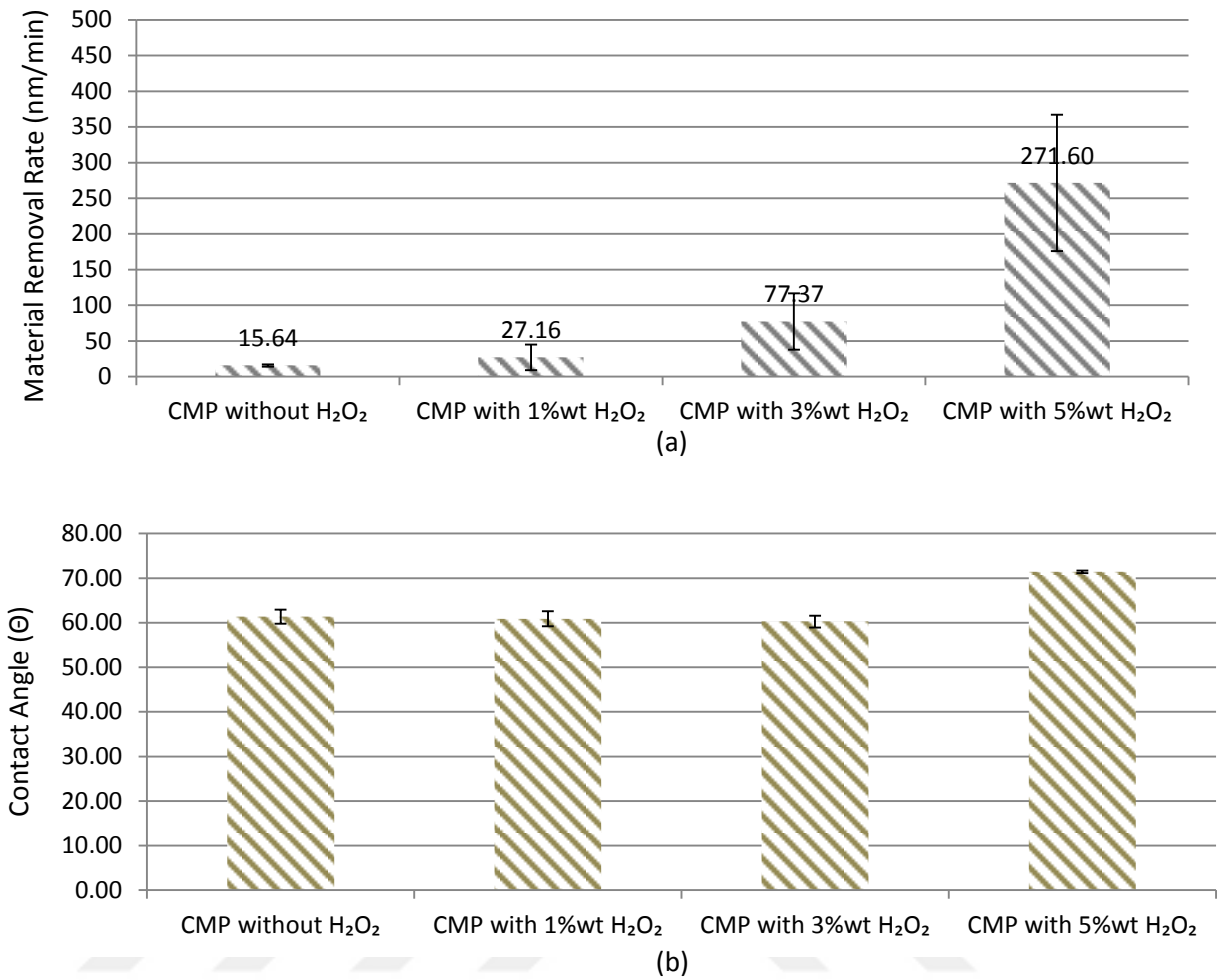

Figure 3.13 CMP performance of the Ti plates as a function of the oxidizer concentration with TiO_2 abrasive containing slurry (a) material removal rate and (b) contact angle.

The concentration of the H_2O_2 affected the oxidation reaction and hence increased oxidizer concentration increased the wettability response due to the thick oxide film formation since oxides are known to be more wettable. Optimal concentration of the oxidizer ensures a passive film formation on the metal surface. 3wt% H_2O_2 containing CMP treatment ensures lower material removal rate due to passivation of the surface which is also verified by lower wettability response with the SBF solution. The characterization of the formed native oxide film will be discussed in the next chapter more in detail.

In addition to MRR and wettability responses, surface topography analyses were also evaluated through roughness measurements. Figure 3.14 gives the RMS, Ra and Rz values of the CMP treated titanium samples in the presence of the oxidizer as compared to the bare sample. Baseline sample showed a higher roughness value due to the thick and porous anodized oxide layer as compared to the CMP treated samples. All three methods of roughness measurements are in good agreement for the samples polished with CMP treatment. The increased oxidizer concentration resulted in negligible change in the roughness values of the titanium films.

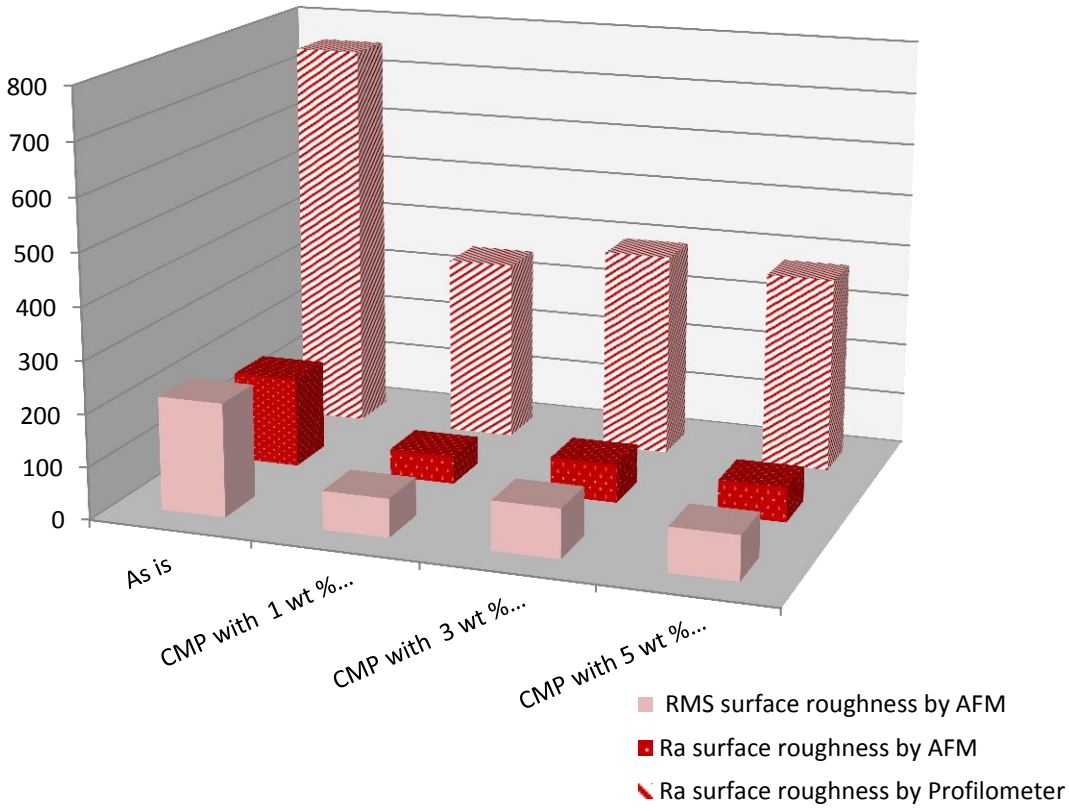

Figure 3.14 Surface roughness evaluation based on RMS, Ra and Rz evaluation polished of Ti with Al_2O_3 slurry as a function of the oxidizer concentration.

3.3.1.3 Effect of polishing pad

After evaluating the effect of slurry abrasive type and oxidizer concentration, the pad materials were also evaluating as they relate to the CMP performance. Control of the CMP variables such as slurry, oxidizer type and dosage and pad type enable the control of surface properties post CMP. In the case of bio-applications, surface nature and biocompatibility relates to surface roughness and wettability performance. Therefore, different pad variables were evaluated in this part of the dissertation with selected optimal slurry particle type (Al_2O_3 at 5wt % solids loading) and oxidizer concentration (3wt% H_2O_2) conditions.

The baseline titanium plates were anodized and hence had a porous oxide layer on the surface as it is seen in Figure 3.1a. In order to understand the impact of the presence of oxide as well as the nature of the oxide film on the titanium surface, initially the baseline sample was subjected to surface characterization and biological evaluations. In addition, another sample was prepared by implementing CMP treatment by using 5 wt% alumina nanoparticle containing slurry at pH 4 without addition of the H_2O_2 oxidizer. This approach tunes the CMP process to function only mechanically and helps remove the surface oxide of the plates and expose the bare titanium without planarization due to the lack of chemical component. In addition, CMP was performed in the presence of oxidizer addition to the alumina slurries at 3 wt% H_2O_2 concentration. This helped comparing the titanium oxide films which form during the CMP process to the baseline anodized oxide film in terms of bioactivity performance. In these preliminary CMP evaluations, a relatively soft polytex buff-pad was used on top of a SUBA IV subpad to provide smooth surface finish while protecting the macro scale topography of the surface such as the screw crests and roots of the dental implants. Following these treatments, two types of abrasive papers were also used in place of the polishing pad to induce micro-scale roughness on to the titanium plates. Consequently, five types of sample surfaces were prepared as (i) baseline, (ii) CMP without H_2O_2 which exposes bare titanium surface, (iii) CMP treated in the presence of H_2O_2, (iv) CMP treated in the presence of oxidizer by using 45-μm grid abrasive paper and, (v) CMP treated in the presence of oxidizer by using 90-μm grid abrasive paper.

These five samples were treated and characterized for their CMP responses, surface nature as well as the biological performances. Titanium plates treated with the five conditions as described above were initially characterized for the CMP material removal rate, wettability, and surface topography responses evaluated through surface roughness measurements. Table 3.2 summarizes the post CMP evaluations of the conducted experiments. It can be seen that the material removal rates of the samples polished on the polymeric pads were negligible. Particularly, the CMP test conducted without the addition of oxidizer resulted in only 0.007 μm/min material removal rate. This result is expected since the material removal is driven by the continuous chemical attack on the surface by the oxidizer during the CMP operation. Consequently, when the oxidizer is added into the system, material removal rates within a 0.5–0.9 μm/min range were obtained. On the other hand, polishing with the abrasive papers resulted in much higher removal rates due to the highly pronounced mechanical action provided by the fixed abrasive particles embedded into the polishing papers. Although, this very high level of material removal rates are typically not desired for the CMP applications, it must be noted here once again that the abrasive papers help modulate the surface roughness significantly to understand the effect of roughness on the bio-implant performance.

Table 3.2 Material removal rate, wettability and surface roughness responses of the titanium plate samples treated with five different experimental conditions.

Sample	CMP Conditions		Material Removal Rate (nm/min)	Wettability Contact Angle (θ)	RMS Surface Roughness (nm)	Profilometer Surface Roughness (nm)	
	Time (min)	Pad Type				Ra	Rz
As is	-	-	-	84.4±0.7	486±17	425±40	2660±50
CMP without H_2O_2	2	Polytex pad	7±2	45.6±1.2	205±32	410±20	2570±60
CMP with 3wt.% H_2O_2	2	Polytex pad	505±395	34.3±2.6	128±41	350±30	2470±120
CMP with 3wt.% H_2O_2	2	Ab.P.(45μm)	30113±3039	54.2±0.2	423±56	350±50	2770±60
CMP with 3wt.% H_2O_2	2	Ab.P.(90μm)	37260±3882	65.1±0.7	517±88	540±220	4170±1800

Figure 3.15.a illustrates the trends in the material removal rates of the samples treated with selected CMP conditions. It highlights the much higher removal rates with the abrasive papers. Figure 3.15.b summarizes the contact angle measurements taken with the simulated body fluid on the titanium plates representing the wettability of implant surface in the body environment. The high contact angle value obtained on the untreated baseline titanium sample can be attributed to the surface oxide formed by anodization which has a porous structure [Bic02, Hsu10]. The trapped air in the porous titanium oxide is believed to increase the hydrophobicity of the surface. The CMP process performed without the oxidizer addition resulted in removal of the top oxide layer and exposed the titanium surface with an approximately 45° contact angle measured, which is nearly half of the value measured on the baseline sample (85°). This observation confirms that the thick anodized oxide film was removed from the titanium surface during the polishing with water since the wettability response of the sample changed significantly.

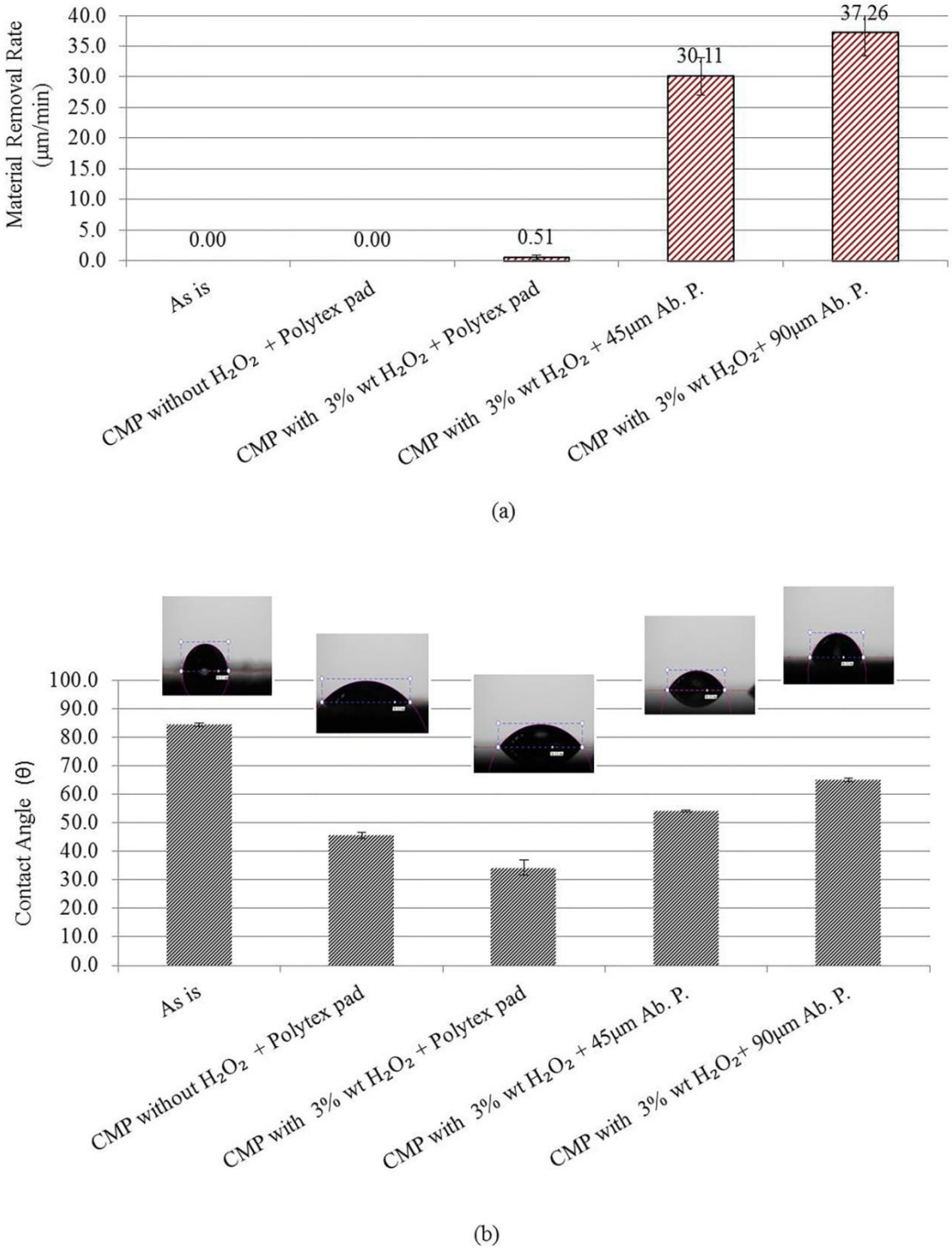

Figure 3.15 Results of the (a) material removal rate and (b) surface wettability of the baseline and CMP treated Ti plates.

The decrease in the contact angle of the bare titanium surface can be attributed to the higher surface energy of the freshly exposed titanium atoms resulting in higher interaction with the water molecules that leads to higher surface wettability and hence a decrease in the contact angle value. In the following treatments where CMP was conducted in the presence of an oxidizer, the effect of surface roughness on the contact angle response started to dominate in parallel to the observations in the literature [Kur05, Mir07].

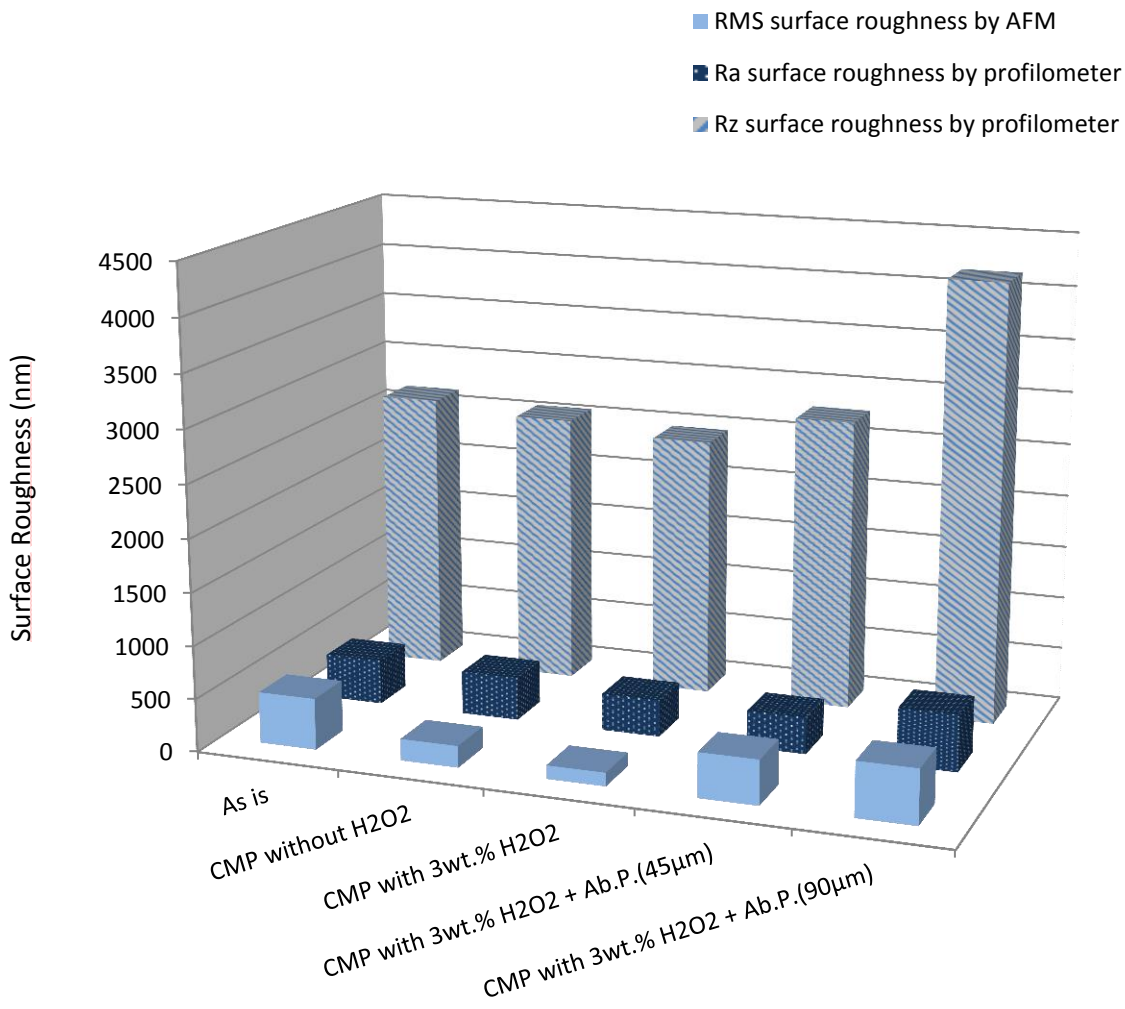

Figure 3.16 Surface roughness evaluations based on RMS, Ra and Rz values of Ti treated with Al_2O_3 slurry with different pad types.

Figure 3.16 gives the surface roughness values of the samples treated with the five different experimental conditions (4 mm profilometer range and 10×10 μm surface scans averaged on three samples). As summarized in Table 3.2 the original sample had a high root mean square (RMS) surface roughness (~486 nm) that can be attributed to the porous oxide layer formed by anodization. When the surface was buffed with CMP without the addition of the H_2O_2, the porous surface oxide was removed and the surface topography reduced to~205 nm. CMP process in the presence of the oxidizer at 3wt% and using the polytex buff pad further reduced the surface roughness to ~128 nm, achieving a smoother surface finish. When the abrasive papers were used, on the other hand, surface roughness increased as the grid size increased reaching up to ~517 nm with 90 μm grit size paper.

The larger scale roughness measurements conducted with the profilometer were consistent with the AFM roughness values on the rougher samples including the baseline sample and the samples processed with CMP by using the abrasive papers. As it is detailed in Figure 3.16 and Table 3.2, the baseline sample was measured to have an rms of 486 nm by AFM and ~ 425 nm (Ra) by the profilometer. These values are statistically the same. However, for the samples processed by using the soft polishing pad in the absence and the presence of the oxidizer, AFM roughness values were reported as ~205 nm and ~128 nm, while the profilometer roughness were measured as ~410 nm and ~350 nm, respectively. For these smoother samples, the local roughness measurements by AFM are giving lower roughness measurements as compared to the larger scale measurements by the profilometer. Consequently, the results are statistically different. Yet, this finding is supporting the outcome that the CMP treatment by the smooth pad usage is decreasing the surface roughness locally while still protecting the global curvature of the sample as desired. This result is also

confirmed by the Rz measurements taken by the profilometer, in that, the average roughness heights are comparable for the relatively smoother samples (~2400–2800 nm) yet the sample treated by using the largest grid abrasive paper had a Rz value of 4170 nm. These results further support the utilization of CMP as a method to control the surface roughness to enable the surface tuning for the needed biocompatibility.

Figure 3.17 shows the AFM micrographs and corresponding cross sectional analyses of the titanium plates treated by selected five different experimental conditions. Here, it can be seen that the surfaces with a smoother surface finish, such as in the case of CMP application in the presence of the oxidizer, resulted in more wettability and hence a lower contact angle. Yet the surfaces with the induced micro-roughness (such as the samples polished with abrasive papers) resulted in a higher contact angle that can be attributed to the lowered wettability through the trapped air pockets within the grooves on the surface. One more important factor that can be observed by comparing the micrographs in Figure 3.17 is that, the CMP of the surfaces by using the soft polytex pad helps smoothen the surfaces locally while protecting the macro scale topography. This effect can be seen when the cross-sectional profiles of the baseline sample and the CMP treated sample are compared.

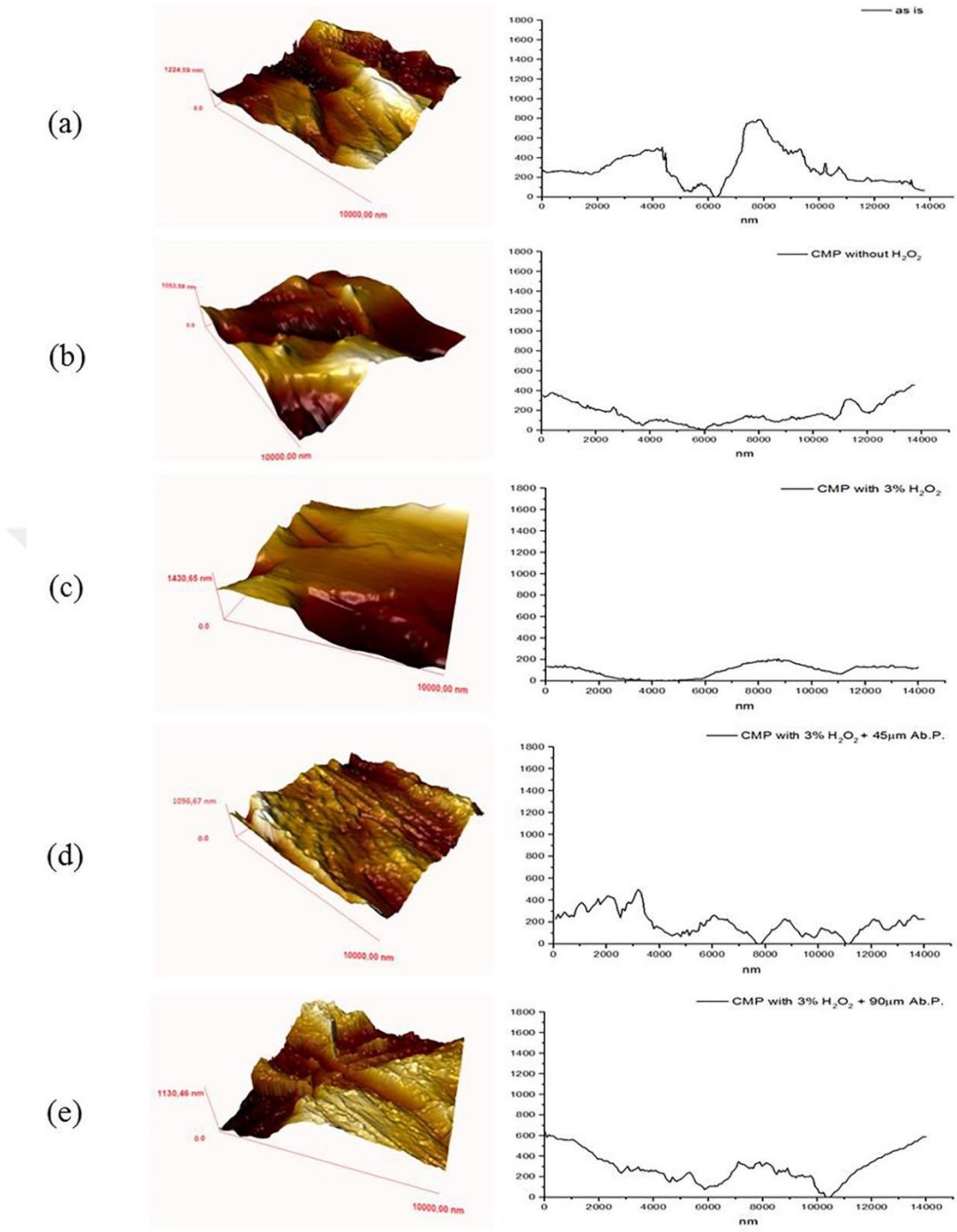

Figure 3.17 Post CMP treatment AFM micrographs and pre and post CMP cross sectional images of the titanium plates (a) as received baseline sample (b) post CMP without oxidizer (c) post CMP with 3% H_2O_2 oxidizer (d) post CMP with 3% H_2O_2 oxidizer with 45µm grit abrasive paper and (e) post CMP with 3% H_2O_2 oxidizer with 90µm grit abrasive paper.

3.3.2 Evaluations of Mechanical Properties for 2D Samples

Since CMP process has a mechanical impact, mechanical properties of the metal surfaces exposed to CMP may change during the treatment. In order to evaluate to mechanical properties of the samples which were exposed to CMP treatment, they were examined with Vickers hardness measurements and tensile tests as compared to the baseline sample.

3.3.2.1 Hardness measurements

Vickers hardness measurement values taken on the CMP induced samples shows higher hardness values as compared to bare titanium sample as shown in Figure 3.18. Indeed, CMP process resulted in work hardening effect on the Ti samples during the polishing because of the mechanical action. In addition, hardness results showed similar values even through different removal mechanism were active during the process. When a soft pad is used with a nano-sized abrasives, the contact angle mechanism is active due to the promoted chemical activity in CMP process. Yet, when the harsh abrasive papers are used, the indent volume mechanism takes over which is more mechanically pronounced as can be seen in the Figure 3.19 schematically.

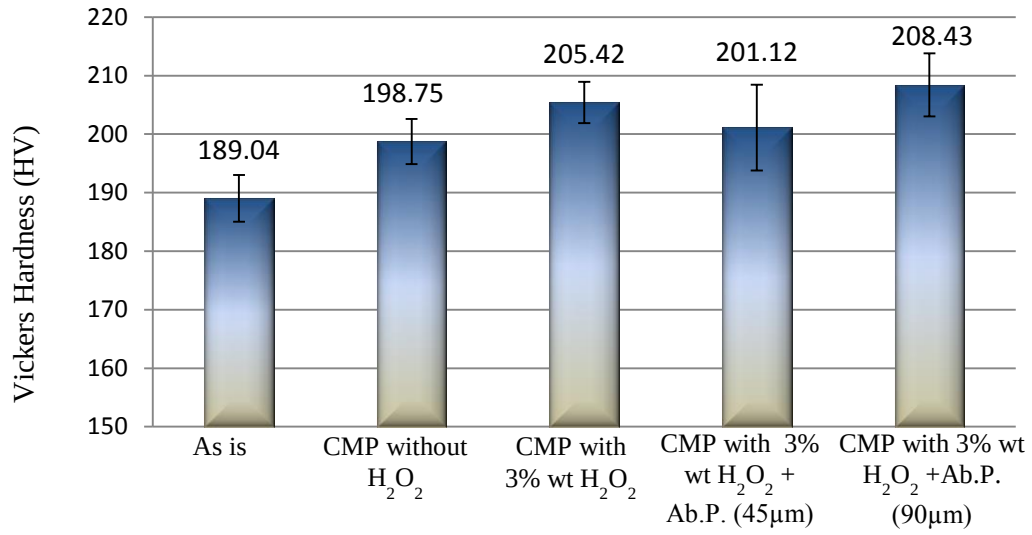

Figure 3.18 Micro hardness evaluations of CMP applied surfaces by Vickers Hardness.

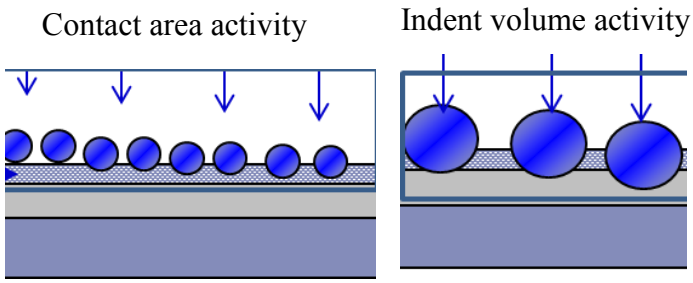

Figure 3.19 Schematics of removal mechanisms

3.3.2.2 Tensile strength testing

Tensile strength measurements were conducted on the CMP treated samples as compared to baseline samples. Samples were cut to the specifications of the tensile strength tool measurement holder on which CMP test were implemented under different conditions. Figure 3.20 gives the stress/strain measurements of the samples. Elastic modulus of the titanium samples vary with the implemented CMP treatment type. Highest elastic modulus value was obtained on the CMP sample treated in the presence of the oxidizer. Its modulus was 33.5 GPa while the lowest value of 13.5 GPa was observed on the sample treated with the coarse abrasive paper as expected. Elastic modulus values calculated according to equation (3.1) and summarized in Table 3.3. The decrease in the yield strength of the rougher samples can be attributed to the modulated surface roughness acting as the stress concentration point while the higher elastic modulus on the smoother surfaces can be attributed to the more effective cold working activity when the small size abrasive particles are used for the regular CMP applications.

$$E_{[MPa],[psi]} = \frac{stress}{strain} \qquad [\, Stress = {}^{F}/_{A},\ Strain = {}^{dL}/_{L}\,] \tag{3.1}$$

Table 3.3 Modulus of elasticity values of the samples

Sample	Elastic Modulus (GPa)
Baseline	31.9
CMP without H2O2	29.8
CMP with 3% wt H2O2	33.5
CMP with 3% wt H2O2 + 45 µm Ab.P.	27.2
CMP with 3% wt H2O2 + 90 µm Ab.P.	13.5

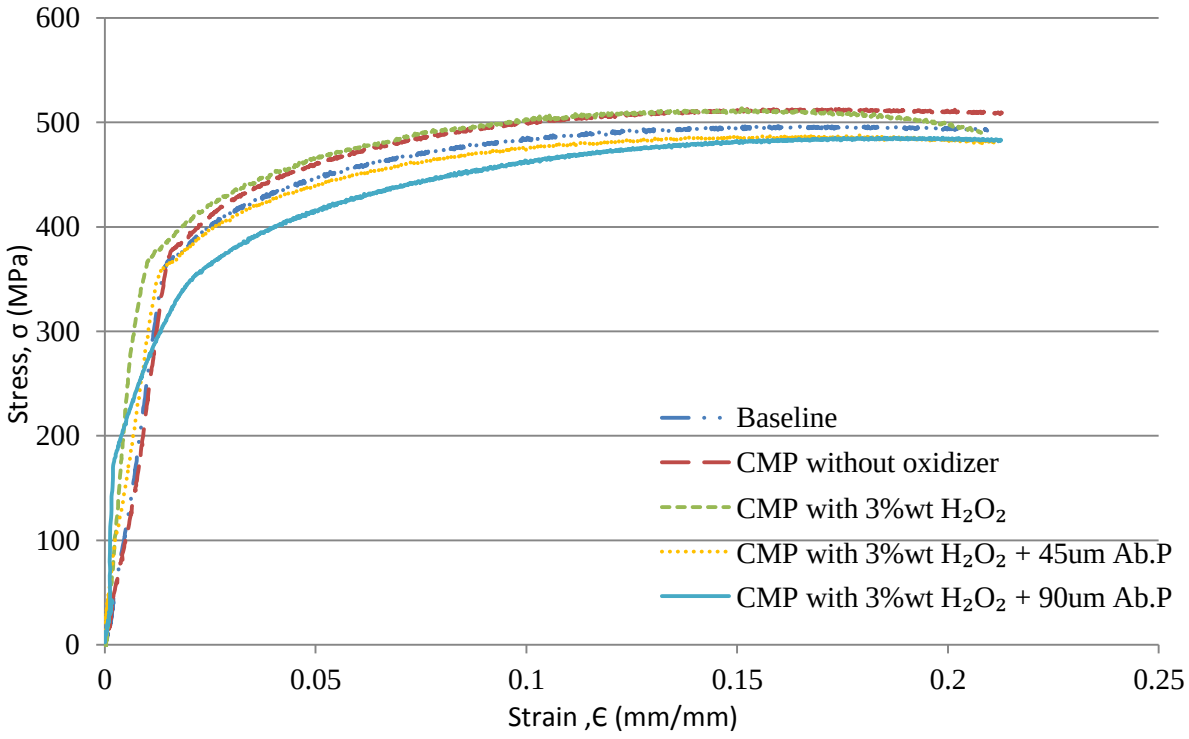

Figure 3.20 Stress versus strain plots of the CMP implemented surfaces as compared to the baseline sample.

3.3.3 Material Removal Rate Response for the 3D Implant Samples

In scope of this dissertation, CMP treatment is suggested as an alternative method for implant material surface engineering. Hence, beyond the preliminary testing on the titanium plates, titanium dental implants were also treated according to the pre-selected CMP conditions.

3.3.3.1 Effect of slurry abrasive particles

Among the slurry particles tested for titanium plates (Al_2O_3, SiO_2 and TiO_2), TiO_2 was neglected in this part due to its affinity of sticking particles on the surface. Figure 3.21 gives the material removal rate and wettability performances of the treated dental implants in the presence of the 3%wt H_2O_2 with silica and alumina based slurries. Silica (SiO_2) based CMP slurry showed slightly higher material removal rates as compared to the alumina (Al_2O_3) slurry. On the other hand, wettability performance of the 5wt% Al_2O_3 slurry was lower with 61.88° contact angle indicating a hydrophilic surface nature formation.

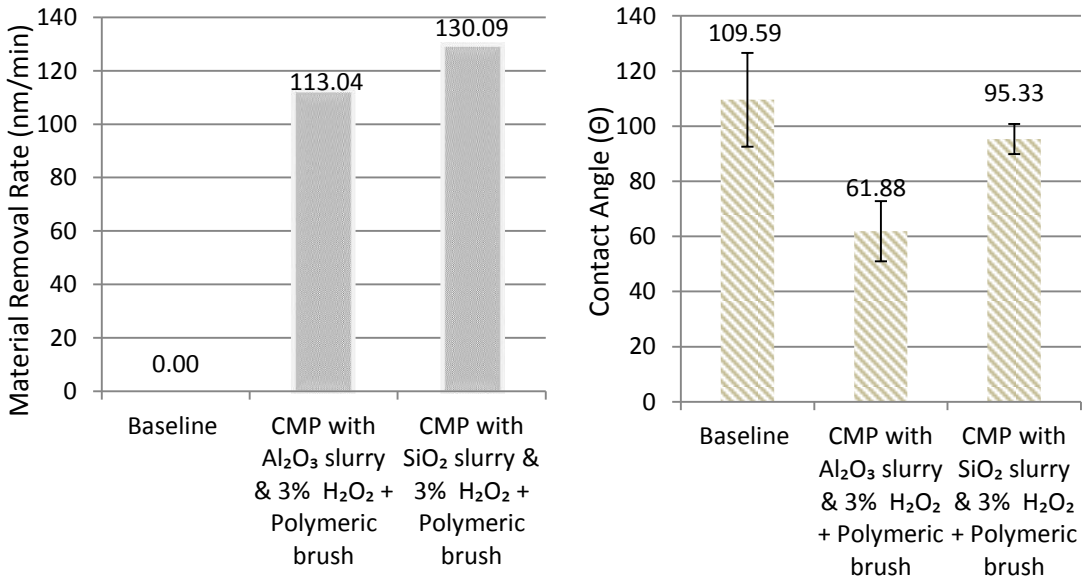

Figure 3.21 Material removal rate and wettability performance of CMP treated titanium dental implants in the presence of 3 wt% H_2O_2 by using 5%wt Al_2O_3 and SiO_2 slurries.

3.3.3.2 Effect of slurry oxidizer concentration

The effect of oxidizer concentration was also investigated on the machined dental implants by using 5wt% Al_2O_3 slurry. Furthermore, to evaluate the effect of the oxidizer directly, etching process was applied to the samples at 3wt% and 30wt% H_2O_2 concentrations. Furthermore, the CMP treated samples (at optimal conditions) were also exposed to dipping process at 3 wt% and 30 wt% concentrations. Figure 3.22 gives the material removal rates of the etched samples with respect to the contact angle values. Removal rate values of the samples showed increase with the higher oxidizer concentration due to the formation and delamination of the porous and non-stable oxide layer. Lowest material removal rate, 17.87nm/min value was obtained after the CMP treatment in the absence of the H_2O_2, as expected. This is due to the protective nature of the surface oxide film. Dissolution of the material from the metal surface increased when the CMP treatment was followed by the chemical dissolution. On the other hand, wettability evaluations of the treated surfaces showed that strong etching process with 30 wt % H_2O_2 has the highest contact angle value 140.00° which is highly hydrophobic. Etching process with 30wt% H_2O_2 has resulted in increased surface hydrophobicity as compared to the baseline and CMP treated samples. Surface finishing with the CMP process in the presence of 3wt% H_2O_2 and 3wt% H_2O_2 etching showed the lowest wettability response among all the samples and they responded hydrophilic against the SBF solution.

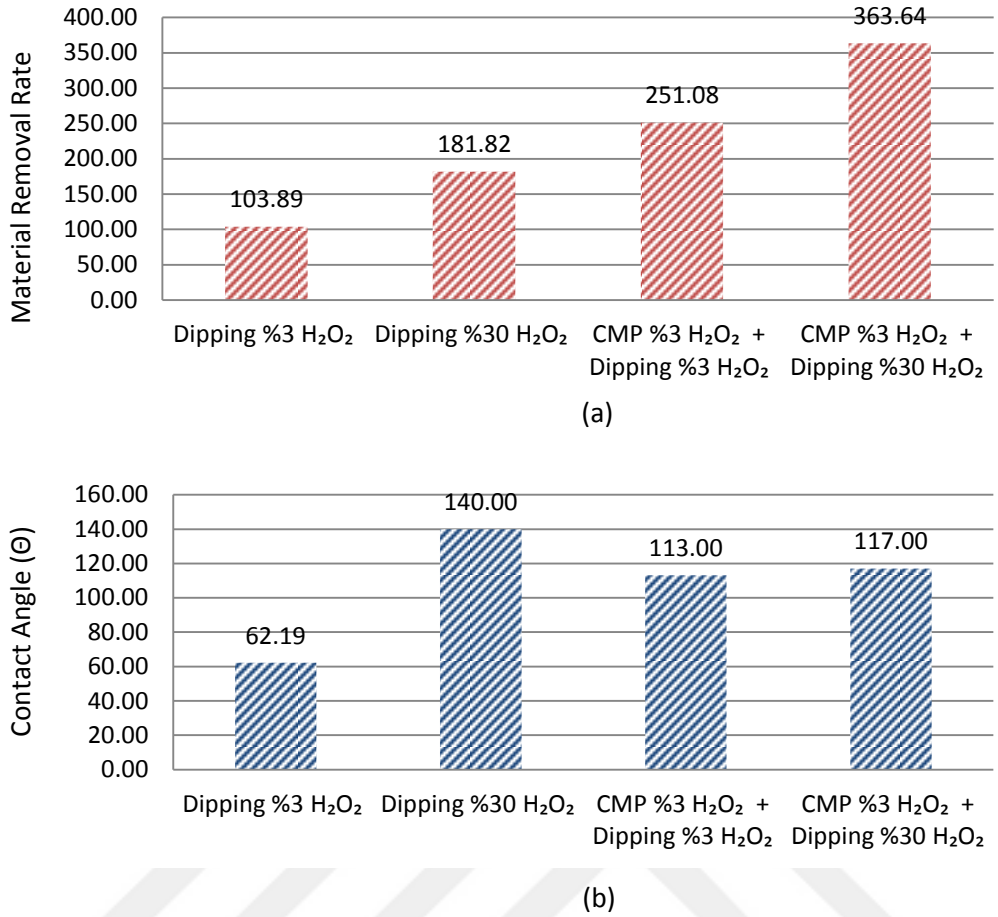

Figure 3.22 Material removal rates and wettability performance of etched and CMP treated titanium dental implants

3.3.3.3 Effect of pad type on CMP performance of 3-D Implants

Figure 3.23 summarizes the CMP performance of the 3-D dental implant samples when different pads were used in preperation. The same experimental procedure was followed on the 3-D dental implant samples by replacing the polymeric pad with a polymeric brush and hand polishing the samples all over their exposed surfaces with the alumina based polishing slurry. CMP performances were evaluated based on the material removal rates measured by the change in unit volume as a function of time and also measuring the wettability responses of the implant surfaces on a pre-selected region where the screw pitch is the same. It can be observed that both the material removal rate responses (Figure 3.23.a) and the wettability results maintained the same trend as observed on the titanium plates. These results are encouraging in that the biological responses of the 3-D implants are expected to be similar to the 2-D equivalents.

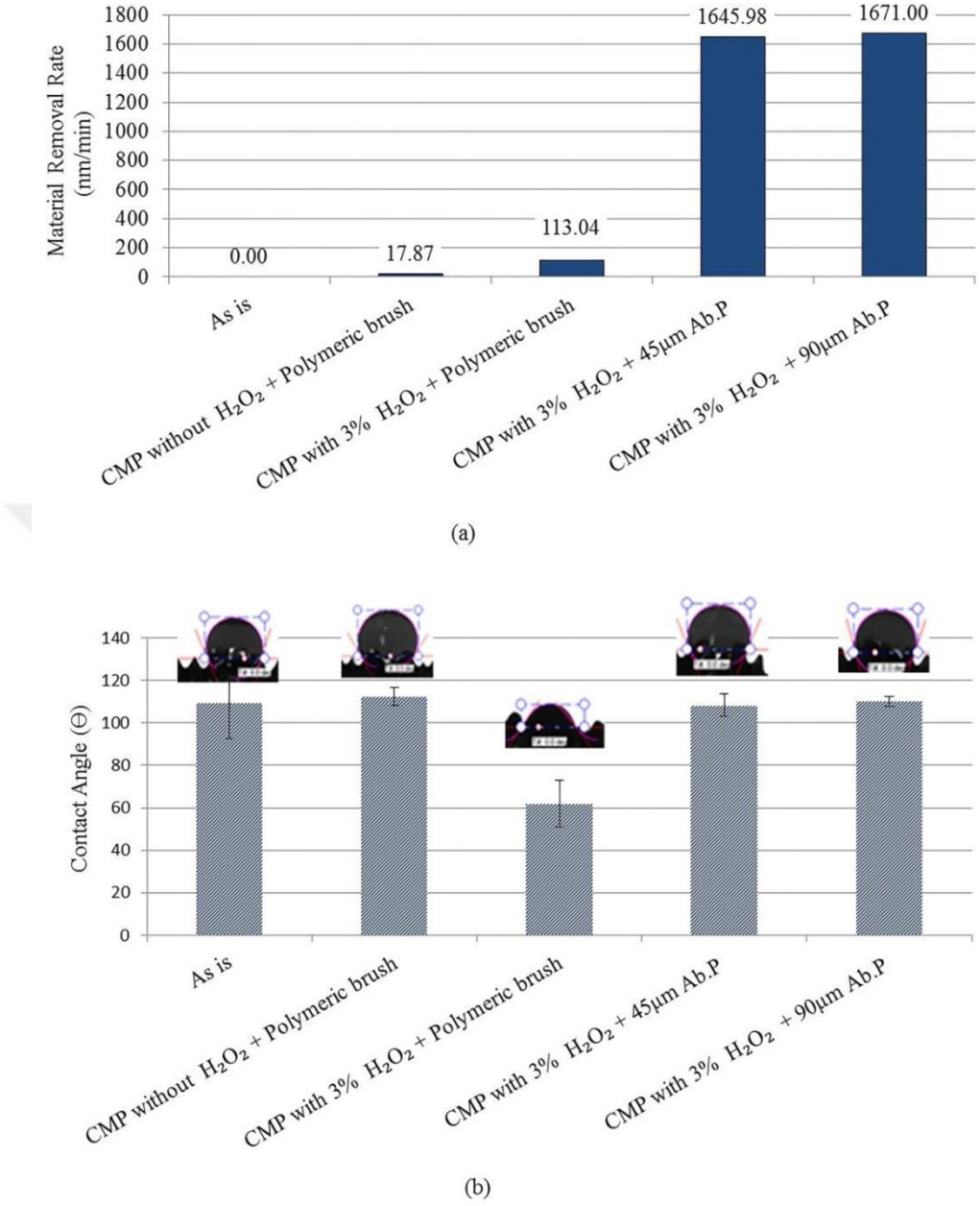

Figure 3.23 CMP performance of the 3-D dental implants (a) material removal rate analyses and, (b) wettability responses post CMP treatment.

3.4 Summary

In this chapter we examined CMP process as an alternative technique to engineer the titanium based implant surfaces to induce smoothness or controlled surface roughness while simultaneously forming an oxide layer which will be examined with detail in the next chapter. The impact of the CMP process variables were evaluated by using Al_2O_3, TiO_2 and SiO_2 based slurries at different oxidizer concentrations. To modulate the surface roughness, in addition to general CMP pad materials, SiC abrasive papers with two different particle sizes were used in place of the pad material. Material removal rates, surface roughness and wettability analyses showed that the optimal slurry and oxidizer combination for the surface engineering depended on the process variables. In the case of biomaterial application, both of the smooth and roughened surfaces were evaluated as it is discussed in Chapter 5. Furthermore, mechanical properties of the titanium surfaces after the CMP treatment were also examined through Vickers hardness and tensile strength analyses and results showed that CMP implementation did not affect the sample performance significantly. Finally, the application of the CMP on the 3-D dental implant surfaces also resulted in similar CMP responses as compared to the 2-D plates confirming that the CMP application can help enhance the surface properties of the titanium based implants.

CHAPTER IV

NATIVE SURFACE OXIDE FILM FORMATION AND CHARACTERIZATION OF CHEMICAL MECHANICAL POLISHING INDUCED TITANIUM SAMPLES

4.1 Introduction

Titanium tends to form a native oxide layer in air which is similar to the stoichiometric TiO_2 characteristics based on its amorphous and defective nature [Cox92, Gem07]. This native oxide layer helps the biocompatible behavior of the titanium surface [Alb81]. In addition, this oxide film prevents the ion dissolution into the surrounding tissue and promotes the osseointegration due to active bio-ceramic nature [Gem07]. Cell interaction and bone interlocking between the implant material and the tissue depends on the composition, homogeneity, and thickness of the oxide layer [Wen98, Li02]. Furthermore, the mechanical functionality of the implant might also be affected by the properties of the surface oxide. General surface treatment methods tend to result in formation of a thick and porous oxide films, which show decreased biocompatibility and degraded corrosion resistance as compared to thin, homogenous and pore free layers.

In this chapter, the oxide layer which forms on the titanium surface by the CMP treatment has been characterized through X-ray diffraction (XRD), X-ray photoelectron spectroscopy (XPS) and Energy-dispersive X-ray spectroscopy (EDX) analyses in order to understand the chemical composition, morphology and crystal structure of the film. In addition, surface free energy analyses were conducted on the samples through contact

angle measurements to qualify the adhesion propensity of the treated titanium surface in the host tissue [Sam09]. Moreover, protective properties of the oxide layer were evaluated through Pilling-Bedworth Ratio (PBR) calculations, which is an expression of the volume ratios of the oxide layer as compared to the metallic material underneath. Furthermore, electro-kinetic behavior of the surface oxide layer in different oxidizer media was evaluated through potentiostatic measurements in order to simulate the body environment.

4.2 Experimental Analyses

4.2.1 Surface crystallographic structure analyses

In order to analyze the changes in the nature of the very top thin film which is modified by the chemical action of the CMP process, grazing angle GIXRD analyses were conducted by using PANalytical, X'PERT Pro MPD model XRD analyzer. The XRD profiles were collected between 20–80° of 2Θ angles with a step interval of 0.02° using grazing angles for the measurements.

4.2.2 Surface chemical composition analyses

The chemical nature of the titanium surfaces were studied through X-ray photoelectron spectroscopy (XPS) and Energy Dispersive X-ray (EDX) analyses. PHOIBOS HAS 3500 150 R5e XPS [HW Type 30:14] tool was used to compare the electronic states of the Ti2p and O1s of the titanium plates pre and post CMP. Furthermore, EDX analyses were performed on a JEOL JIB-4501 MultiBeam Scanning Electron Microscope (SEM). The titanium peaks were investigated at 0.4 and 4.5 eV energy level and the oxygen peak was analyzed at the 0.525 eV as reference values [Kim08].

4.2.3 Surface energy and Work of adhesion analyses

Surface free energy of the solid material is equal to surface tension of the liquid which is in contact with the solid surface. Surface wettability properties were determined through the contact angle of the liquid which depends on the type of the liquid utilized. In order to determine the surface energy of the treated titanium materials, contact angle measurement based approach was used which involves Lewis acid-base theory [Sam09]. Furthermore, work of adhesion was also evaluated as another useful measure to calculate the adhesion propensity of the surface. Mathematically work of adhesion is expressed as;

$$\gamma_{sl} = \gamma_s + \gamma_l - W_a \qquad (4.1)$$

Where the "W_a", is the work of adhesion and "γ", is the interfacial tension between the considered phases (surface free energy). Subscripts "*s*" and *"l"* stand for the phases for solid and liquid respectively. In order to determine the work of adhesion for a substrate, it requires the measurement of three interfacial tension values. This interfacial tension (surface energy) can be calculated according to Van Oss et. al's suggested theory, which involves the Lifshitzs-van der Waals (LW) and polar acid-base (AB) interactions as given in Equation 4.2;

$$\gamma_s^{tot} = \gamma_s^{LW} + \gamma_s^{AB} \qquad (4.2)$$

The first term on the right hand side is the dispersive component and second one is the polar (acid-base) component, which plays a major role on the surface tension. Polar component of the surface free energy is the geometric mean of two parameters as shown below in Equation 4.3;

$$\gamma_s^{AB} = 2\sqrt{\gamma_s^- \gamma_s^+} \qquad (4.3)$$

where γ^- is the electron donor (Lewis base) and γ^+ is the electron acceptor (Lewis acid) parameter. Combining Equations (4.1), (4.2) and (4.3) results in the Equation (4.4) in which W_a depends on the three components of the surface free energy:

$$W_a = 2\left(\sqrt{\gamma_s^{LW} + \gamma_l^{LW}} + \sqrt{\gamma_s^+ \gamma_l^-} + \sqrt{\gamma_s^- \gamma_l^+}\right) \qquad (4.4)$$

Combining this equation with Young-Dupre equation gives Equation 4.5;

$$\gamma_s = \gamma_l cos\theta + \gamma_{sl} \qquad (4.5)$$

In this part of the study, 1-bromonapthalene (B), ethylene glycol (E), formamide (F), glycerol (G), dimethylsulfoxide (D) and distilled water were used as probe liquids on the titanium substrate. Their total surface tension properties are given in Table 4.1. The sessile drop method was used for contact angle measurements under ambient conditions at room temperature. The contact angles measured at five different points on the material surface and averaged for the calculations. The dispersive component (γ^{LW}) of the total surface energy was calculated as in Equation 4.6;

$$\gamma_s^{LW} = \gamma_l \frac{(1+cos\theta)^2}{4} \qquad (4.6)$$

The electron donor (γ^-), electron acceptor (γ^+) and polar component parameters were calculated according to the McCafferty linear plot method which is a plot of;

$((1 + cos\theta)\gamma_L/2) - (\gamma_s^{LW}\gamma_L^{LW})^{1/2})/\ (\gamma_L^+)^{1/2}$ versus $(\gamma_L^-/\gamma_L^+)^{1/2}$

This plot produced a straight line, where the line slope gives the $(\gamma_s^+)^{1/2}$ and intercept gives the $(\gamma_s^-)^{1/2}$ values [McC02, Bar09]. Following these calculations all the data was inserted into the Equation 4.2 and 4.4 in order to find the surface energy and work of adhesion values.

Table 4.1 Total surface tension and its components of probe liquids (in mN/m) used for contact angle measurements [Sam09]

Liquid	γ^{total}	γ^{LW}	γ^{-}	γ^{+}
1-Bromonaphthalene (B)	44.4	44.4	0	0
Water (W)	72.8	21.8	25.5	25.5
Glycerol (G)	64	34	57.4	3.92
Ethylene glycol (E)	48	29	47	1.92
Formamide (F)	58	39	39.6	2.28
Dimethylsulfoxide (D)	44	36	30	0.5

4.2.3 Surface electrochemical analyses

The electrochemical behavior of the treated samples was also evaluated through potentiostatic and potentiodynamic polarization measurements by using a Gamry Potentiostat/Galvanostat (model 1000 Interface). Titanium samples were placed in a Teflon sample holder on which 10x10mm area was exposed to the electrolyte solution. A conventional three-electrode electrochemical cell was used. Ti plates were used as the working electrode, a platinum (pt) wire was used as the counter electrode and a saturated calomel electrode (SCE) was used as the reference electrode. Different H_2O_2 concentrations (0M= 0wt%, 0.3M=1wt%, 1M=3wt% and 1.6M=5wt%) were used as the electrolyte in 150mL solution volume. The potentiostatic scan period was set to 1100 seconds with an input potential of 0V vs. E_{ref}. Potentiodynamic scans were performed with scan range from -5V to 8V with a scanning speed of 10mV/s and a step of 1mV for each point. All electrochemical tests were carried out at room temperature and under ambient conditions.

4.3 Results and Discussion

4.3.1 Characterization of titanium surface as a function of selected CMP treatment

Ti and its alloys tend to growth an amorphous air-formed TiO_2 oxide layer on top of the substrate [Roe02]. The nature of this oxide layer nature depends on the surface characteristic of the material and the processing technique. It has been documented that oxidation at high temperatures promotes the formation of a crystalline form of the oxide film with increased thickness [Tho97]. The oxide layer formed on the titanium substrate was examined in detail in this chapter as a function of implemented conditions of surface treatment.

4.3.1.1 Characterization of surface oxide film on titanium substrate

Preliminary evaluations were conducted on the titanium samples to shows the difference in the nature of the oxide films between the CMP implemented and mechanically polished samples. Figure 4.1 compares the XRD analysis on the CMP treated and standard polished samples. XRD analysis on standard polishing as compared to the CMP applied Ti samples, showed that CMP treatment generates a different form of oxide layer on the Ti sample surfaces.

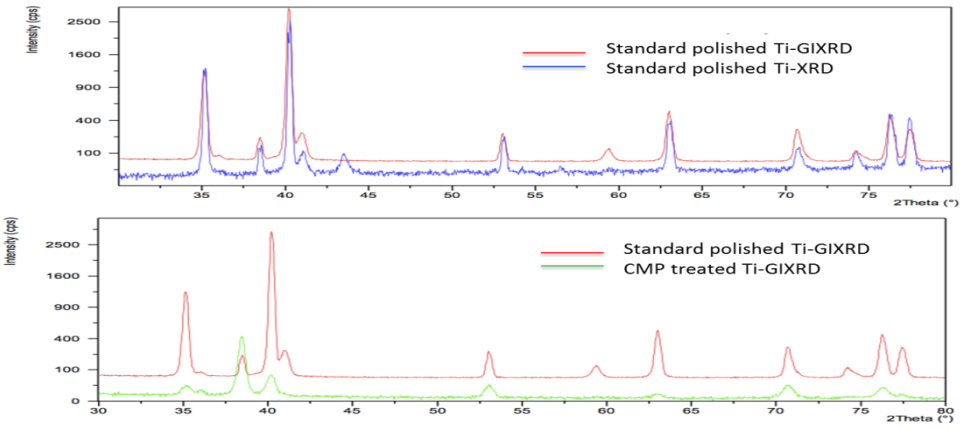

Figure 4.1 XRD analysis on titanium with Mechanical Polishing vs CMP treatment.

The nature of the surface oxide forming on the titanium plates was characterized for elemental composition as well as for the crystal structure. In order to determine the elemental composition, XPS analyses were performed. Furthermore, the changes in the crystallographic nature of the titanium surface in the absence and presence of the oxidizer in the CMP slurries were analyzed by XRD analyses to understand the protective nature of the surface oxide. Figure 4.2 shows the XPS spectrum of CMP treated titanium plates in the absence (only by using water in the CMP slurry) and presence of 3wt% H_2O_2 at the 2p orbital region of the titanium (Ti2p-region), and the 1s orbital region of the oxygen (O1s-region). This analysis was conducted to determine the changes in the intensities of the typical titanium and the oxygen peaks of the titanium plates as they are known to confirm the protective oxide formation on the surface [Oka09]. A prominent Ti 2p3/2 peak was observed at 459 eV region (Figure 4.2.a), which corresponds to the binding energy of Ti 2p3/2peak conformed to that of Ti in TiO2. Similarly, O 1s peak is positioned at the 530–535 eV region as seen in Figure 4.2.b, which can be assigned to the three chemical components of oxygen namely (i) the lattice oxygen O^{2-} (530.3 eV), (ii) the bridging and terminal OH^- (532.0 eV) and (iii) the adsorbed H_2O peaks (533.2 eV) [Lee12, Mob09]. The samples polished by CMP in the presence of the oxidizer showed a higher intensity of the O1s peak relative to the samples polished by using only water in the slurry as seen in Figure 4.2 b. Yet, the Ti 2p3/2 peaks of the titanium overlapped for both samples as seen in Figure 4.2 a. These results confirm the surface oxidation of the titanium plates when the oxidizer is used in the CMP slurry and indicate the formation of a protective oxide on the surface of the titanium [Var08, SaM99].

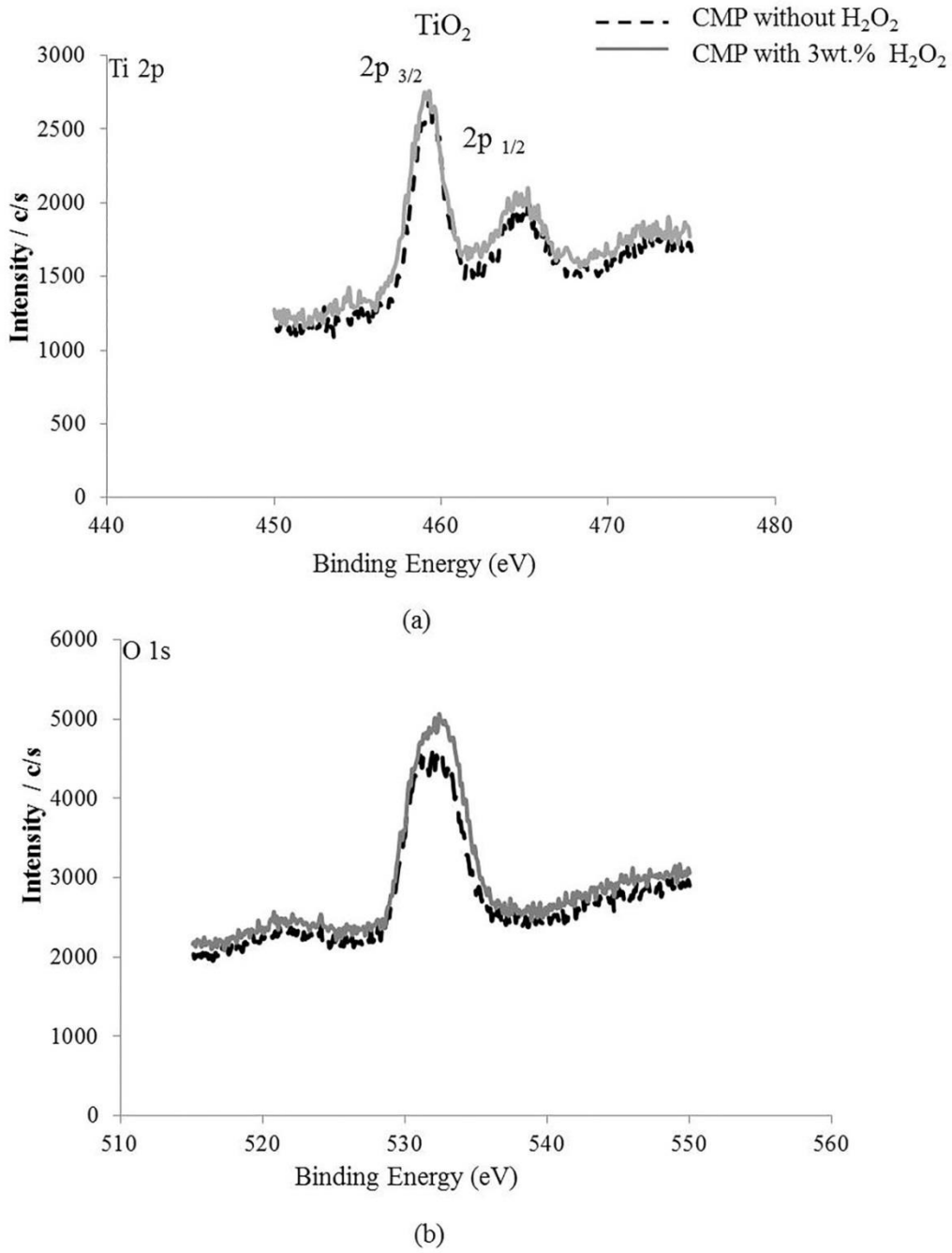

Figure 4.2 XPS spectrum of CMP treated titanium plates in the absence (only by using water in the slurry) and presence of 3 wt% H_2O_2 at (a) the Ti2p region and, (b) the O1s region.

Figure 4.3 shows the EDX analyses performed on the CMP treated samples in the presence and absence of the oxidizer with the soft pad. The results showed the surfaces of both samples are composed of titanium and oxygen. The net value of the oxygen was 5.30% on the sample treated with CMP by using only water, whereas the surface treated with CMP in the presence of oxidizer had a value of 9.02% as summarized in Table 4.2. As expected, the sample treated in the presence of oxidizer had a higher net value of oxygen and the corresponding titanium percentage was relatively lower in agreement with the XPS results.

Table 4.2 EDX analyses results on CMP applied Ti plate samples in the absence and presence of H_2O_2 as an oxidizer.

Sample	Element	Net	Nor. C (wt. %)	Atom C. (at.%)
CMP without H_2O_2	Titanium	19954	93.95	84.49
	Oxygen	1145	5.35	14.39
CMP with 3wt.% H_2O_2	Titanium	17997	88.01	72.94
	Oxygen	2045	9.33	23.15

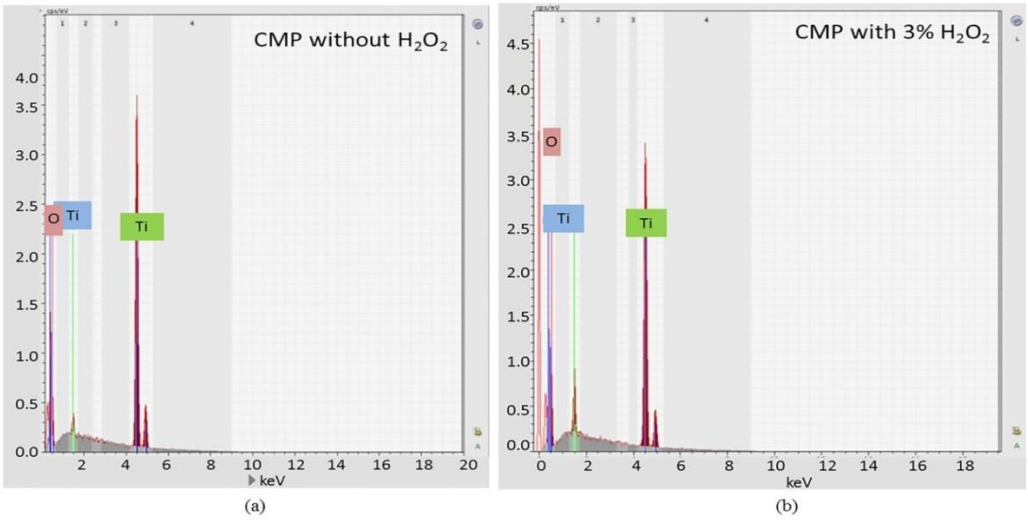

Figure 4.3 EDX analyses on the titanium samples CMP treated with water only suspension versus with the addition of 3% H_2O_2

In order to verify the protective nature of the CMP induced titanium oxide, the changes in the surface crystallographic nature of the titanium plates exposed to CMP treatment with and without the oxidizer addition were also studied by grazing angle X-ray diffraction analyses. This technique has the advantage of focusing on the thin film region of the sample surface and hence can give a precise comparison of the oxide thin film crystal structure forming during the CMP process. As it can be seen in Figure 4.4, when hydrogen peroxide is added into the CMP slurries, the relative intensity of the Ti peak reduced by 23% from 175 to 135, while the relative intensity of the titanium oxide peak (the anatase form of titania) [Hsu10] increased by 17% from 410 to 480. This data further agrees with the formation of a thin film of oxide layer on the surface of titanium plate when it is treated with the oxidizer in the slurries during the CMP process.

It can be concluded that a denser film of titania is formed when oxidizer is used as compared to the sample CMP treated by using only water. This is due to the faster conversion of the titanium atoms into titanium dioxide in the presence of the H_2O_2 by oxidation reaction enhancing the protective nature of the oxide film on the implant material surface [Ila05, Nat10].

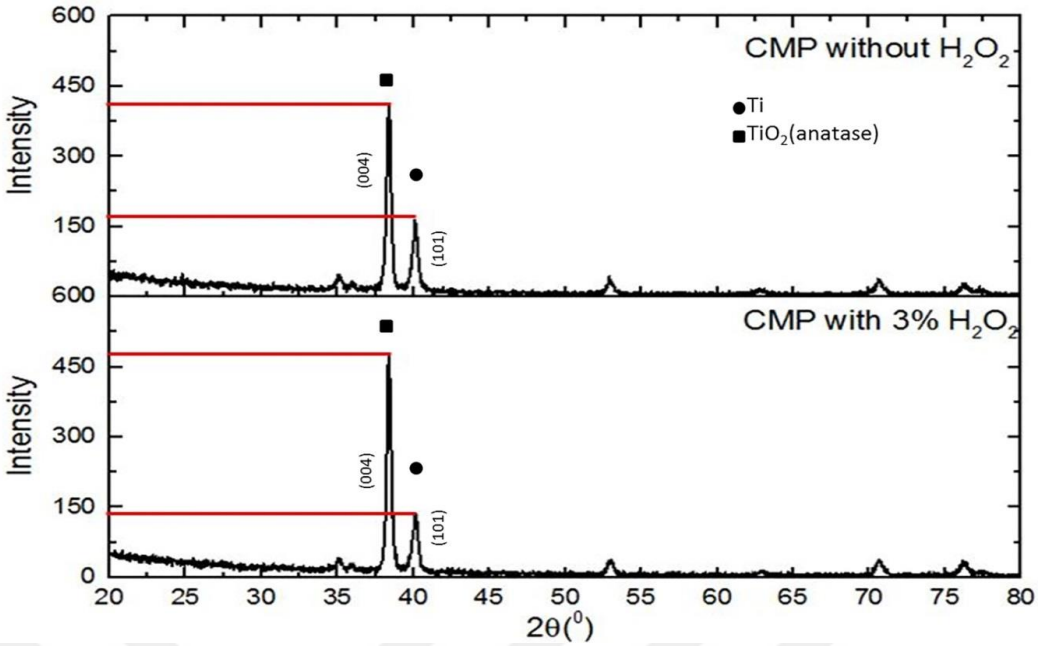

Figure 4.4 XRD analyses on the titanium samples CMP treated with water only suspension versus with the addition of 3% H_2O_2.

4.3.1.2 Surface energy analyses on the baseline and CMP implemented samples

Surface wettability of the implantable materials has a significant effect in its adaptability in a biological system. The nature of the surface hydration force directs the healing process with adsorption and cell adhesion promotion [Eug05, Suc07]. Cells have a negative surface charge naturally which directly affects the work of adhesion performance between the cells and the substrate material [Vog98]. The average contact angle values obtained with all the selected probe liquids are given in Figure 4.5. As it can be seen in the figure, all the liquids showed reproducible wettability hence hydrophilic performance. Glycerol gave the highest contact angle values due to high surface energy values followed by the DI water. Also, Figure 4.5 indicates that there is a little decrease in the contact angle values with increasing roughness. Surface energy and work of adhesion performances of the samples were also evaluated using the contact angle data by using equations given in section 4.2.3, previously.

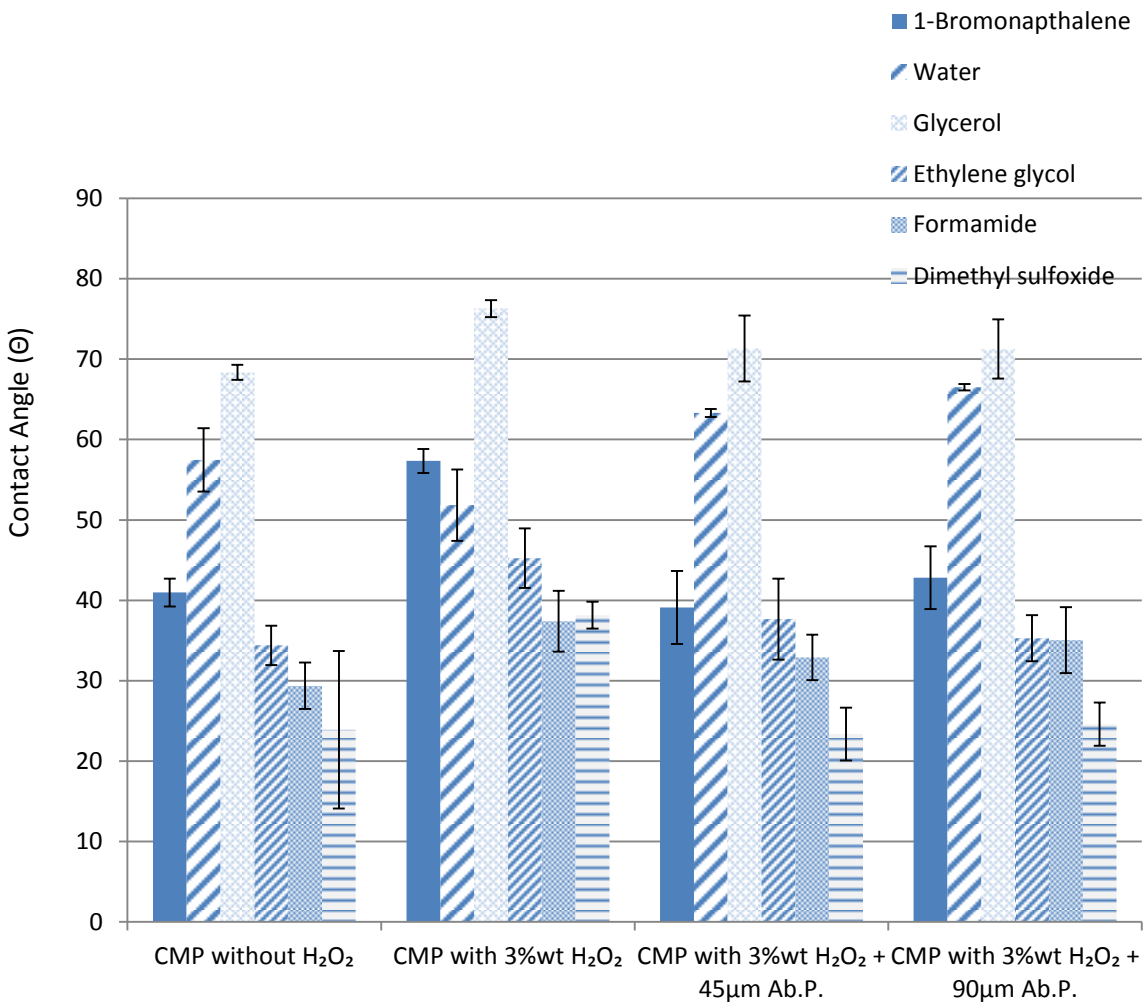

Figure 4.5 Contact angle values obtained with the six probe liquids as a function of titanium surface treatment.

In order to predict the cell responses in the human body (in vivo), surface free energy and work of adhesion performances were analyzed in more detail. Figure 4.5 summarizes the calculated surface free energy and work of adhesion responses of the titanium surfaces. Highest surface energy values obtained with the standard CMP implemented sample with ~66.19 J/m^2 value as can be seen in Figure 4.6.a. The surface free energy values decreased with increased surface roughness value. The lowest surface energy data obtained with the samples on which CMP was implemented by using the coarse abrasive papers to induce micro scale roughness to the surfaces.

The increased surface roughness values resulted in increased contact angle values with DIW as can be seen from the contact angle data in Figure 4.5. However, increased contact angle data resulted in decreased surface energy responses when Figure 4.5 is compared to Figure 4.6.a. On the other hand, work of adhesion data shows correlation with the surface energy response as can be seen in the Figure 4.6 and Figure 4.6.b shows the reduced adhesion performance with the induced roughness values. These trends are expected to correlate to the surface healing performances of the titanium surfaces in vivo.

In general, the cell response (in the case of aqueous media) is expected to increase with the decreasing surface energy. The wettability, which forms surface energy and work of adhesion evaluations based on the contact angle measurements vary with the type of surface oxide film which forms on top of the titanium surface. The intrinsic factors such as hydroxyl groups on the surface mainly influence the surface energy response. However, beyond the intrinsic factors, extrinsic factors such as surface roughness also have a great contribution on the surface energy and adhesion responses. In the following chapter, response of the fibroblast and osteoblast cells will be evaluated according to the adhesion properties on the treated samples.

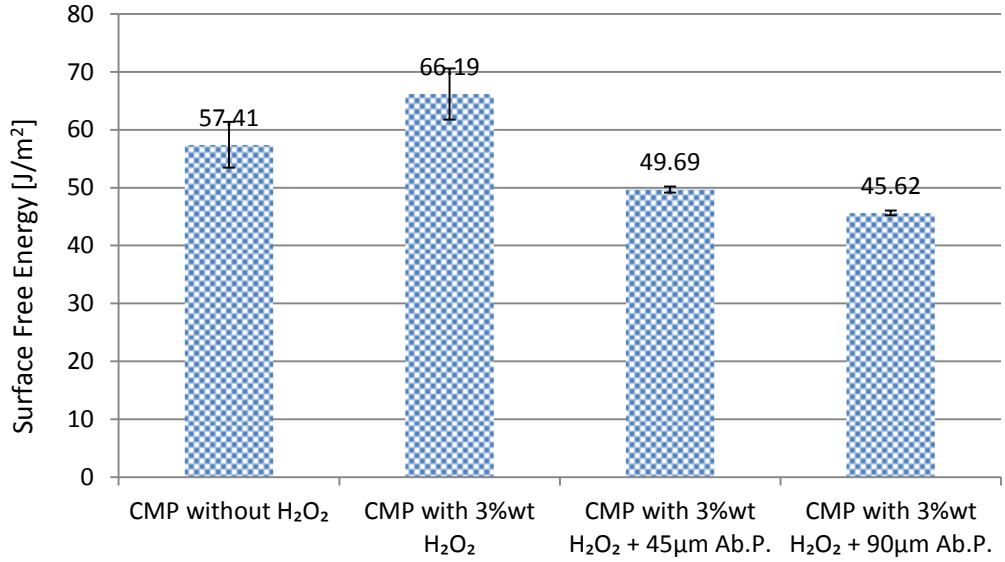

(a)

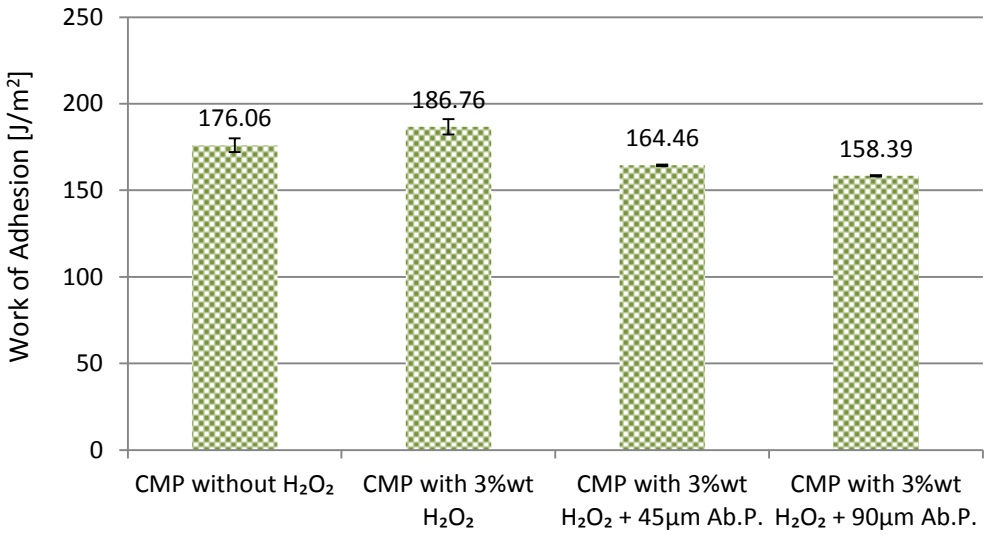

(b)

Figure 4.6 Surface responses of the treated samples via (a) surface free energy (J/m^2) and (b) work of adhesion (J/m^2) calculations based on the measurements given in Figure 4.5

4.3.1.3 Effect of oxidizer concentration on the protective nature of the titanium oxide layer

Table 4.3 summarizes the XRR results of the treated titanium samples as a function of the thickness, density and roughness of the layers treated with the CMP process in the presence and the absence of the H_2O_2. In addition, etching treated sample was also evaluated through the XRR analyses as compared to the CMP implemented samples. The data shows that a multilayer structure is observed on the sample surfaces after the CMP treatment. The structural analyses suggested that an intermediate layer is formed which is mainly titanium dioxide and taken as the baseline on the measured density value. However, beyond the intermediate layer, the very top oxide layer on the substrate also contains TiO_2 film formation with potential contaminations. We assumed that the reason of this contamination is due to the porosity on the top surface layer. Table 4.3 suggests that a porous structure is formed on the top layer of the titanium substrate as concluded from the lower density data measured from the XRR analyses. Porosity content of each layer was calculated according to Equation 4.7 and the obtained porosity values are summarized on Table 4.4.

$$Porosity(\%) = \left(1 - \frac{\rho_a}{\rho_c}\right) \times 100\% \qquad (4.7)$$

Table 4.4 shows that the top layer of the titanium samples has higher porosity ratio as compared to the bottom layers (the bulk material was assumed to have a pore free structure). CMP implemented samples's porosity ratios were closer to each other, which can be attributed to the uniform surface treatment. Furthermore, Figure 4.7 gives the XRR curves of the treated sample film structures. When we compare the CMP process with etch treatment XRR results, there is a clear difference on the formation of the oxide layer when the samples were dipped into 30% H_2O_2. All these values were

than used to calculate the Pilling Bedworth ratios in between each layer as reported in Tables 4.3 and 4.4.

Table 4.3 XRR data of the CMP implemented titanium as compared to the etched samples (through dipping) with density (D), Thickness (T) and Roughness(R) values.

	CMP without H_2O_2			CMP with 1 wt % H_2O_2			CMP with 3 wt % H_2O_2			CMP with 5 wt % H_2O_2			Etching with 30 wt % H_2O_2		
	D *(g/cm^3)*	T *(nm)*	R *(nm)*	D *(g/cm^3)*	T *(nm)*	R *(nm)*	D *(g/cm^3)*	T *(nm)*	R *(nm)*	D *(g/cm^3)*	T *(nm)*	R *(nm)*	D *(g/cm^3)*	T *(nm)*	R *(nm)*
Layer 1	1.95	1.31	0.65	2.51	1.42	0.69	2.54	1.52	0.68	2.63	1.55	1.32	3.33	1.18	1.78
Layer 0	3.21	2.52	0.43	3.26	2.27	0.42	3.27	2.19	0.25	3.51	3.49	0.60	3.61	3.65	0.3
Ti substrate	4.04	$6x10^5$	0.4	4.11	$6x10^5$	0.4	4.02	$6x10^5$	0.4	4.12	$6x10^5$	0.4	4.13	$6x10^5$	0.4

Table 4.4 Composition of the surface layers based on the XRR measurements

		CMP without H_2O_2	CMP with 1 wt % H_2O_2	CMP with 3 wt % H_2O_2	CMP with 5 wt % H_2O_2	Etching with 30 wt % H_2O_2
	Composition	% Ratio	% Ratio	% Ratio	% Ratio	% Ratio
Layer 1	Porosity	48	33	32	30	12
	TiO_2	52	67	68	70	88
Layer 0	Porosity	25	22	22	17	11
	TiO_2	21	36	35	29	57
	Ti	54	42	43	43	32
Ti substrate	Ti	100	100	100	100	100

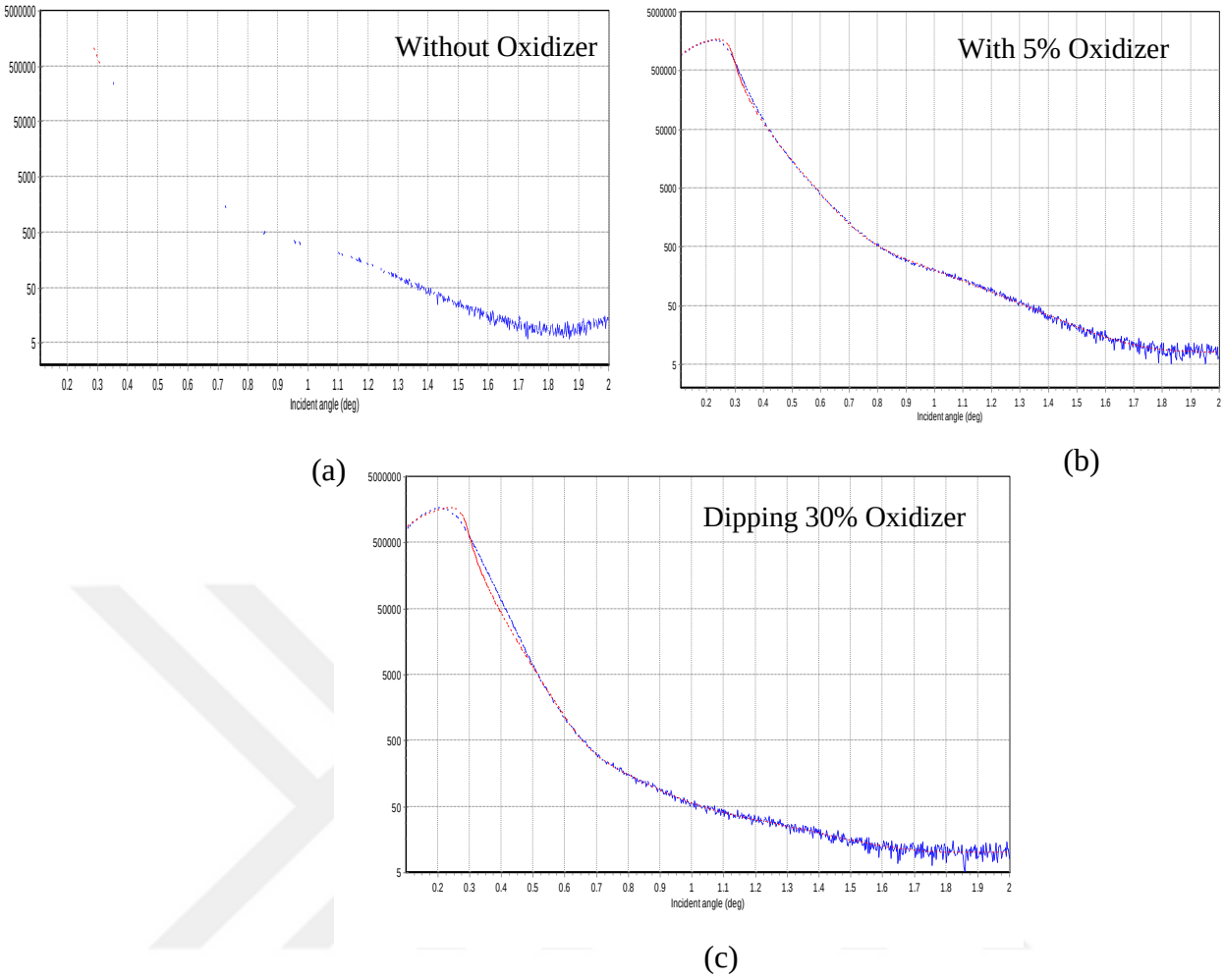

Figure 4.7 XRR curve profiles of the oxidized surface films on the titanium samples (a) CMP implemented in the absence of the H_2O_2 (b) CMP treated in the presence of 5% H_2O_2 and (c) etching with 30% H_2O_2

Protective nature of the formed oxide film on its native metal through oxidation is related to the relative specific volumes of the oxide and the metal. When an oxide film forms at the metal/oxide interface, oxygen atoms tend to diffuse from surface through interior layers while metals atoms diffuse through the upper layers which results in consecutive transition layers to form. When the P-B ratio <1, which means that the volume of the oxide is less than the metal volume, tensile stresses form at the interface. On the other hand, when the P-B ratio is >2 then compressive stresses start to develop at the interface. In order to be a protective oxide film, P-B ratio should be in

between 1 and 2. Based on this rule of thumb, P-B ratios were calculated as given in Equation 4.8.

$$PB\ Ratio = \frac{Volume\ of\ oxide}{Volume\ of\ metal} = \frac{A_O \rho_M}{A_M \rho_O} \qquad (4.8)$$

In previous sections, we summarized the XRR and XRD data as an indication of the formation of protective oxides on Ti surfaces. Here, we use the XRR characterization results to determine the protective nature of the natural oxide of titanium as a function of the selected treatment. Table 4.5 summarizes the P-B ratio calculations as a function of the layers distinguished by measured density from the XRR results. P-B ratio values showed that the CMP implemented samples in the presence of the oxidizer have similar protective film formation based on the PB ratios. However, most favorable P-B ratio was obtained when 3wt% H_2O_2 was used in the CMP treatment with 1.38 PB ratio value (the lowest value obtained). On the other hand, etched samples showed the highest P-B ratio value of 1.96, which is very close to 2 menaing that the film may have a tendency to flake off due to building compressive stresses at the interface.

Table 4.5 Compositional analyses and P-B ratio calculations on the treated samples

		CMP without H_2O_2	CMP with 1 wt % H_2O_2	CMP with 3 wt % H_2O_2	CMP with 5 wt % H_2O_2	Etching 30 wt % H_2O_2
Layers	*Composition*	*P-B ratio*	*P-B ratio*	*P-B ratio*	*P-B ratio*	*P-B ratio*
Layer 0/Layer 1	Porosity TiO_2	2.33	1.88	1.79	2.24	2.45
Subtrate/Layer 0	Porosity TiO_2 Ti	1.89	1.41	1.38	1.53	1.96

4.3.2 Electrochemical evaluation of the surface oxide film formation

Potentiostatic and potentiodynamic polarization measurements were conducted on the titanium samples with different oxidizer ratios in the measurement solutions. Potentiostatic polarization allows the observation of the cathodic and anodic behaviors of the metallic surface. Potentiosatatic measurements of the titanium samples showed that, initially all the samples have positive current values. The higher oxidizer concentrations change the time to reach stability as can be seen in Figure 4.8. However 3% H_2O_2 treated samples reached to a zero current point and stayed as stable passived regions throughout the measurements.

On the other hand, potentiodynamic tests were implemented to the samples to evaluate the corrosion resistance trends. Figure 4.9 gives the potentiodynamic polarization curves of the samples showing a correlation between the potentiostatic behavior with the change in current. The current density increased with the increasing corrosion potential. The current is suppressed at zero and remained at this particular level. It is believed that the formation of a protective passive film is resulting in this linear behavior.

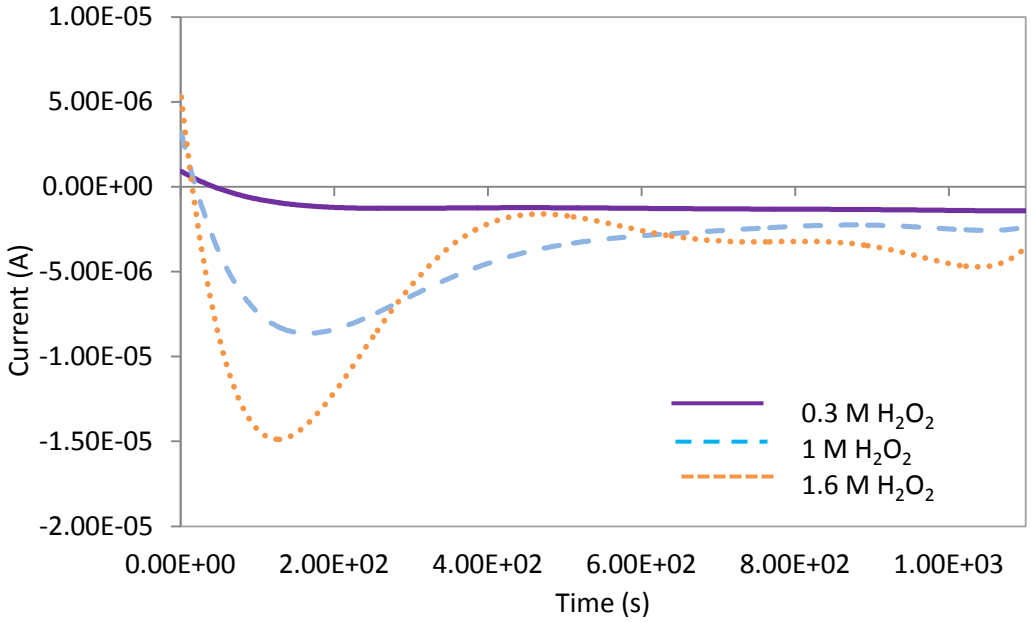

Figure 4.8 Potentiostatic measurements in 0.3M, 1M and 1.6 M H_2O_2 at 0V applied potential

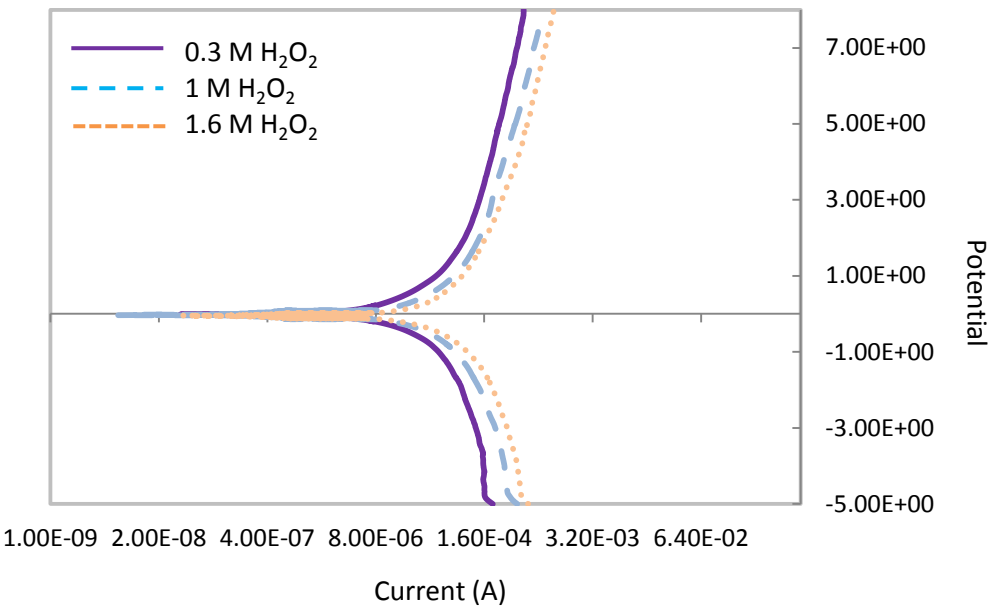

Figure 4.9 Potentiodynamic polarization measurements of titanium samples treated with 0.3M, 1M and 1.6 M H_2O_2 containing electrolyte solutions

3.4 Summary

The CMP implementation results in an oxide film formation on the titanium surfaces, which is the chemically modified top layer. In this chapter, these films were evaluated based on their chemistry, composition and surface energy responses. Chemical analyses showed that the formed oxide film is TiO_2 in composition which is preferable for a better biocompatibility on the implant material. Additionally, XRD analyses showed that CMP implemented samples had crystalline structures, which are different as compared to the polished samples. Furthermore, oxidizer concentration also resulted in different oxide layer formation on the surfaces.

Surface free energy analyses were conducted on the samples to predict their bio-response against the tissue cells in the body environments. It was observed that the surface oxide composition and roughness level are affective in determining the adhesion propensity of the surfaces, which can be used to evaluate the adhesion propensity of the cells in vivo.

In addition, oxide film's passivation and protective natures were evaluated through the electrochemical measurements and PB ratio calculations. The potentiodynamic behavior of the curves showed that the samples processed in the presence of the oxidizer formed a passive film on the titanium surface. The most favorable PB ratio value was obtained with the 3wt% H_2O_2 used sample indicating the formation of the most protective oxide film which is favorable in vivo. Following these results, the impact of the formed TiO_2 film on the biological responses will be further evaluated in detail in the next chapter.

CHAPTER V

BIOLOGICAL EVALUATIONS OF TI BASED IMPLANT SURFACE TREATED BY CMP

5.1 Introduction

Titanium implants are applied with a high success rates today. However, bone-to-implant connection problems still occur for some patients in the early period after implantation, which may lead to loss of implant. Another important issue of implantology is the long waiting periods for the bone-implant connection after the surgery. The fact that the titanium implants do not have periodontal tissues like natural teeth, they have low resistance against the external conditions in the mouth. Eliminating these inefficiencies is the basis of research efforts for titanium-based implants in the recent years. In order to provide an optimal and long-term combatable bone-implant interface, the main goal is to create an appropriate interface. In the long term, rapid migration of osteoblast cells and formation of extracellular matrix, in addition to production of a bio-surface that performs as a pathogen leak-proof interface with bone and soft tissue is required. On the other hand, behavior of the cells on the biomaterial-tissue interface also depends on the physico-chemical properties of the implant sample such as surface free energy, wettability and chemical composition of the material surface [Pon03]. Many studies have shown that beyond the physico-chemical properties, surface roughness is another major parameter, which influences the cell adhesion behavior [Pon03, Lin98, Rol11].

It has been shown in that there are many processes for altering the surface roughness of the implantable material to modify surface for a better cell adhesion as mentioned previously [Ani11, Gar12, Mdo04, Gup10]. Beyond these methods, Chemical mechanical polishing (CMP) process is suggested as an alternative method to change to surface properties through inducing controlled smoothness or roughness on Ti surface in this study [Bas14, Ozd16]. In addition, using oxidizer during the CMP process forms an oxide layer on the surface which enables improved biocompatibility and also prevents the surface contamination and ion release from titanium surface [Cac01]. In scope of this chapter, analyses are aimed to evaluate in vitro cell viability and attachment behavior with respect to surface modifications through CMP implementation on the Ti material.

5.2 Experimental

5.2.1 Cytotoxicity Experiments

ISO 10993-5 cytotoxicity test procedure was adapted to evaluate the cell viability on the samples treated with and without CMP process. L929 mice fibroblast cells were used to represent the mammalian tissue system. Cells were counted and seeded onto the well plate at a concentration of 10^4 cells/plate. The titanium samples were kept in the solutions prepared as per the ISO 10993-5 procedures for 72 hours and the solution extracts were added to the cell plates at 37°C and retained for 24 hours in a %5-CO_2 media. Cell viability was evaluated via WST-1 agent by colorimetric testing.

5.2.2. Bacteria attachment evaluations

Titanium plates were sterilized in an autoclave at 120 °C temperature for 20 min before the microbiological analysis. Cronobacter sakazakii (Gram-) bacteria was used as the species to evaluate the bacteria attachment. 100 µl of microorganisms from the

nutrient broth microbial stock were spread on nutrient agar plates under sterile conditions. After the cultivation of bacteria, sterilized Ti samples were placed into each plate and incubated at 37 °C. The bacteria growth zone was observed over 1, 3 and 7 days and quantified by measuring the thickness of the colonies grown at the periphery of the plates through photographs taken on the samples as can be seen on Figure 5.1a.

5.2.3 Cell Adhesion Experiments

5.2.3.1 L929 Fibroblast Cell Analyses

Titanium plates were cut into circular disks for the cell-growth evaluation to fit into well plate-18 and sterilized with UV radiation. L929 fibroblast cells were amplified in the laboratory for the proliferation on the samples. The cells were seeded directly on top of the Ti plates which were placed at the bottom of the wells. The nutrient medium was changed every 3 days to help keep the fibroblast cells alive. After 1, 3, and 5 days of incubation periods, the grown cells were washed off the titanium plates. In order to test the cell attachment on the titanium plates, initially 7.8g DMEM-F12 (Dulbecco's Modified Eagle Medium, D8900 Sigma) and 0.6g $NHCO_3$ (dissolved in 450ml ultra-pure water) was mixed to prepare a total 500ml solution. The pH of the solution was adjusted to 7.3 with the addition of NaOH. 50 ml FBS (fetal bovine serum) was added afterwards to make a 10wt% FBS concentrated solution. 5 ml of antibiotic Penicillin Streptomysin (100X) was added as the last component and the solution was mixed thoroughly and filtered as a final step. L929 fibroblast cells were grown in the prepared nutrient media inside the well plates in the presence of the prepared Ti samples. The excessive solution was removed from the well plates with vacuum and the plates were washed with phosphate buffer solution (PBS). The grown cells were separated from the plates by using Tripsin into the well plates. The cells were placed into the falcon tubes

and centrifuged at room temperature at 1300 rpm. The settled cells were diluted to a 10^4 cells/cm^2 concentration and transferred on to the Thoma lamel for counting under the microscope as can be seen on the Figure 5.1 c.

5.2.3.2 SaOS-2 Osteoblast Cell Analyses

In order to simulate the bone response human osteoblast like SaOS-2 cells were cultured on the Ti samples. Ti samples were cut according to well plate hole size and after sterilization with UV radiation placed into the wells. SaOS-2 cells were cultured in DMEM medium with 10% fetal calf serum (FCS), 2mM L-glutamine and 10U/mL penicillin. Cells were harvested in the suitable media and plated on the titanium samples. Numbers of attached cells were determined over 3 and 5 days as incubation period, through counting number of the cells on the Thoma lamel by microscope as in the fibroblast cell attachment evaluation.

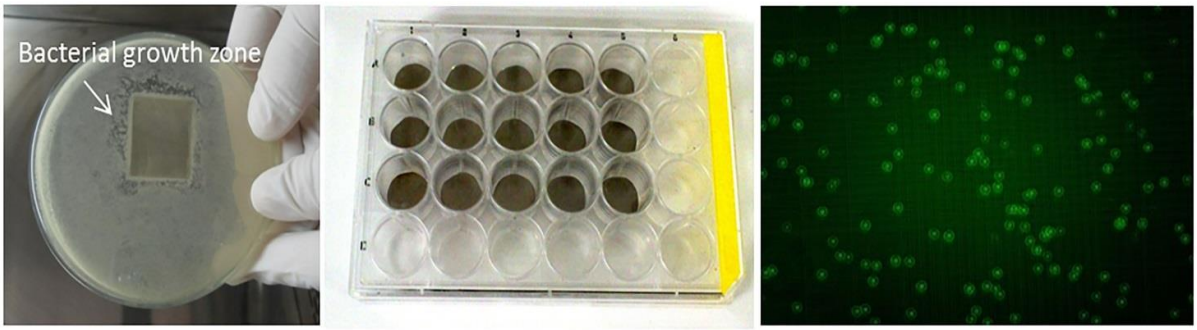

Figure 5.1 Biological evaluation set-up for (a) bacterial growth analyses, (b) cell attachment test incubation well plates and (c) microscopic image of L929 cells on Thoma lamel used for counting fibroblast cells.

5.2.4 Hydroxyapatite Attachment Analyses

Hydroxyapatite (HA) is known to be mimicking the bone tissue and known to promote the osteoblast cell attachment as a coating on the implants due to its bio-ceramic chemical composition of the compound [Sho13, SaM99, Bic02, Hsu10]. In order to mimic the bone cell response, HA attachment was evaluated on the titanium implants by preparing a solution by using Ca and P routes namely the calcium nitrate ($Ca(NO_3)_2$) and diammonium hydrogen sulphate ($(NH_4)_2HPO_4$) according to the reaction given in the following chemical Equation 5.1 [Sho13].

$$10Ca(NO_3)_2 + 6(NH_4)_2HPO_4 + 8NH_4OH \rightarrow Ca_{10}(PO_4)_6(OH)_2 + 20NH_4NO_3 + 6H_2O \quad (5.1)$$

Before deposition, titanium samples were washed in distilled water in an ultrasonic bath. Deposition was carried out by dipping the titanium plates into the HA solutions for 72 h. The HA growth was evaluated through weight differences pre and post the coating procedure. This evaluation is an indication of how well the osteoblast cells will attach to the CMP processed surface in addition to the plausibility of coating the implant surfaces with HA to further promote biocompatibility.

In addition to general mass difference detection method, an easy approach was developed to evaluate the HA attachment performance through Vickers Hardness (HV) test protocol. The standard micro hardness tests were applied to the baseline and HA coated titanium samples with ARS9000 Full-Automatic Micro Hardness Testing System and data was processed through software. After the indent on the surface, the formed

pattern is used to characterize the HA layer through the color difference between the coated HA layer and the bulk material as seen in Figure 5.2. This color difference is accounted for the layer change on the surface. According to the specific HV indenter shape on the edge, pattern depth and layer depth were determined as sketch in Figure 5.3, The thicknesses of the HA coating layer can be calculated through this color coded areas as given Equation 5.2.

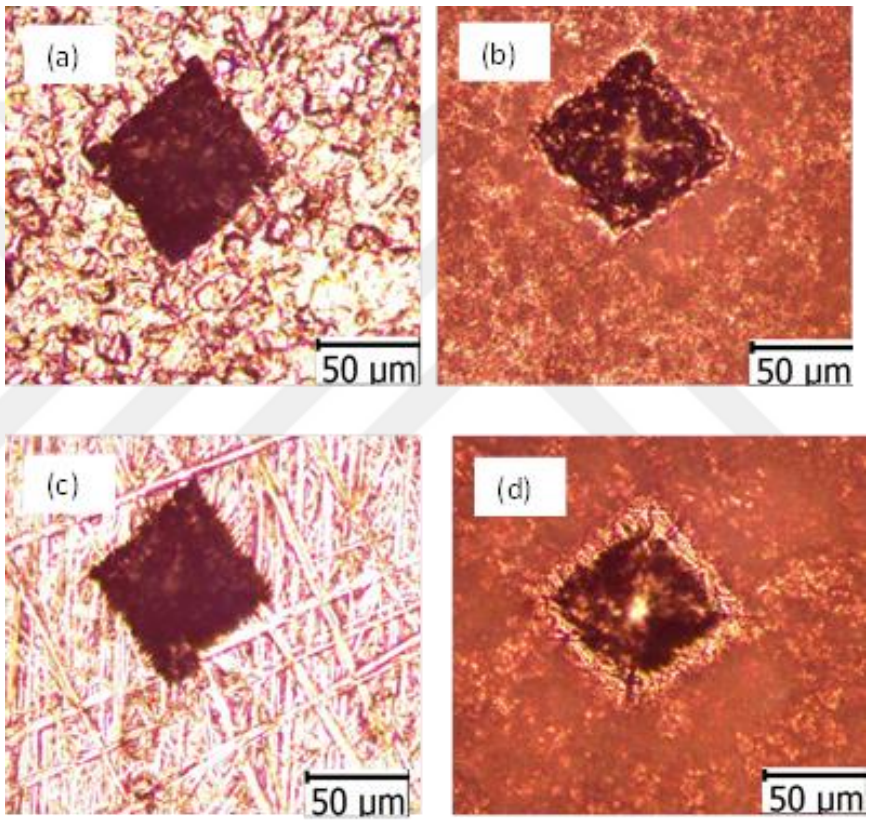

Figure 5.2 Micro hardness measurement indentation pattern on the (a) sample CMP treated in the absence of an oxidizer, (b) sample from part (a) coated with hydroxyapatite (HA), (c) sample CMP treated in the presence of an oxidizer with abrasive paper (45µm-grid), and (d) sample from part (c) coated with hydroxyapatite.

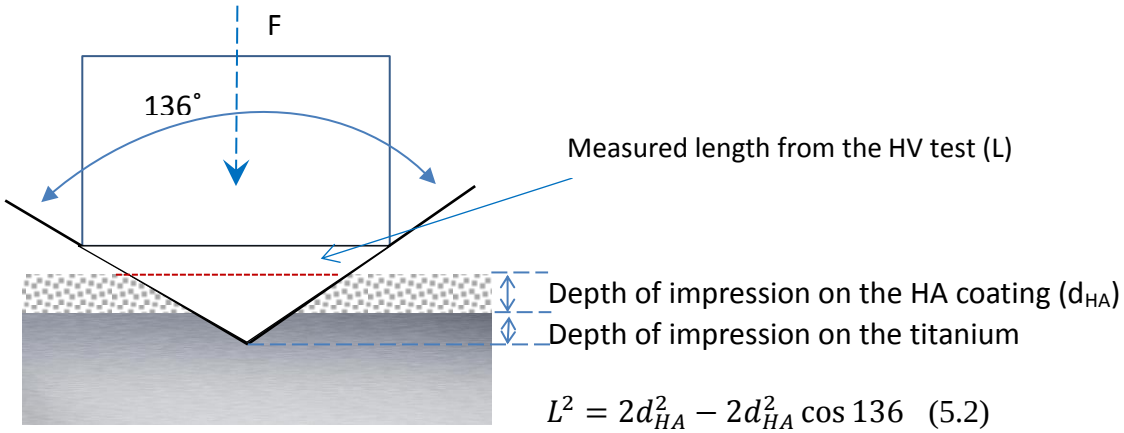

Figure 5.3 Hydroxyapatite coating thickness measurements through micro hardness measurement indentation tool.

5.3 Results and Discussion

5.3.1 Cell viability analyses

Preliminary cytotoxicity analyses were conducted to test the cell activity after the CMP application in order to understand if there are any adverse effects of CMP treatment on the titanium implant material. The results were compared to the untreated sample with negative and positive controls. Figure 5.4 shows the cytotoxicity test results conducted to evaluate the percent cell viability on the polished surfaces as compared to the baseline and the known positive and negative samples [Bas13]. The results confirmed that the cell viability was not affected by the CMP process within the 72 h of the testing period. Furthermore, it is expected that the formation of the protective oxide films of titanium will further limit the titanium dissolution in longer term and hence improve the cell viability, which needs to be studied through in vivo evaluations.

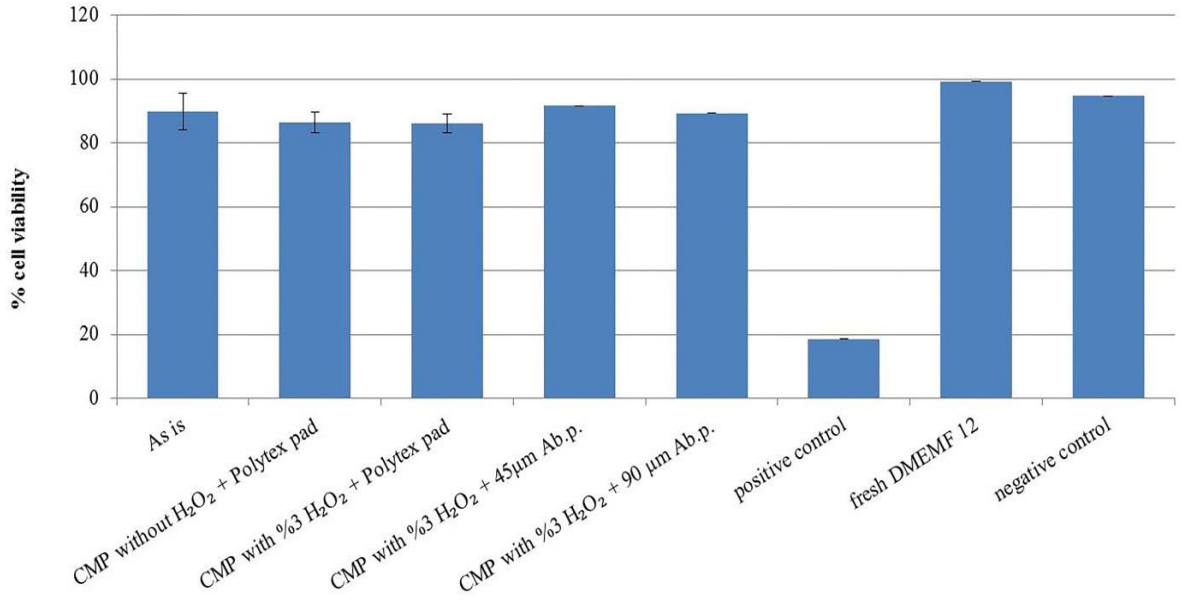

Figure 5.4 Cell viability on the titanium samples treated with CMP as compared to the baseline and control samples to observation of the CMP process and chemical applied samples biocompatibility [Hsu10].

5.3.2 Bacteria growth analyses

Post CMP treatment biological evaluations were also performed through the bacteria growth analyses in order to evaluate the tendency of biofilm formation on the material surfaces. Figure 5.5 illustrates the growth zone thickness of the bacteria when the treated titanium plates were plated upside down inside the petri dishes which are containing the nutrient agar. The test results were evaluated after 1, 3 and 7 days [Bas12]. The baseline sample which has a porous and thick titanium oxide layer has shown an increase in the bacteria growth zone after the first day as detected by the layer thickness (increased nearly 0.4mm from ~1.4 mm to ~1.8 mm). The same observation with a more pronounced effect has been noted on the titanium plate on which the oxide layer was removed through CMP application without using an oxidizer. The bacteria zone thickness increased up to ~1.9 mm from the first day value of 0.9 mm. This is believed to be due to the oxidation of the bare titanium surface in the nutrient medium. As the bacteria are known to grow on the oxide surfaces, the increase in the bacteria

growth zone is potentially promoted when the oxide is formed [Eli08, Var08]. This trend can also be explained by the increased hydrophobicity of the surface by the formation of the oxide, which promotes the biocompatibility [Zur13]. When CMP is performed with 3 wt% H_2O_2 addition, however, the results indicate that the increasing surface roughness promoted the bacteria zone thickness which can be attributed to the better adhesion of the bacteria on the rougher surface. Yet, all the samples were observed to retain an almost constant bacteria growth zone as a function of time after the CMP application. The consistency of the bacteria growth response of the CMP treated samples is believed to be due to the formation of a nano-scale protective oxide layer on the surface during the CMP process. Therefore, it is plausible that the control of surface roughness through CMP application can further be used to control the infection resistance.

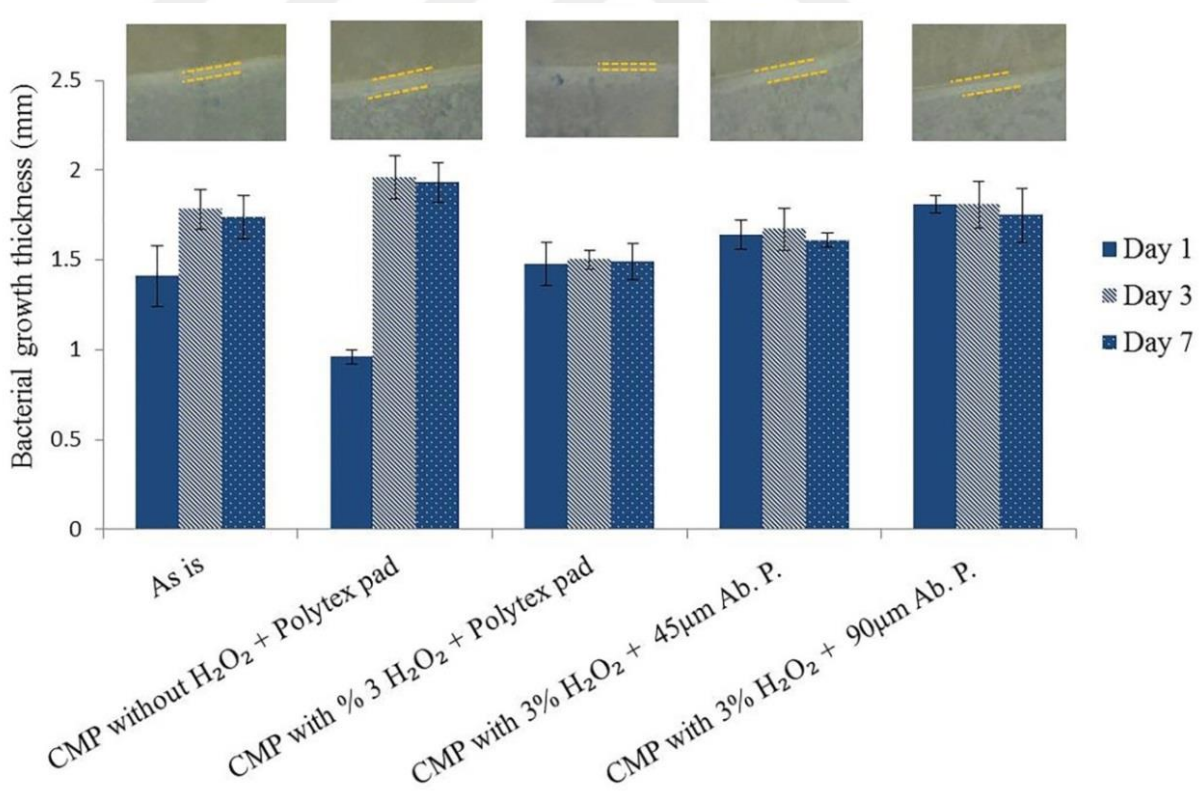

Figure 5.5 Bacteria growth analyses on titanium plates quantified by thickness of the bacteria zone surrounding the titanium plates after 1, 3 and 7 days

5.3.3 Cell attachment analyses

The fibroblast type L929 and osteoblast type SaOS-2 cells attachment behavior was also evaluated on the titanium plates in order to observe surface response on different cell type, the samples prepared by five different surface finishing method through CMP process. Figure 5.6 shows the change in the number of cells after 1, 3, 5, 7 and 15 days incubation period in the well plates. The cell growth increased on all the samples in consistency with the cell viability results. Yet, the growth rate showed a tendency to change by the surface roughness of the titanium plates. Samples surfaces which were CMP treated with the coarse abrasive papers and hence had a surface roughness of 400 nm and above (polished with 45 and 90 μm grit abrasive papers) have shown less amount of cell attachment. As it is schematically illustrated in Figure 5.6 on the cross sectional images of the actual samples, it can be suggested that the reason for this response is the sharp edges forming on the surface topography, which cause some of the cells to rapture as they try to approach and attach to the surface. Similarly, the baseline sample with a high RMS roughness value (~486 nm) also showed lower trend in cell attachment. On the other hand, the samples treated with CMP by using the polymeric polishing pads had smoother surface finish as it can be seen from their cross section images and the RMS surface roughness values reported in Chapter 3 previously. Between these two surfaces, the best cell attachment was observed on the titanium plate which was CMP treated in the presence of the oxidizer. This plate had the smoothest surface finish (RMS surface roughness of ~120 nm) and a protective oxide film formed on its surface as shown previously. On the other hand, cell attachment was limited when the CMP was performed without an oxidizer and the pure titanium was exposed on the surface of the plate. This may be due to the dissolution of the Ti^{+4} ions in the absence of the protective oxide layer on the surface that limits the attachment of the cells.

However, the standard deviations calculated based on three measurements do not show a statistically significant difference among the samples tested as observed by other researcher earlier [Cro12]. Hence it can be stated that the CMP implementation increases the tendency of cell attachment when it is applied in the presence of oxidizers and using a soft pad promoting the smoothness. The sensitivity to the surface structuring is aligned with the earlier literature findings where the nano-scale structuring was observed to enhance the cell attachment [Ken13, Obe13]. In addition cell response after the fifth day showed that the cells tend to die due to the lack of nutrient. Consequently a decreasing number of cell attachment was observed as seen in Figure 5.6.

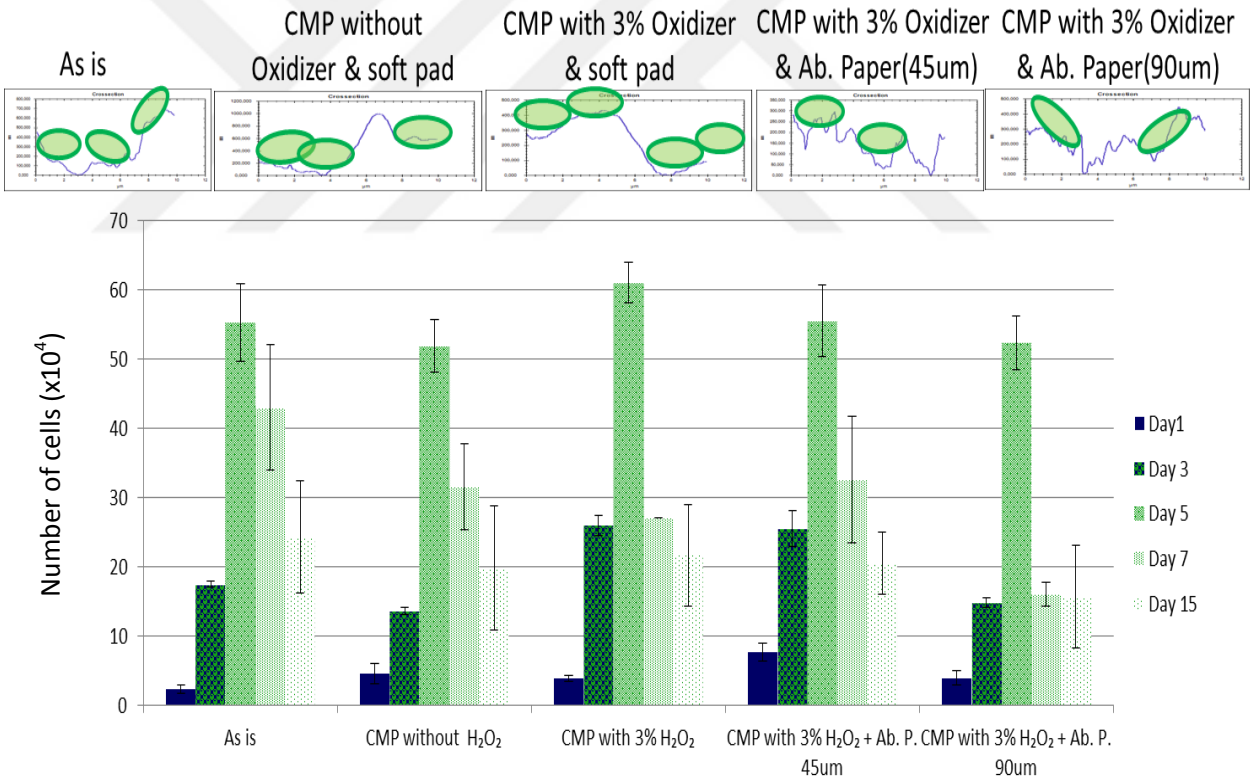

Figure 5.6 L929 fibroblast cell attachment test results according to surface modification with CMP within a 5 days test period to observation proliferation distribution of cell.

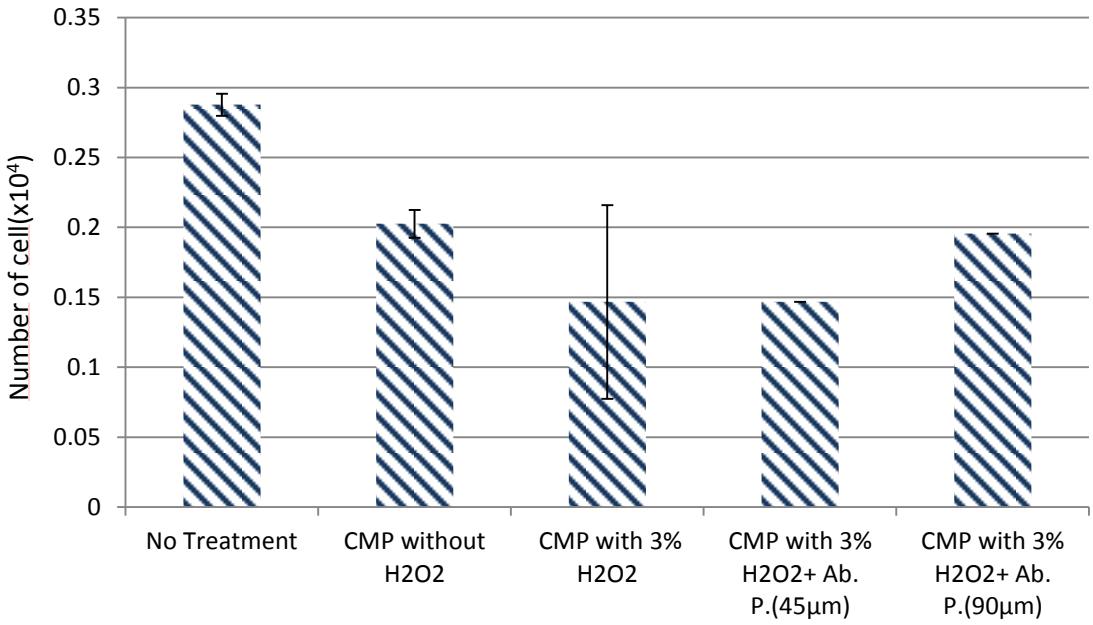

Figure 5.7 Saos-2 type Osteoblast cell attachment evaluations after 3 days

Osteoblast type SaOS-2 cell attachment analyses after 3 day test period showed that rougher surfaces had the highest cell activity for cell attachment as can be seen in Figure 5.7. There were significant differences as compared to the fibroblast cell behavior. Increased surface roughness resulted in increased surface area on the titanium samples which resulted in increased cell attachment for the osteoblast-like cells. As seen in Figure 5.7 CMP implemented samples in the presence of oxidizer showed relatively lower cell activity as compared to the ones without H_2O_2 treatment. This is due to the controlled surface roughness and pore free surface oxide layer. Cell attachment test were also continued after 3 days up to 5 day test period. However, after 3 days cells started to die as documented previously by L.Postiglione resulting in increased standard deviation on the number of the cell attached and hence those results were not presented here.

5.3.4 Hydroxyapatite attachment analyses

Hydroxyapatite (HA) is widely used as a coating material for dental implants due to its similar chemical composition to the natural bone mineral and its capability to promote bone regeneration [Lum01, Li12, Xu15, Nay10]. In this part of the study,we have evaluated the HA attachment on the samples treated with CMP and once again compared the attachment performance to the baseline sample. Figure 5.8 a and b illustrate the HA attachment and the change in the RMS surface roughness values as a function of the HA coating, respectively. It can be seen that the attachment of HA increased with the increasing surface roughness. The smoothest surface obtained by the CMP in the presence of the oxidizer and the polytex pad resulted in the minimum amount of HA attachment which was 1.4 mg/72 h. In contrast, the surface with the highest roughness (polished with 90-μm grid paper) resulted in 2.1 mg attachment/ 72 h. In addition, the post HA coating surface roughness values were higher when the original surface roughness was higher. The AFM micrographs given in Figure 5.8b also clearly shows the change in surface morphology with the HA coating. It is interesting to note that although the pre-HA coating surface roughness of the baseline sample was similar to the roughness values obtained when the abrasive papers were used for CMP applications (45 and 90- μm size sandpapers), the HA attachment was not necessarily similar on these samples. Figure 5.9 demonstrates the difference much better when the cross sectional AFM micrographs of all the samples are compared pre and post HA deposition. Obviously, CMP induced surface roughness helped promote the HA attachment with a thicker layer deposited on the surface. This observation also supports the enhanced biocompatibility of the surfaces when CMP is applied since the HA attachment is known to promote the osteoblast-like cell activity with increasing

roughness on the HA coated surface is reported to increase the osteoblast cell attachment in the earlier studies [Li12, Xu15].

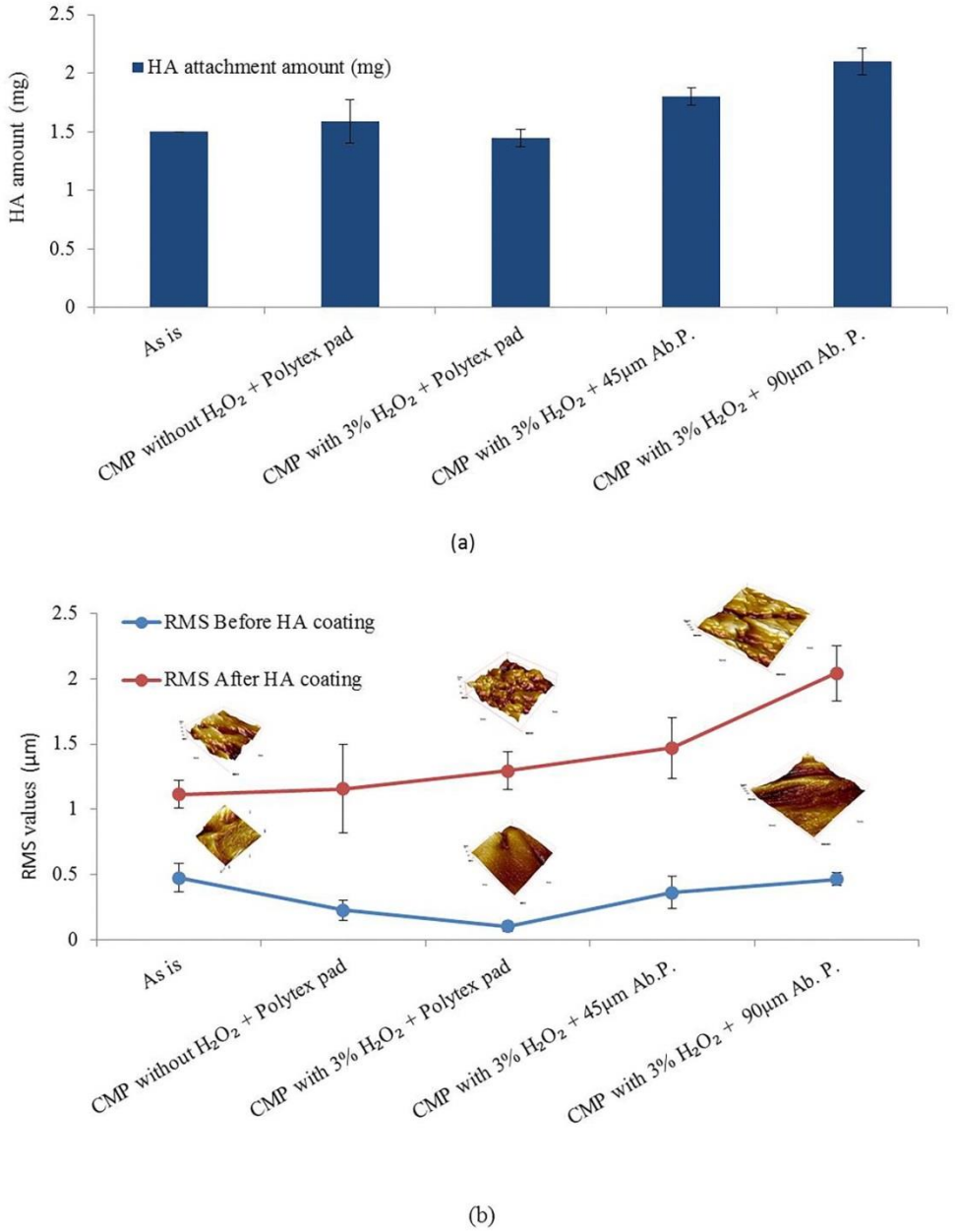

Figure 5.8 HA attachment evaluation of the titanium samples (a) amount of HA attachment as a function of surface treatment and (b) measured RMS roughness values pre and post HA coating.

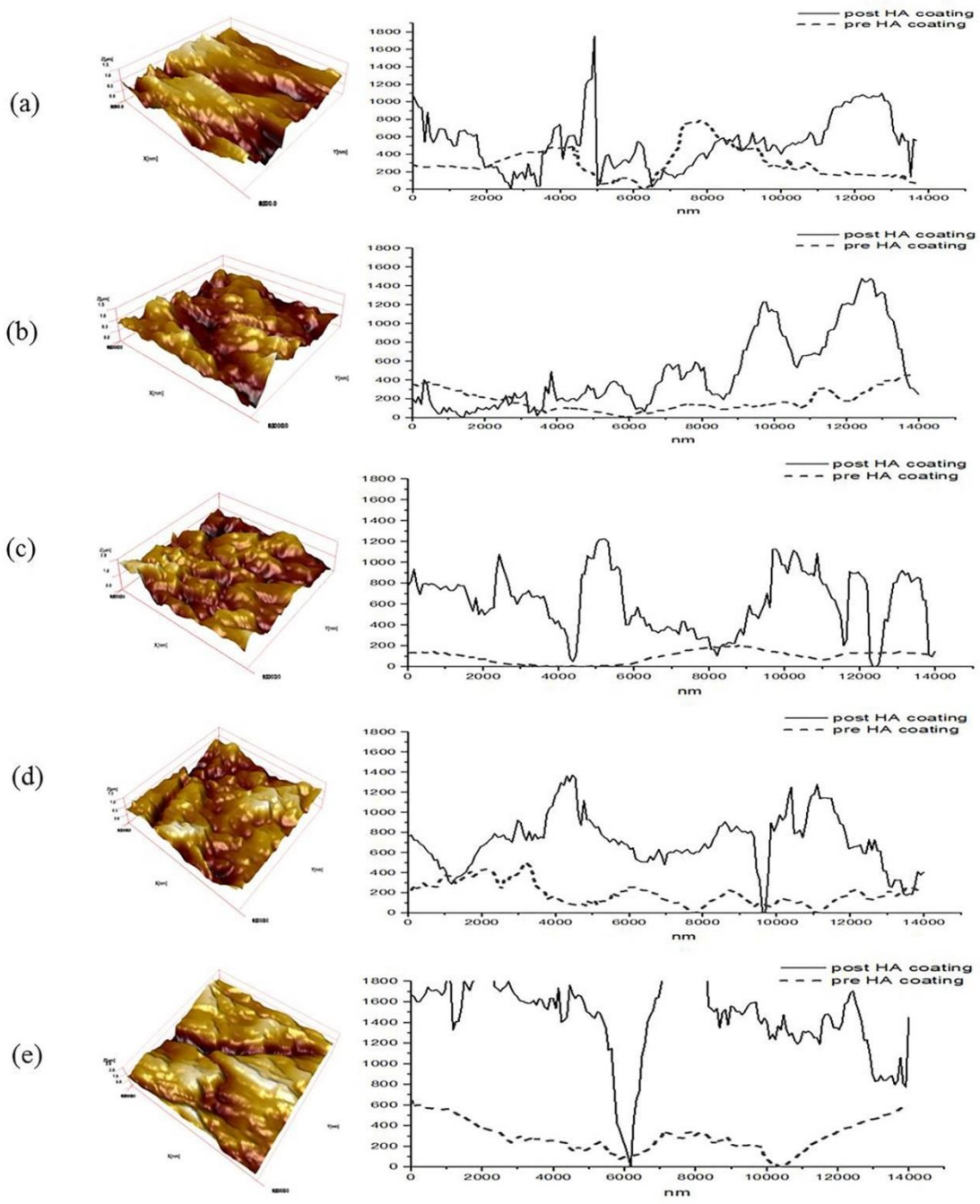

Figure 5.9 Post HA coating AFM micrographs and pre and post cross sectional analyses of the titanium plates (a) as received baseline sample (b) post CMP without oxidizer (c) post CMP with 3% H2O2 oxidizer (d) post CMP with 3% H2O2 oxidizer with 45 μm grit abrasive paper and (e) post CMP with 3% H2O2 oxidizer with 90 μm grit abrasive paper.

Previously it has been documented that, HA shows similarities with the bone structure and therefore after the osteoblast cell tests HA attachment tests were also implemented on the samples. According to the surface enhancement method, HA coating amount showed difference as mentioned previously. HA layer on titanium sample can be considered as a composite material. Therefore, the changes in hardness can be evaluated through HV measurements by using layer thicknesses as illustrated in Figure 5.10. Pre HA coating, the samples showed similar hardness values excluding the baseline sample. The porous oxide layer on the baseline sample resulted in lower hardness values since the CMP process can strain harden the material surface, higher hardness values were observed after CMP. Figure 5.10 shows clearly that, the HA coated samples have relatively higher hardness values. The lowest HV value obtained on the rougher sample due to thick HA layer coating formed on the sample. The highest HV value was observed on the CMP implemented sample in the absence of an oxidizer due to the thin HA layer thickness resulting in hardness values close to the uncoated samples. Hardness measurements on the HA coated samples were also used to calculate HA layer depth. Table 5.1 compares the calculated values through pre and post weight measurements as well as the HV measurements. The results also correlate with the osteoblast cell attachment test results obtained after 3 days of incubation.

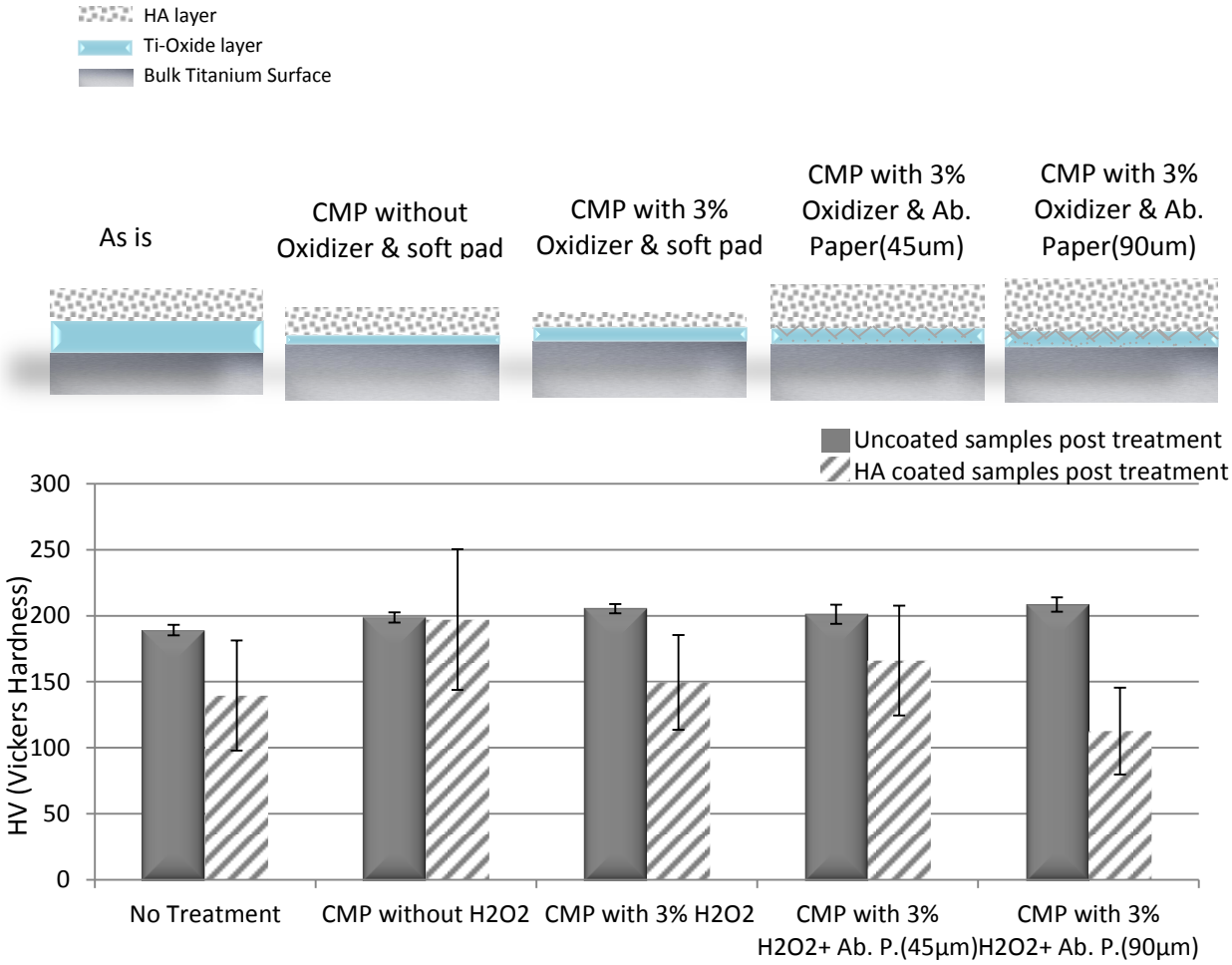

Figure 5.10 Micro hardness test results for the CMP applied samples pre and post and HA coating and schematic representation of the surface layers drawn to the scale.

Table 5.1 HA coating depth calculations based on pre and post weight measurements as compared to the calculations conducted based on the hardness test profile analyses.

	HA deposition depth	
	Weight based calculation	Hardness measurement profile based calculation
No Treatment	6.68±1.25	6.67±0.01
CMP without H_2O_2	5.64±1.65	7.07±0.18
CMP with 3% H_2O_2	6.57±1.07	6.44±0.07
CMP with 3% H_2O_2 & Ab. P.(45µm)	7.83±2.49	8.00±0.07
CMP with 3% H_2O_2 & Ab. P.(90µm)	9.84±0.01	9.33±0.11

In addition to quantitative analyses of the HA layer, qualitative analyses were also conducted as FT-IR and XRD measurements. Chemical characterization of the HA coating on titanium samples by infrared spectrum is given in Figure 5.11, which shows the FT-IR spectrum of the samples with the corresponding peaks of the HA layers. CMP treated samples in the presence of an oxidizer showed higher HA affinity as compared to the no oxidizer treated samples. On the other hand, HA peaks showed higher intensity on the rougher samples. This behavior correlates with the HA depth profile results. In that context, higher surface roughness samples have the higher peak intensities on the spectrum with the highest value observed on the sample treated with the coarsest abrasive paper (90µm).

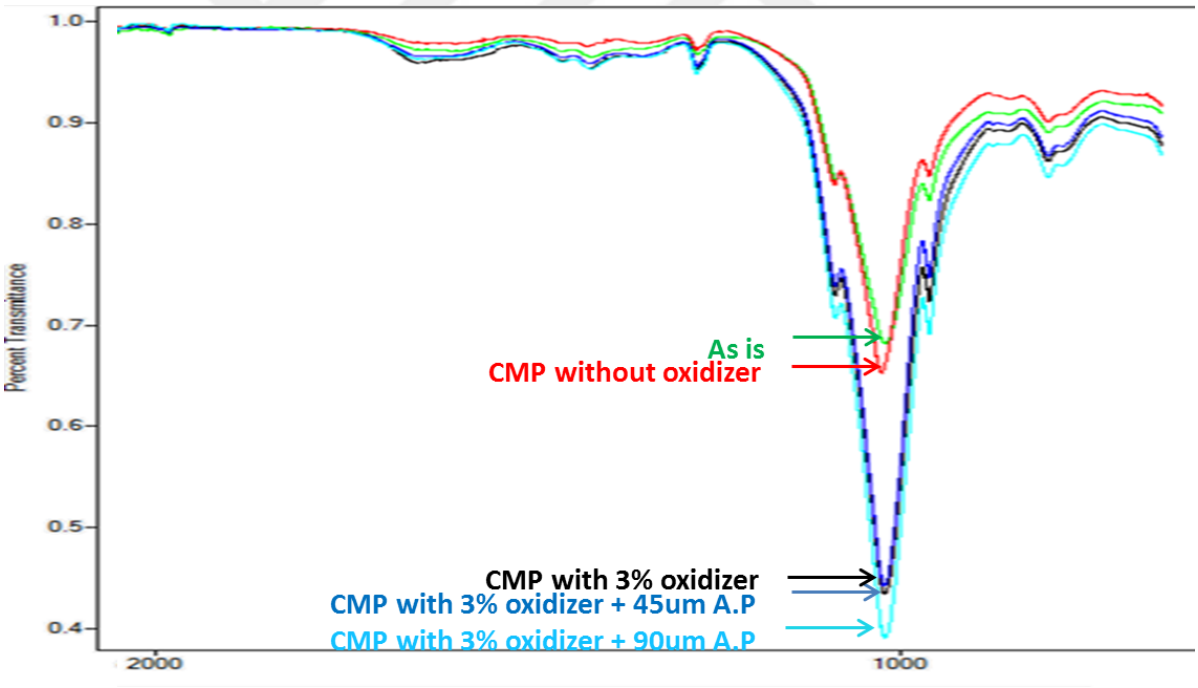

Figure 5.11 FTIR analyses on the HA coated titanium samples with corresponding HA peaks on the spectrum.

Furthermore, XRD analyses on the HA coated samples were also utilized to characterize the coated Ti surfaces. Corresponding peaks of the titanium and HA layers were observed on the XRD spectrum as given in Figure 5.12. Changes in the relative peak intensities show the correlation between the coated layer and the bulk material. CMP treated samples in the presence of oxidizer showed higher peak intensities for HA on the spectrum as expected.

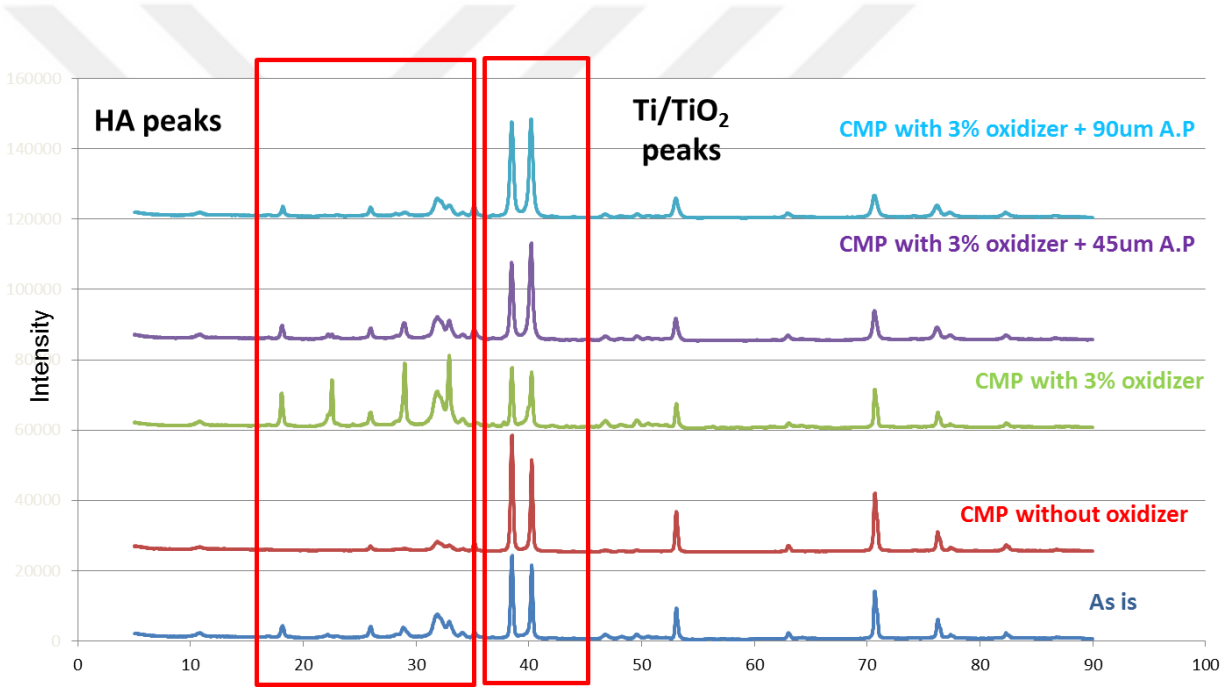

Figure 5.12 XRD analyses of the HA coated titanium samples with both Ti/TiO2 and HA peaks on the spectrum.

5.4 Summary

The interaction of hard and soft tissues with implant material is the main issue for the surface engineering of the implants. After the CMP treatments titanium sample surfaces were characterized through cell viability, adhesion and proliferation evaluations. Cytotoxicity results of the treated samples were also presented as an evidence for the inertness of the suggested methodology on cell health. Furthermore, the cell growth analyses for fibroblast and osteoblast-like cells were correlated to the surface morphology of the treated samples. The cell growth was observed to be affected more by the surface roughness whereas the cell attachment tests have illustrated that there is an optimal roughness value where the cells are better adhering on the implant surfaces when their sizes match the surface roughness better.

Furthermore, HA attachment results have also confirmed that the CMP treated surfaces tend to help the HA deposition more than an oxidized surface although the surface roughness values were comparable. Coating characterization was also performed to study surface composition after the HA coating implementation. These results indicated that the treated surfaces may contribute to better biocompatibility for bone regeneration due to better bioactivities and furthermore the formed surface oxide layers and HA coatings may help ensure insulation against the ion release from the titanium implants.

CHAPTER VI

CMP BASED DESIGN CRITERIA FOR OPTIMALLY PERFORMING IMPLANT MATERIAL SURFACES

6.1 Introduction

Surface properties of the implantable materials are deterministic factors for the healing process. There are number of studies conducted on the implant material surfaces to obtain a better osseogenesis at the implant-bone interface. While the type of implant material has been proposed to affect the cell response, the surface treatment, wettability and roughness values also influence the osteogenic interactions [Pos03]. During the implantation process, tissue cells respond to the implant material in a few seconds. Initially, water molecules make a contact with the implant surface and a hydrated layer is formed on top of the implant. Integration process is followed by the protein adsorption on to the surface and the cells start to adhere to these regions [Sha06]. Therefore, the implant surface should have an optimal morphology to be attractive for the tissue or the bone cells. However, previous studies showed that there is no exact definition for the optimal surface parameters. As a part of this dissertation, we examined the cell adhesion behavior on different roughness induced titanium implants in Chapter 5 and the results showed that, the roughness value is a selective parameter and its effect is dependent on the cell type.

A number of approaches have been suggested in an attempt to obtain rapid and long term success of the implantation process. As detailed in Chapter 2, these processes

include implementation of various surface roughness types, changing morphology and application of coatings on the implant material for an ideal surface finishing. Beyond all these suggested methods, we introduced a new approach in order to enhance the implant surface morphology through the CMP process. As mentioned in Chapter 2, CMP process has variable components (such as polishing pad, slurry and applied pressure) which can alter the surface finishing quality both chemically and mechanically.

In this chapter we examined the optimal CMP conditions statistically to determine the best surface treatment conditions. Initial CMP analyses were conducted with 70N applied load, 3wt% H_2O_2 added into the slurry and using a polymeric soft pad (in order to induce roughness two types of abrasive papers were also used in place of pad material). CMP performance of the treated titanium samples were evaluated in terms of material removal rate, wettability and surface roughness responses. Since, the cell response has been evaluated according to surface morphology in Chapter 5, predicted cell attachment responses were examined as a function of the implemented surface treatment for improved desirability in the surface finish. The optimal surface treatment methodology was established based on varying applied load, grain size of the pad material and the oxidizer concentration. Design of experiment (DEO) methodology was used with a Central Composite Design (CCD). The obtained responses were plotted by material removal rate, wettability performance and surface roughness values. These evaluations provided a systematic approach for optimizing the CMP inputs, which affect the biocompatibility performance of the implants via changing the surface properties.

6.2 Experimental Approach

6.2.1 Chemical mechanical treatment of the surface

CMP experiments were conducted with the Tegrapol-31 polisher as mentioned previously. However, in this section CMP conditions were determined based on the Design Expert software suggested values. CMP was conducted by using 5%wt alumina (Al_2O_3) slurry and the H_2O_2 oxidizer added into the slurry for a duration of 2 minutes. The selected polishing pad type, oxidizer concentration and the applied down-force were set by the suggested values of the design of experiment.

6.2.2 Evaluation of the responses

Three responses were evaluated after the conducted tests namely; (i) material removal rate, (ii) wettability and (iii) surface roughness values. Material removal rates were calculated through weight loss of the samples before and after polishing. Wettability was characterized through contact angle measurements by using simulated body fluid and the sessile drop method. Surface roughness values were measured by Atomic Force Microscopy (AFM) using contact mode on 10 × 10 μm scan area and reported as (root mean square) RMS roughness as an average of three measurements taken on the samples.

6.2.3 Statistical Design of Experiments Set-up

Design-Expert® software was used for the statistical analyses with response surface methodology (RSM) in order to process optimization. Response surface methodology based statistical design model has been applied with the Central Composite Design (CCD) model. Objective of the CCD model depends on the optimization of a response, which is obtained by interaction with the other independent

input variables. The CCD model results were found to be well suited for fitting either a linear or a quadratic surface that generally works well for process optimization. In this study, a three-factor CCD was used for the optimization. As pictured in Figure 6.1, it is based on a core factorial that forms a cube with surfaces, which are coded as -1 to +1 and the stars represent axial points which are extended to 1.68179 coded units away from the center enabling a cubic response beyond the surface. The three factor CCD model revealed 19 test runs that provide an estimate of the experimental standard deviation and variability. The selected design levels are summarized in Table 6.1 and Table 6.2 summarizing the selected design factors and responses with respect to the run order.

CMP experiments were conducted on the titanium samples within the given DoE order. Slurries with 5wt% Al_2O_3 solids loading were used with the abrasive paper with different grain sizes in the presence of the oxidizer (H_2O_2) in the slurry at various concentrations. In addition, IC1000 CMP pad was used in place of the abrasive paper to represent no-grain set-up. Material removal rate (MRR), wettability and surface roughness values were evaluated as the three responses after the polishing tests.

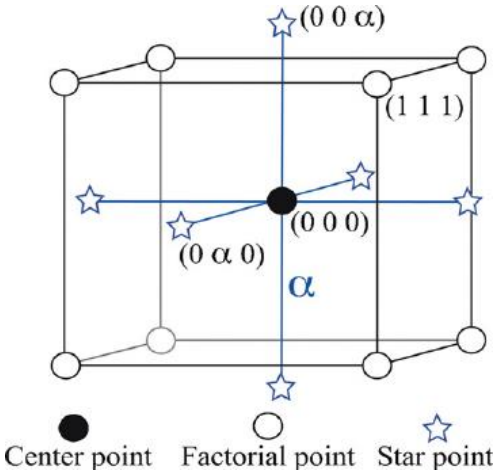

Figure 6.1 Central Composite Design (CCD) for three factors selected for optimization

Table 6.1 Selected design levels for three factorial central composite design

	Design Levels				
	-1.68	-1	0	1	1.68
Applied load(N)	36.36	50	70	90	103.64
Abrasive grain size (μm)	0	21	45	69	90
H_2O_2 concentration (% wt.)	0	1.2	3	4.8	6

Table 6.2 Experimental design by for three factor CCD optimization

Std	Run Order	Space Type	Applied Force (N)	Grain size (μm)	H_2O_2 concentration (%wt.)	MRR (nm/sec) $x10^3$	CA (Θ)	RMS (nm)
1	13	Factorial	50	21	1.2	2374.54	69.67	179.15
2	5	Factorial	90	21	1.2	2786.41	93.27	135.55
3	15	Factorial	50	69	1.2	3193.94	90.38	115.0
4	19	Factorial	90	69	1.2	3731.94	91.98	114.36
5	7	Factorial	50	21	4.8	2502.79	97.13	160.65
6	4	Factorial	90	21	4.8	2580.17	94.826	124.53
7	9	Factorial	50	69	4.8	3512.21	93.05	101.13
8	12	Factorial	90	69	4.8	3636.88	69.79	105.83
9	11	Axial	36.36	45	3	1523.34	94.76	170.09
10	17	Axial	103.64	45	3	3562.74	87.65	130.98
11	16	Axial	70	0	3	26.04	88.20	97.93
12	14	Axial	70	90	3	3949.97	92.45	179.11
13	10	Axial	70	45	0	2911.75	86.57	81.49
14	3	Axial	70	45	6	2860.29	79.42	220.52
15	18	Center	70	45	3	3470.78	92.58	117.58
16	2	Center	70	45	3	3528.96	93.11	102.54
17	1	Center	70	45	3	3343.32	91.56	116.13
18	6	Center	70	45	3	3484.14	93.45	116.55
19	8	Center	70	45	3	3631.96	94.84	127.84

6.3 Results and Discussions

Statistical analyses of the experiments conducted were evaluated through Central Composite Design (CCD) model and the ANOVA analyses satisfied the statistical significance with a p-value of 0.0026. Overall test design levels are given on Table 6.1. It is accepted that the the regular CMP tests by using IC1000 pad and only CMP slurry are representative of 3-phase friction where the abrasives are free to rotate. On the other hand, CMP tests conducted with the abrasive paper are representative of 2- phase friction since the solid abrasive particles are embedded into the paper and cannot rotate freely, as can be seen in the Figure 6.2 schematically. These friction actions contribute to the magnitude of the obtained surface roughness significantly. Results were evaluated based on material removal rate (MRR), RMS surface roughness and wettability responses for each experimental set-up individually.

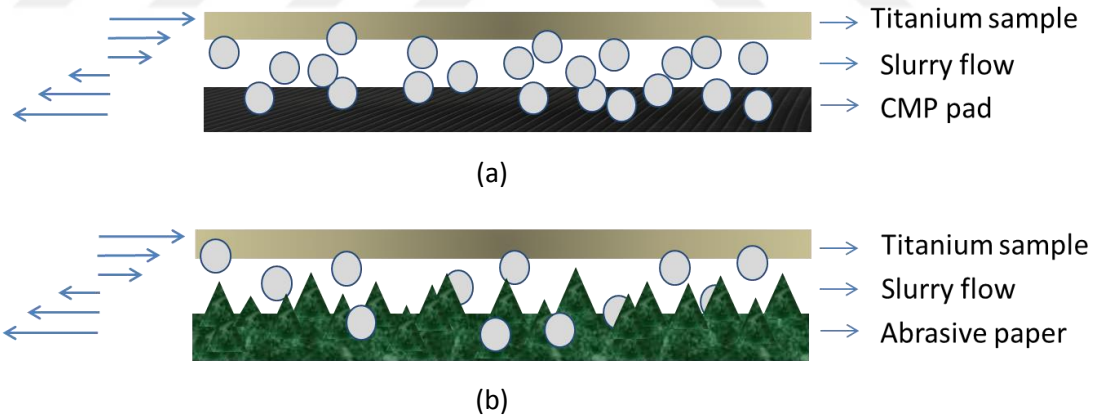

Figure 6.2 Schematics of friction factors during the CMP process with regular pad (a) and abrasive paper (b)

6.3.1 Effect of abrasive particle size on titanium surface structuring

Initial analyses on the surface finishing show that the samples polished with the abrasive papers had higher material removal rates and roughness values as can be seen on Figure 6.3. CCD evaluations have shown that there is a linear correlation between the material removal rates with respect to the abrasive grain size. Figure 6.4 gives the effect of abrasive grain size on each selected response individually as contour images and Figure 6.5 gives the 3D surface responses of the output values.

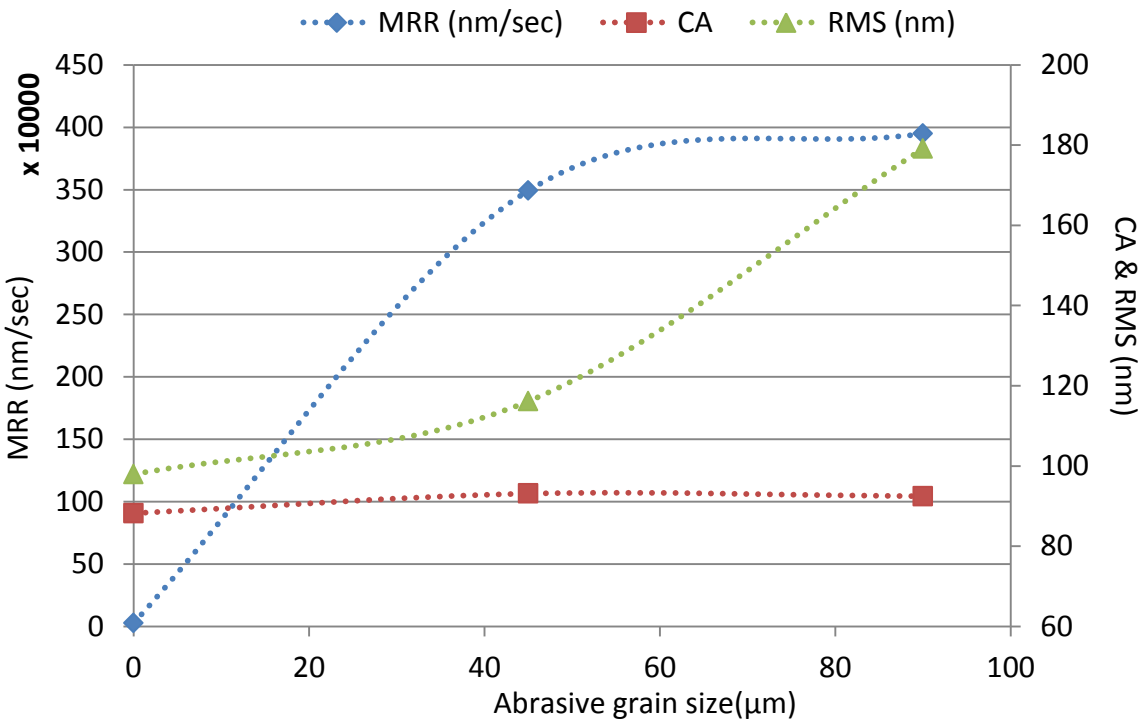

Figure 6.3 Material removal rate, roughness (RMS) and contact angle responses as a function of abrasive grain size.

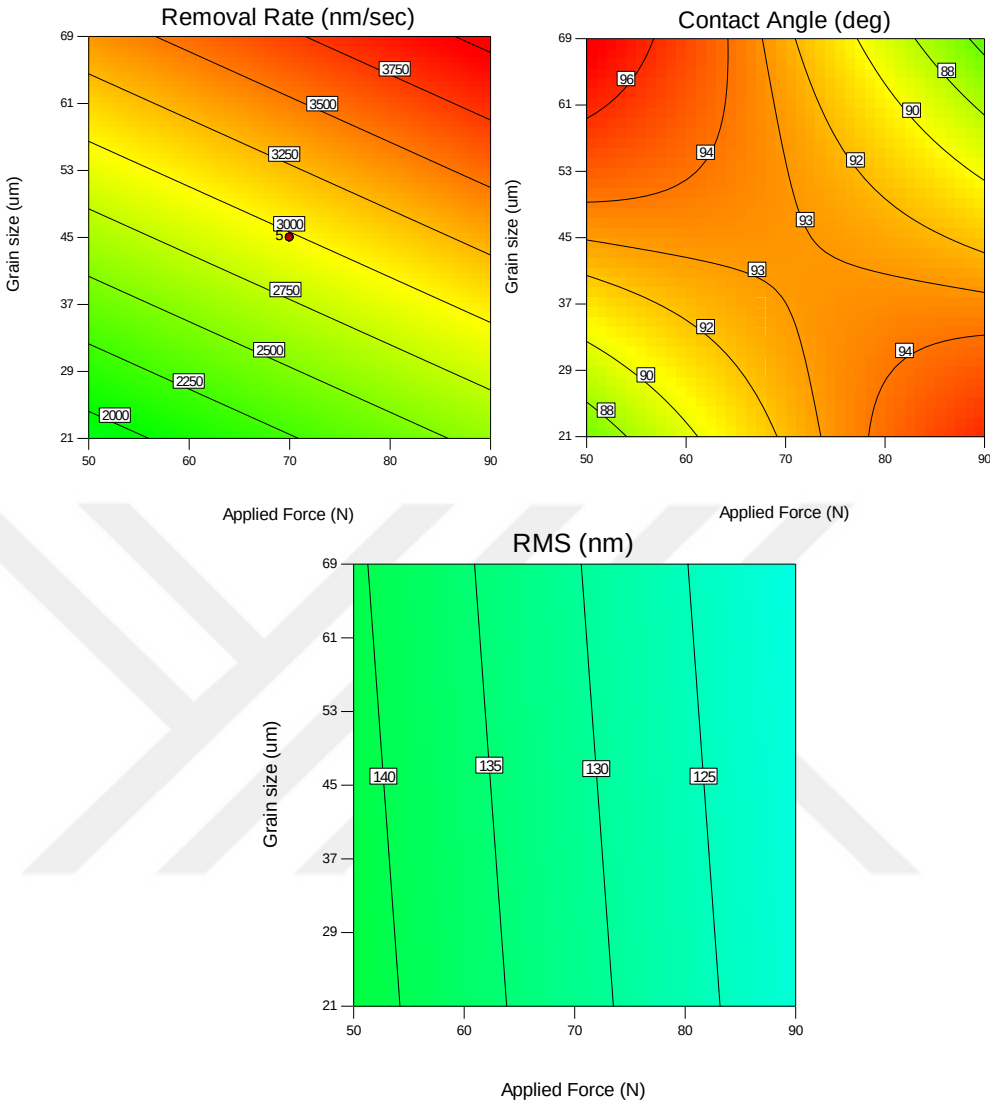

Figure 6.4 Contour graphs of the grain size effect on material removal rate, wettability and surface roughness properties.

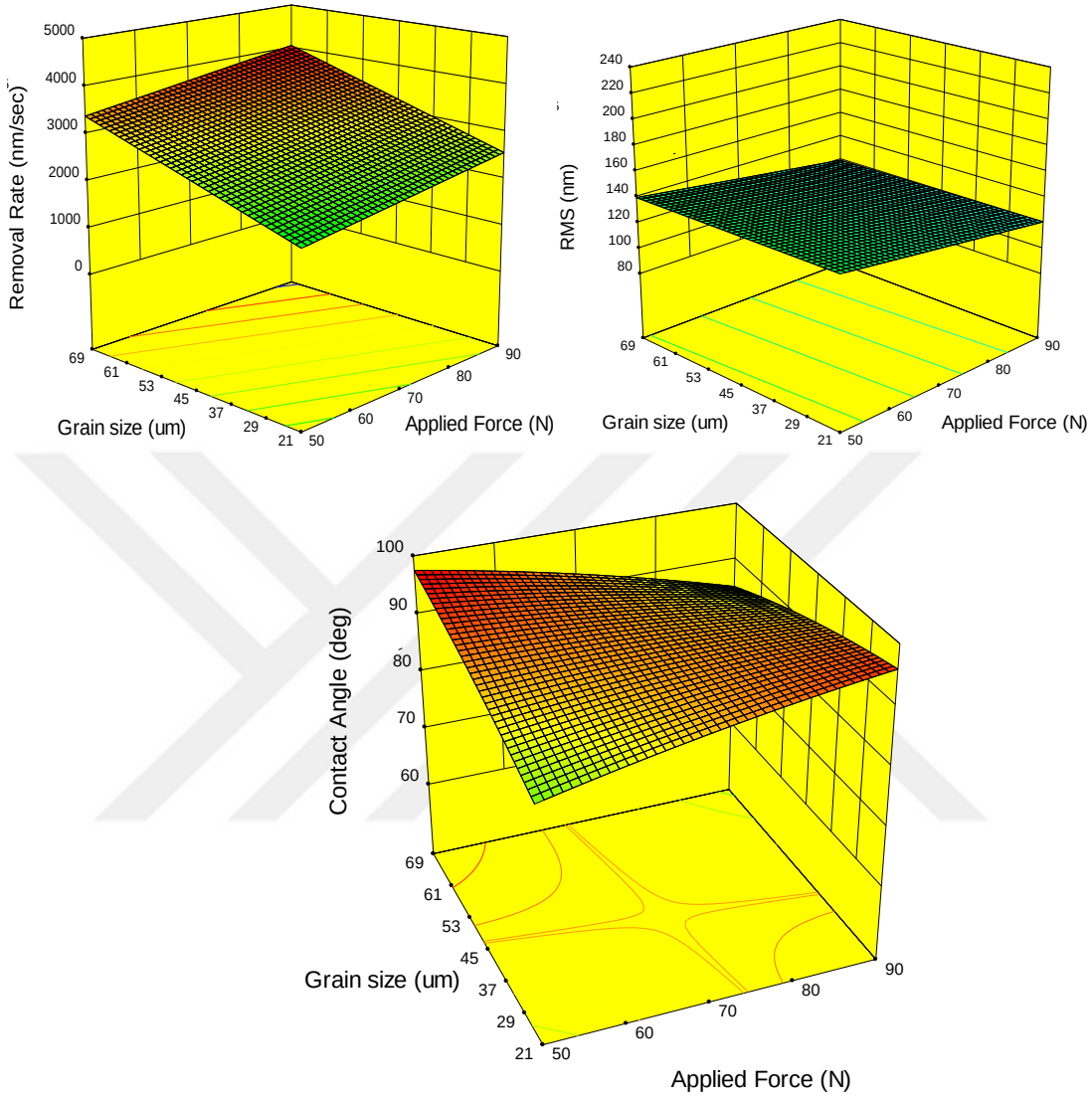

Figure 6.5 Grain size effect on the surface material removal rate, wettability and roughness as 3D response.

6.3.2 Effect of applied head pressure on surface structuring

Applied head load also affects the final surface structure during the CMP implementation. CCD model experiments conducted with various applied load values have shown that increased down force resulted in reduced surface roughness and increased contact angle values as given in Figure 6.6. The increase in the material removal rate with the increasing down force can be attributed to the elevated mechanical interactions under the higher pressures induced. The decrease in the surface roughness is due to the enhanced planarization at the higher pressure values. Nevertheless, the contact angle values tend to remain similar although the roughness values decrease with respect to the low pressures. Figure 6.7 gives the affect of head load on each response in 2D graphs and Figure 6.8 gives the 3D surface responses of each selected output.

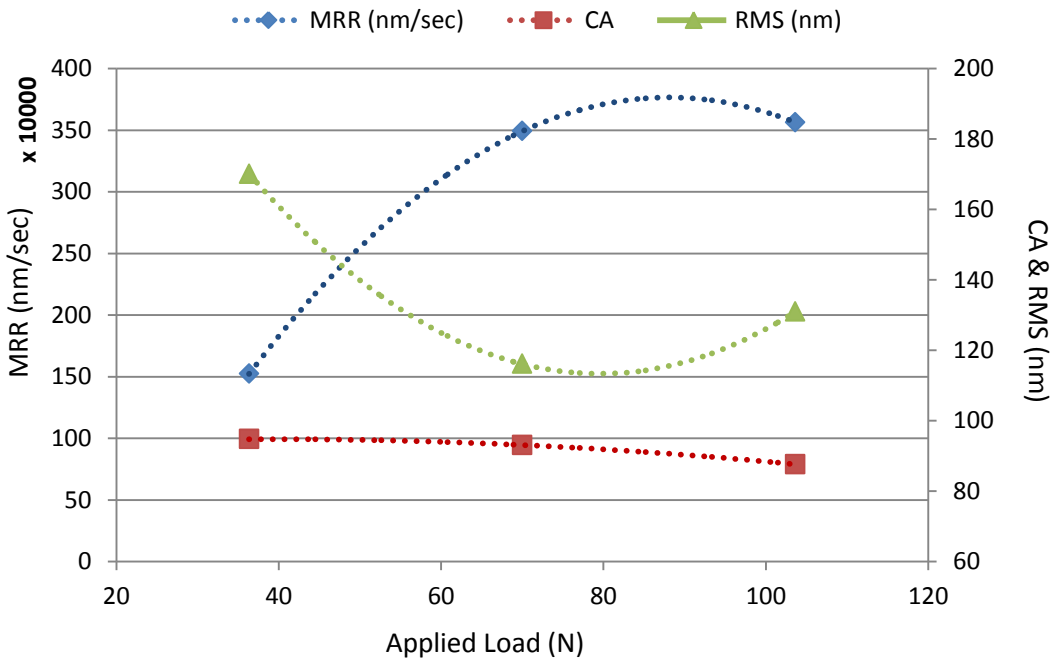

Figure 6.6 Material removal rate, roughness (RMS) and contact angle response as a function of applied down force.

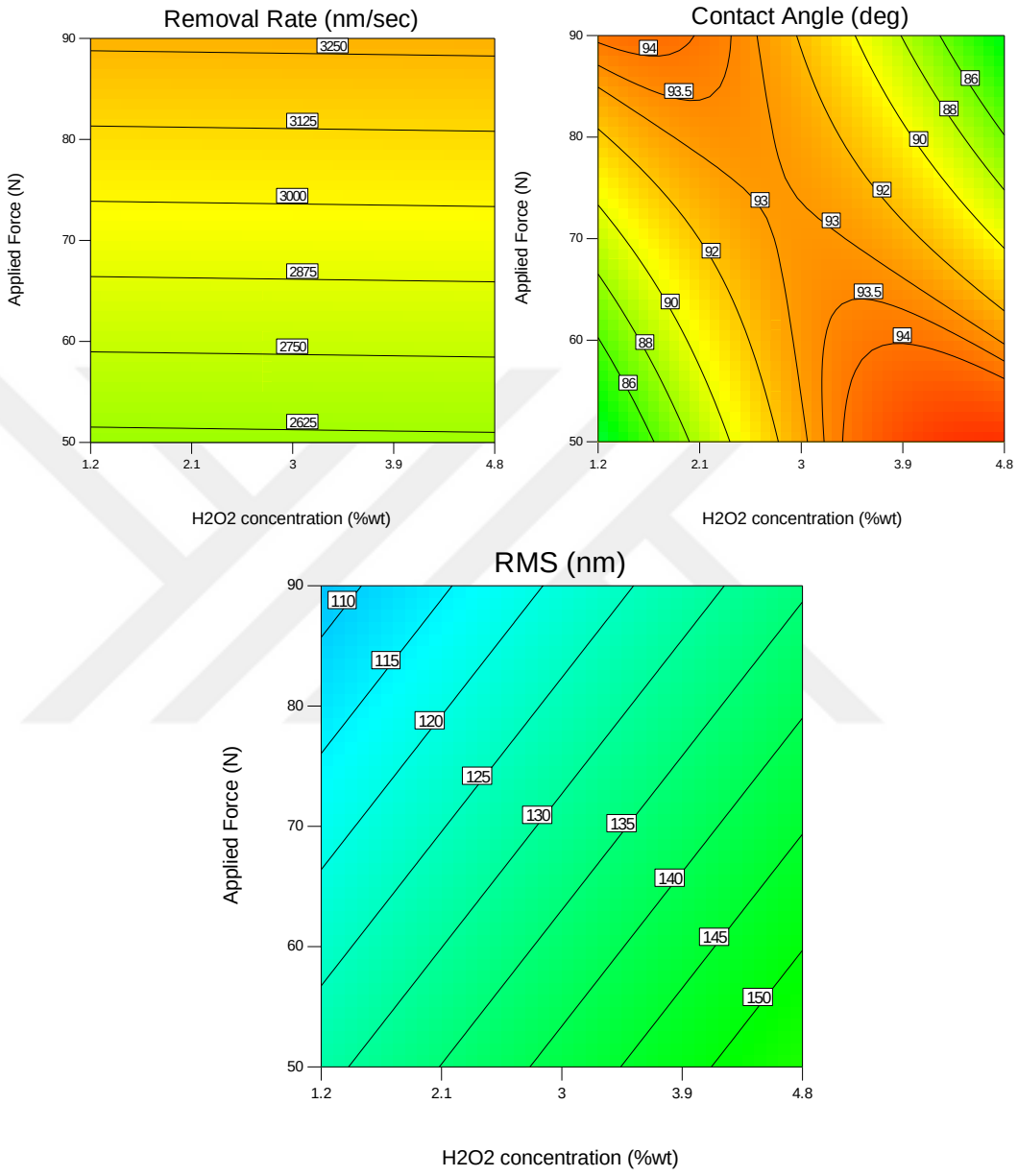

Figure 6.7 Contour graphs of the applied down force effect on material removal rate, wettability and roughness properties.

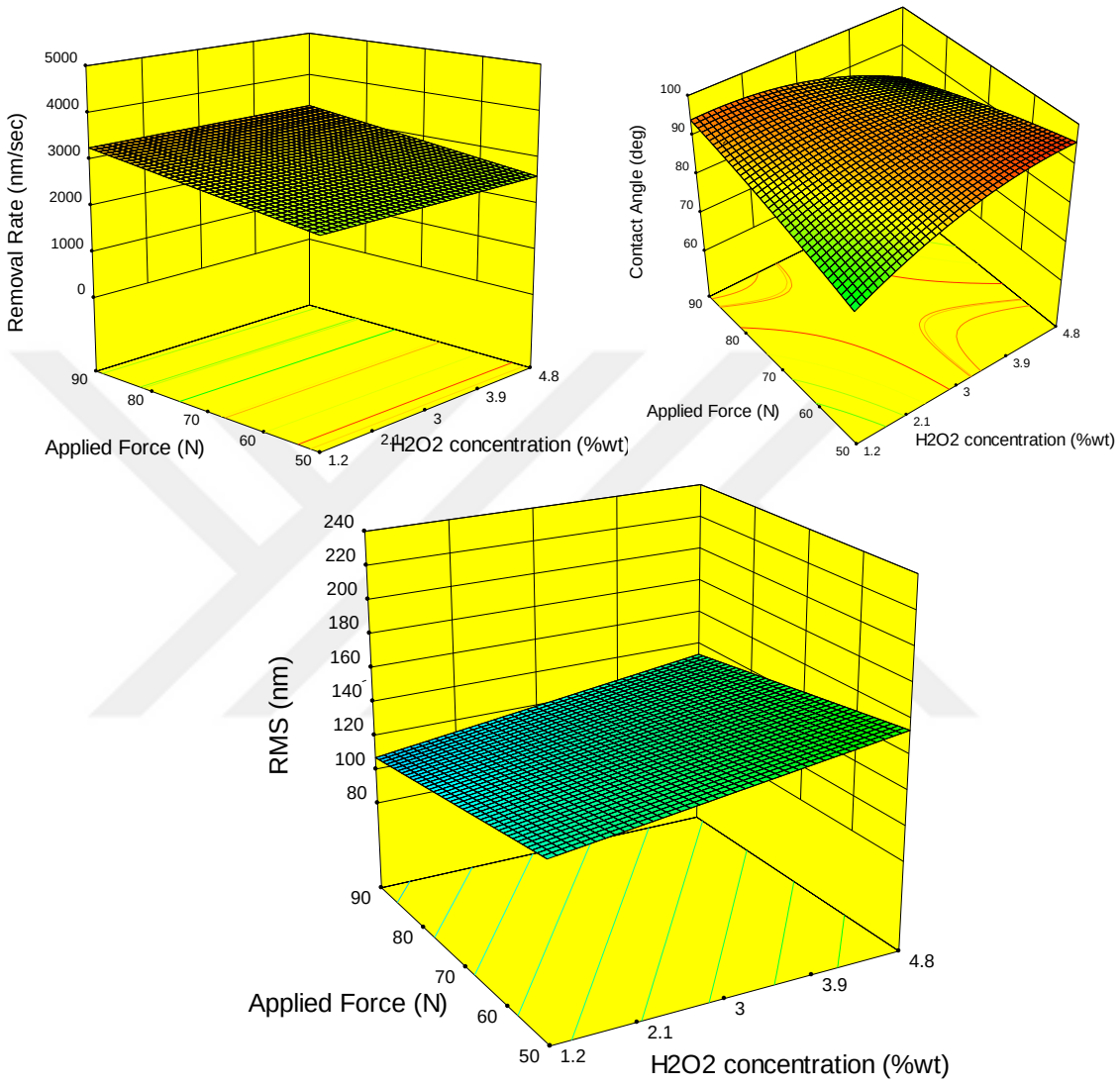

Figure 6.8 Effect of applied down force on material removal rate, wettability and roughness as 3D response.

6.3.3 Effect of oxidizer concentration on titanium surface structuring

The amount of oxidizer added into the CMP slurry changes the thickness of the surface oxide layer as explained in detail in Chapter 3. Therefore, oxidizer concentration was also evaluated as one of the input variables in the DoE model. Figure 6.9 gives the H_2O_2 concentration impact on the material removal rate, wettability and surface roughness responses. As can be seen in the Figure, increased H_2O_2 concentrations resulted in higher surface roughness values. However, increment of the oxidizer concentration is negligible on the wettability performance. Contour graphs of the oxidizer concentration effect on material removal rate, wettability and roughness properties are given in Figure 6.10 and Figure 6.11 as 3D surface responses of the each output units.

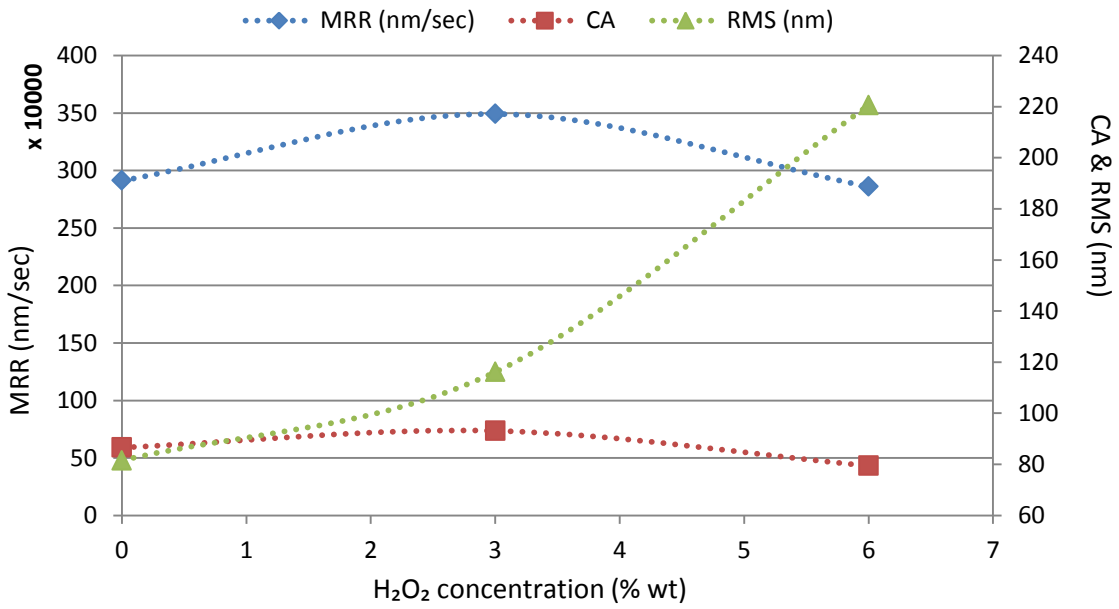

Figure 6.9 Material removal rate, roughness (RMS) and contact angle response as a function of H_2O_2 concentration.

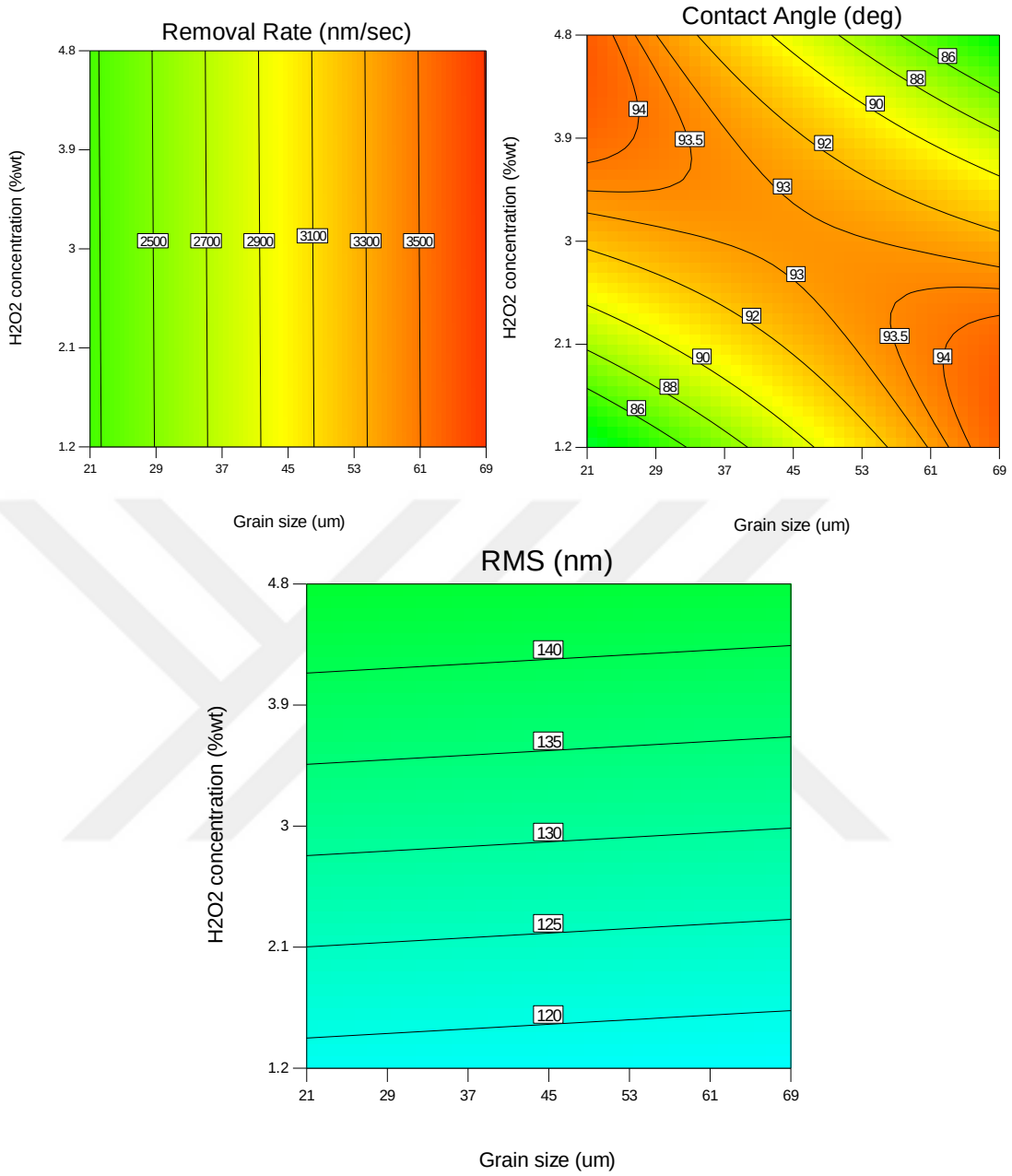

Figure 6.10 Contour graphs of the oxidizer concentration effect on material removal rate, wettability and roughness properties.

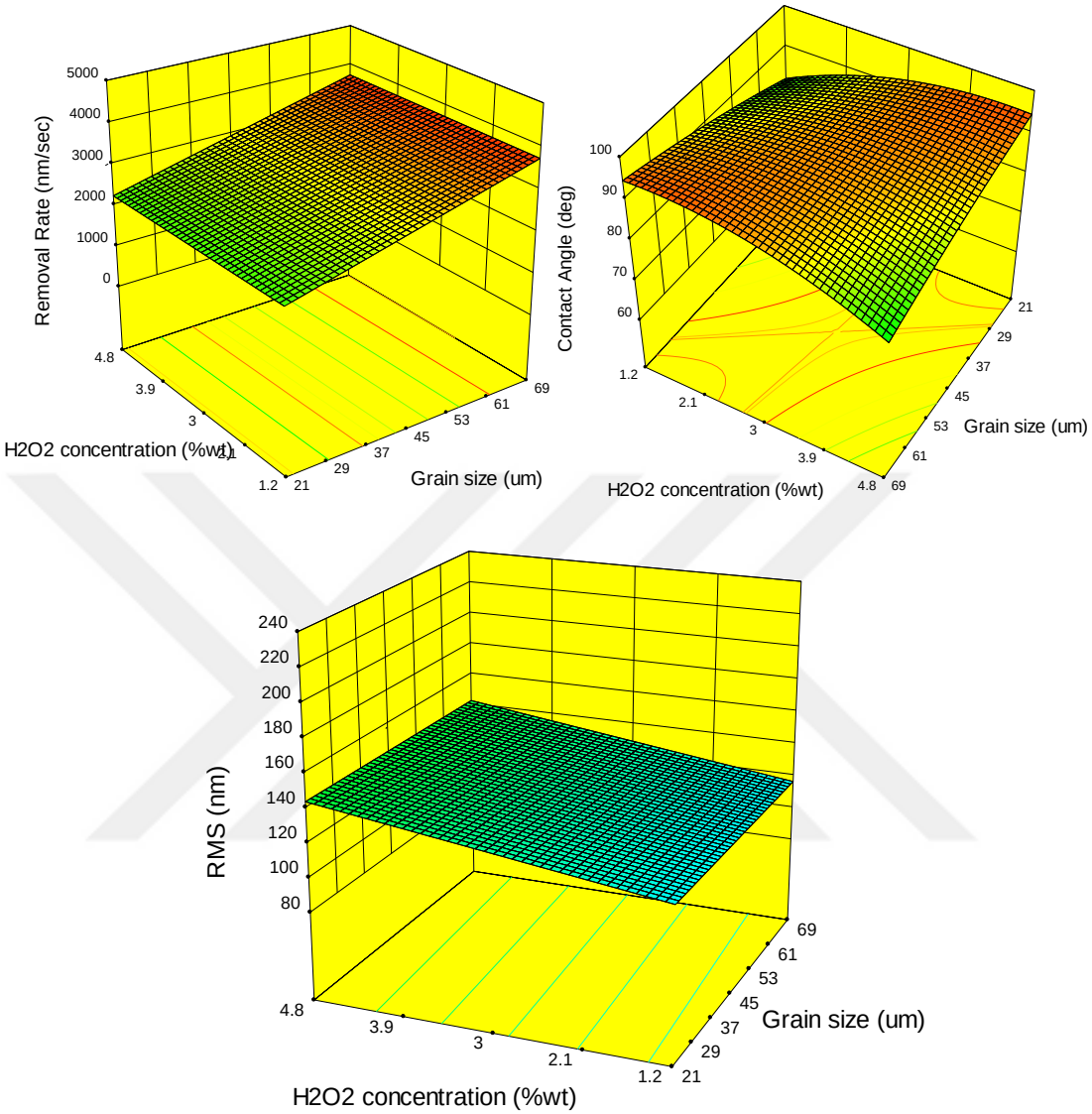

Figure 6.11 Effect of oxidizer concentration on material removal rate, wettability and roughness as 3D response.

6.3.4. Optimization

Design-Expert software's numerical optimization enables to maximize or minimize the responses according to the desired outputs. Since it is known that surface topography directly affects the biological responses such that the most desired outputs need to be optimized by determining the variables to obtain the optimal surface on the implant. Equations 6.1, 6.2 and 6.3 give the relationship of each response i.e, MRR, contact angle and surface roughness to the selected input variables

$$Removal\ Rate = 402.42 + 16.77 \times A + 31.01 \times B + 2.44 \times C \quad (6.1)$$

$$Contact\ Angle = -17.39 + 1.26 \times A + 1.33 \times B + 25.5 \times C - 0.01 \times A \times B - 0.18 \times A \times C - 0.14 \times B \times C - 1.94E^{-003} \times A^2 - 1.49E^{-003} \times B^2 - 1.16E^{-003} \times C^2 \quad (6.2)$$

$$Roughness\ (RMS) = 146.97 - 0.52 \times A - 0.03 \times B + 7.37 \times C \quad (6.3)$$

A: Applied Down Force (N)
B: Grain size (µm)
C: H_2O_2 concentration (wt%)

A dental implant is always in contact with both osteoblast and fibroblast cells when placed in the human month. Therefore, both type of cell reaction is important for a desired implantation performance. The desirability was determined by taking into account the factors that promote the cell attachment based on the biocompatibility analyses presented in Chapter 5. Initial results showed that the surface roughness and wettability are the main factors on the cell attachment response. However, the responses of the cell adherance showed variability depending on the type of the tissue. While higher hydrophilicity and moderate roughness promote fibroblast type cell attachment, high surface roughness with lower wettability is preferable by the osseo-type cells. We assume that, the effect of the roughness on the cell response mainly depends on the morphological properties of the cell. It has been documented in the literature that, fibroblast cells which are also called as soft tissue cells have a size range between 10 to 15μm, on the other hand osteoblast cells have a larger volume and sizes around ~20-30 μm.

Figure 6.12 represents the schematics of the cell adherence performance on the surface as a function of surface roughness and the cell type. As can be seen in the Figure 6.12.a small fibroblast cells cannot contact with the other cells when they are placed into the cavity areas of the rougher surfaces. Therefore, they have a better adherence performance on the smoother surfaces, which do not disrupt the cells proliferation. On the other hand, since it is known that increased roughness results in increased surface area, to ensure sufficient attachment to the larger osteoblast cells increased roughness helps increase the hard tissue cell attachment behavior on the implant surface as can be seen in Figure 6.12.b.

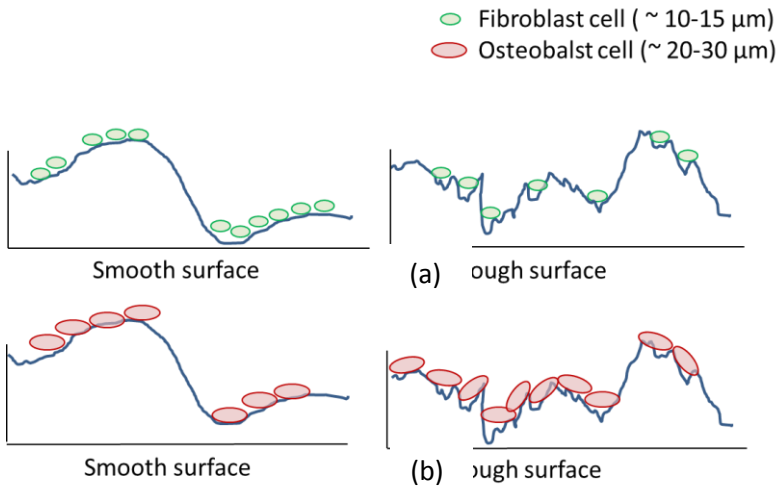

Figure 6.12 Schematics of the adhesion behavior of the (a) fibroblast and (b) osteoblast cells as a function of surface roughness

Based on the cell attachment evaluation, the desirability was evaluated for both of the cell types. The material removal rate is preferred to be at a minimum to keep the designed spec measurements of the implants. Based on the initial test results, higher wettability and moderate roughness were preferred for the desirability of the fibroblast cells. Figure 6.13 gives the desirability response with the chosen parameters with high desirability value 0.906713 obtained at ~80 N downforce and maximum oxidizer concentartion. On the other hand, higher roughness and lower contact angle values have been set for evaluating the desirability of the osteoblast cells. Figure 6.14 shows the desirability as a function of the grain size, and applied down force as a function of the oxidizer concentration on the surface with highest desirability value 1 was obtained. The results of the optimization showed that in order to obtain a sufficient fibroblast attachment, applied down force and grain size should be decreased for a given oxidizer concentration. On the other hand, for osteoblast type cells, it a reverse correlation was observed indicating higher desirability with the increased grain size and applied down force parameters.

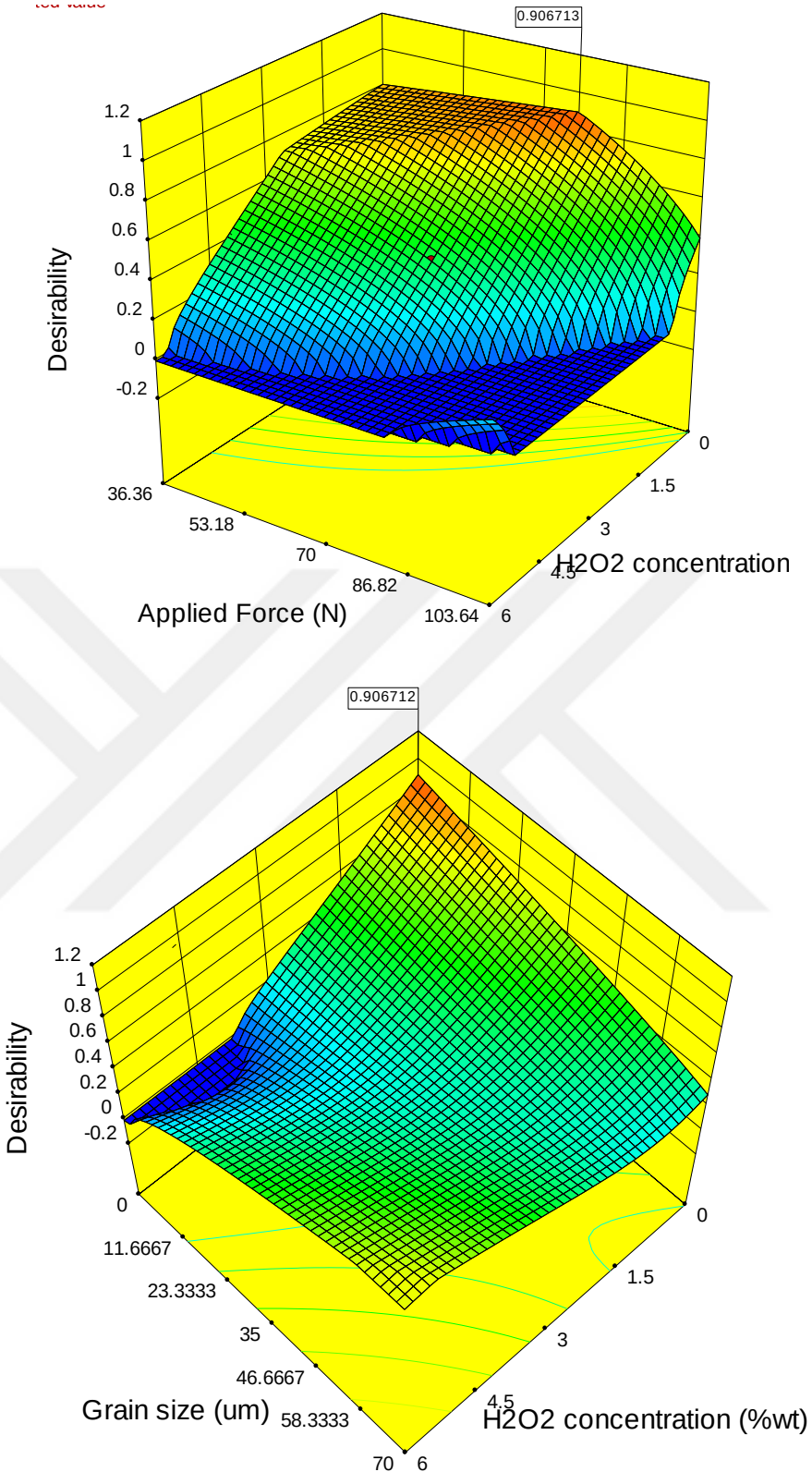

Figure 6.13 Desirability for optimal wettability performance based on the grain size and applied load for fibroblast cells

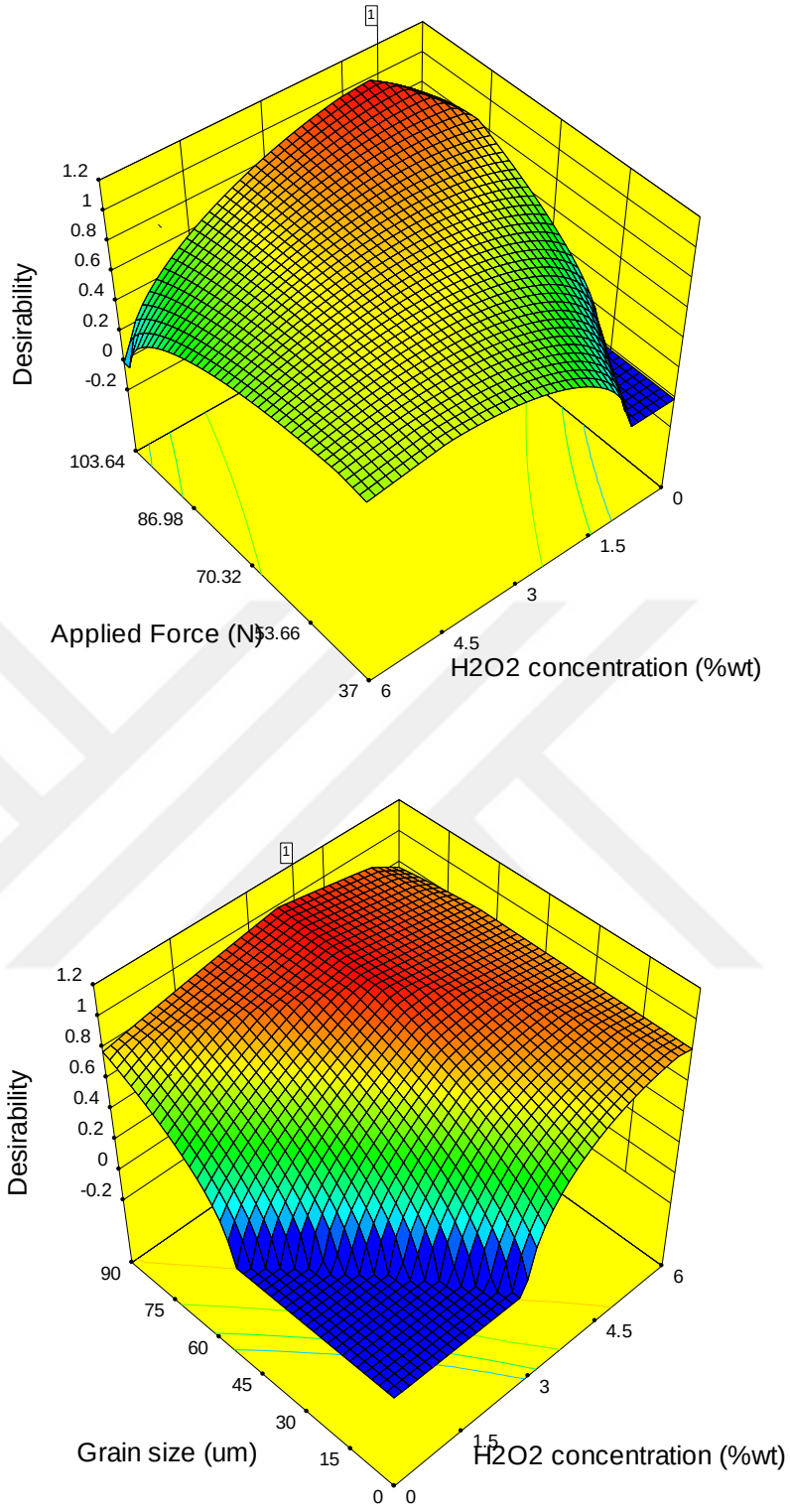

Figure 6.14 Desirability of the CCD model as a function of the surface responses for optimal osteoblast cell attachment.

6.4 Summary

The overall goal of this study is to achieve highly biocompatible implants with rapid and long term healing ability without any side effects in the human body after implantation. CMP process was evaluated on the titanium material as an alternative surface structuring method. After the evaluation of the slurry particle type, oxidizer concentration and pad type, optimization analyses were conducted in the final part of the dissertation.

A central composite design was utilized for the optimization of material removal rate, surface roughness and wettability performances as a function of the applied load, grain size and oxidizer concentration. Obtained results were assessed depending on the projected cell behavior based on the evaluations from the previous chapter with respect to the surface properties. Optimization results showed that the desired surface morphology changes depending on the nature of the cells. In the case of fibroblast cells, most desirable surface structuring was achieved by using small grain size and lower applied pressures. These findings are in agreement with the observations in Chapter 5. Yet the desirability for surface structuring for the osteoblast cells increased with the increased grain size and applied load which result in elevated surface roughness responses.

CHAPTER VII

SUMMARY AND SUGGESTIONS FOR FUTURE WORK

7.1 Summary

The use of titanium and titanium alloys as biomaterials for hard tissue replacement such as in dental and orthopedic applications has found more interest recently. Superior biocompatibility and stability of the titanium promotes implant tissue interactions in the aggressive body environment. Nature of the titanium leads it to form an oxide layer in the air media which is known to contribute to the biocompatibility of the titanium implant and promotes the bone tissue interaction in vivo. However, these excellent properties of titanium are still not sufficient to ensure the optimal healing process in the long term period. Therefore, the mechanical, structural and surface properties of the titanium are still being investigated to find a better implantation process. It has been documented that the manufacturing method of the implant has a major role on the surface quality of the end product. The adapted process directly influences the surface roughness and morphology properties, which are important parameters on the cell attraction ability of the implants. Hence, improvement of the available methods to obtain a desired surface on the implantable material is highly important. There are many processes used at present to alter the implant material surface such as sandblasting, acid etching, combination of blasting and etching process together, laser structuring and coating applications. However, none of them are optimal to ensure the best surface finishing for implant structuring due to the lack of precise control on surface contamination, degree and control of surface roughness and an adherent surface oxide formation.

In this study, we bring a new approach to alter the implant material surface through implementation of chemical mechanical polishing (CMP) process. The CMP process has initially been introduced for glass polishing and extended into the planarization of the interlayer metal connectors in the microelectronics manufacturing. The CMP process involves both chemical and mechanical components to alter the material surface chemically as well as topographically. In CMP, the top film surface of the material is exposed to the chemicals in the polishing slurry, which is made of submicron size particles and chemicals. This interaction forms a chemically altered top film that is removed by the mechanical action of the slurry abrasive particles. Therefore, it is a different method as compared to the mechanical polishing techniques used for implant surface finishing. The chemically altered top film has to be a protective oxide. This is critical for implants in stopping chemical corrosion and futher preventing Ti^{+4} ion dissolution in vivo. Furthermore, it has been shown by an earlier study that the application of CMP on Ti films has been very successful in terms of creating a titanium oxide film on the surface. Moereover, oxides are known to help promote biocompatibility. In addition, CMP can remove contaminated surface layers from machining processes that are used to shape the implant.

In this dissertation, we applied different CMP conditions on the titanium based implants to induce nano or micro scale roughness at the implant/surface interface in a controled manner. Particularly, we focused on the dental implants beyond the other bone replacement materials. In the case of dental implants, material surface should be compatible with both osteoblast and fibroblast tissues. These two different tissue cells have a distinct selectivity on the surface composition and roughness of the biomaterials.

Implementation of the CMP process on titanium bio-implants resulted in a synergy by (i) cleaning the implant surface from potentially contaminated surface layers by removing a nano-scale top layer during the process, (ii) simultaneously creating a pore free and continuous

nano-scale oxide film on the surface to limit any further contamination to minimize risk of infection and prevent corrosion and (iii) inducing controlled surface smoothness/roughness by designing the CMP process variables such as slurry particle size, solids loading as well as the oxidizer type and concentration. In order to demonstrate the use of CMP on dental implants, both titanium plates and dental implants were processed in this study. The CMP process was carried out by using alumina (Al_2O_3), silica (SiO_2) and titania (TiO_2) based slurry abrasives with different oxidizer (H_2O_2) concentrations on commercially pure (cp) Ti samples with different polishing pads to modify surface topography. Initially, CMP process affectivity has been evaluated on the samples through the material removal mechanism, surface roughness and wettability analyses for the optimal slurry and oxidizer combination selection to obtain desired properties. Additionally, mechanical properties of the processed substrates were examined through Vickers hardness and tensile strength analyses after CMP. The results showed that the CMP implementation did not affect the mechanical performance of the implant pieces significantly.

CMP implementation resulted in formation of an oxide film on the titanium. This film and its surface qualities were evaluated based on their crystallinity, composition and surface energy responses. XRR, EDX and XPS analyses showed that the formed oxide layer is TiO_2 and its crystal structure is different from the surface oxide layer which forms in air. In addition, electrochemical analyses of the samples showed that the CMP induced TiO_2 layer ensured passivity on the titanium surfaces. Furthermore, Pilling Bedworth (PB) ratio calculations also confirmed protective nature of the TiO_2 film formed when the baseline CMP process is implemented on the titanium plates. The most favorable PB ratio was obtained in the presence of 3% wt H_2O_2 in the CMP slurry.

In terms of the biological response, in vitro evaluations were performed by cytotoxicity tests in addition to the bacterial and cell attachment analyses as well as hydroxyapatite adhesion measurements through wet deposition. Cytotoxicity results of the CMP treated samples were an evidence of the inertness of the suggested new methodology in vivo. Furthermore, the cell

growth analyses conducted for fibroblast and osteoblast-like expound have confirmed surface morphology contribution to the cell attachment (healing) performance. The cell growth on implants was observed to be influenced more by the surface roughness. Yet, the cell attachment results have illustrated that there is an optimal roughness value where the cells are better adhering on the implant surfaces. This happens when the cell size matches the surface contours better. Furthermore, HA attachment results also confirmed that the CMP treated surfaces tend to help the HA deposition more than an etched surface although the surface roughness values were comparable. Surface free energy and work of adhesion analyses conducted on the samples also correlated to the biological cell responses indicating that the surface oxide composition and roughness impact the cell adhesion performance. These results clearly show that the CMP treated surfaces lead to a high biocompatibility for bone regeneration due to better bioactivities driven by the formed surface oxide layer. Furthermore, HA coating ensures insulation against the ion release from the titanium implants.

Finally, the preliminary CMP tests conducted on the 3-D dental implant surfaces also resulted in similar CMP responses as compared to the 2-D substrates confirming that the CMP application can help enhancing the surface properties of the titanium based implants.

7.2 Suggestions for Future Work

The outcomes reported in this study can be further expanded to investigate several other issues, which are critical to improve implantation performance of the titanium based bio-implants. Although the findings from this dissertation are impeccable and useful in understanding the fundamentals and help development of the CMP process on biomedical implants, several new questions are arised requring some additional directions to be recommended to continue this study in future investigations.

First of all, the CMP process as it is set-up today is suitable for the treatment of the 2D plates. Although the preliminary evaluations were conducted here with the titanium plates in order to evaluate the performance and affectivity of the CMP process, there is a need to expand

the CMP process into a 3-D platform for processing of 3D implants. Hence one of the major challenges facing the adaptability of CMP process in biological implantation is its extension to the 3D objects. The preliminary evaluations were conducted on the dental implants with an automatic polymeric brush in order to evaluate the coherence with the 2D test results. This solution ensures a sufficient pad (brush)-titanium contact for a homogenous surface treatment. Yet, this technique is not suitable for the control of applied force over the given area or in other words the pressure. Therefore, the system needs a new design for 3D CMP process suitable for 3D implant materials. As a suggestion, a preliminary system was designed with a robotic arm that can hold the implant screw towards the CMP pad material. An additional force-torque sensor is adapted in between the robotic arm and the sample holder to ensure the controlled load over the surface area. Various pad materials can be used to enable to best results of polishing on the sample surface. Of course this design should be evaluated based on the slurry abrasive characteristics, pad material type, slurry solids loading and oxidizer concentration perspectives. Once configured, this design can be adapted to different implant structures beyond the dental implants. This proposition may lead to a new industrial application with new consumables, which are needed to be adapted according to the special implant type.

The other suggestion for the CMP treated surfaces may be addition of bioactive coatings after the CMP implementation for a rapid healing process. This can be performed by using bioactive materials that can stimulate cell growth and promote the interaction at the tissue/material interface. Additionally, the induced coating interface may help increase the cell adhesion and proliferation performance on the implant surface.

One final suggestion for future work is the evaluation of the treated samples via biocompatibility performance through in vivo test conditions to observe the real time healing performances. Cell responses of the treated samples were examined in vitro in this dissertation but the cells are known to have a complicated and sensitive healing reaction when in contact with the biomaterials which needs to be further investigated. In order to have a well-defined implant surface finish, animal tests must be conducted for biocompatibility. Therefore, in vivo

studies are suggested following the 3D CMP as a part of the future work in order to understand the complete adaptability of CMP as a new and novel method for titanium based implant material surface engineering.

LIST OF REFERENCES

Ade81 R. Adell, U. Lekholm, B. Rockler, P.I. Brånemark, International Journal of Oral Surgery, 10, 387-416 (1981).

Alb81 T. Albrektsson, P.I. Branemark, H.A. Hansson, H.A., J. Lindstrom, J. Acta orthopaedica Scandinavica, 52, 155-170 (1981).

Ali05 T. Aliouane, D. Bouzid, Belkhir, S. Bouzid, V. Herold, J. phys, 124,123,128 (2005).

Ani11 S.Anil, P.S. Anand, H. Alghamdi and J.A. Jansen, Implant Dentistry - A Rapidly Evolving Practice", ISBN 978-953-307-658-4 (2011).

Ank98 R. Anklekar, M., Borkar, S. A., Bhattacharjee, S., Page, C. H. and Chatterjee, A. K., Colloids Surf. A, 133, 1–2, 41–47 (1998).

Ans00 K. Anselme, et al., Biomaterials, 21, 15, 1567-77 (2000).

Arc01 I. arc a, D. Drees, J.P. Celis, Wear, 249, 452-460 (2001).

Att94 AT&T Bell Laboratory, Solid State Technol. 37, 12, 26 (1994).

Bal11 A. M. Ballo, O. Omar, W. Xia, A. Palmquist, Implant Dentistry - A Rapidly Evolving Practice, ISBN: 978-953-307-658-4 (2011).

Bas11 G.B. Basim, Lambert Academic Publishing, ISBN 978-3-8433-6346-4 (2011).

Bas12 G.B. Basim, Z. Ozdemir, A. Karagoz, MRS Proceedings, 1464, http://dx.doi.org/10.1557/opl.2012.1469. (2012).

Bas13 G.B. Basim, A. Karagoz, Z. Ozdemir, MRS Proceedings, 1560, http://dx.doi.org/10.1557/opl.2013.876, (2013).

Bas14 G.B. Basim, O. Bebek, S.O. Orhan, Z. Ozdemir, Mater. PCT Patent Application, PCT/TR2014/000530 (2014).

Bau13 S. Bauer, P. Schmuki, K. von der Mark, J. Park, Proggree in Material Science, 58, 261-326 (2013).

Bha03 S.S. Bhasin, V. Singh, T. Ahmed, B.P. Singh, Ceram Eng Sci Proc, 24, 245-254 (2003).

Bic02 J. Bico, U. Thiele, D. Quere, Colloids Surf. A Physicochem. Eng. Asp. 206, 41–46 (2002).

Bla92 J. Black, Biological Performance of Materials: Fundamentals of Biocompatibility Marcel Dekker, New York, (1992).

Born08 M.M. Bornstein, P. Valderrama, A.A Jones, T.G Wilson, R. Seibl, D.L. Cochran, D.L. Clinical oral implants research, 19, 233-241 (2008) .

Bou12 D. Bouzid, N. Belkhie, T. Aliouane, IOP Conf. Series: Materials Science and Engineering 28 (2012).

Bra00 A. E. Braun, Semiconductor International, 23 (10), 55 (2000).

Bra09 I. Braceras, M.A De Maeztu, J.I. Alava, C. Gay-Escoda, Int J Oral Maxillofac Surg, 38, 3, 274-278 (2009).

Bra69 P.-I. Brånemark, U. Breine, R. Adell, B.O. Hansson, J. Lindström, Å. Ohlsson, Scandinavian Journal of Plastic and Reconstructive Surgery and Hand Surgery, 3, 81-100 (1969).

Bud04 D.R. Buddy, S.H. Allan, J.S. Frederick, E.L. Jack, Biomaterials science: an introduction to materials in medicine, second ed. Elsevier (2004).

Bus98 D. Buser, T. Nydegger, et al, Int J Oral Maxillofac Implants, 13, 611-619 (1998).

Cac01 P. Cacciafesta, K.R. Hallam, et al., Surface Science, 491, 405-420 (2001).

Caw03 J.Cawley, et. al, Wear 255, 7, 996-1006 (2003).

Cha03 V.S. Chathapuram, T. Du, K.B. Sundaram, V. Desai, Microelectron. Eng. 65, 478–488 (2003).

Cho03 S.A. Cho, K.T. Park, Biomaterials, 24, 3611-3617 (2003).

Cho11 Y.J. Cho, S.J. Heo, J.Y. Koak, S.K. Kim, S.J. Lee, J.H. Lee, Int. J. Oral Maxillofac. Implants 26,1225–1232 (2011).

Coc98 D.L. Cochran, R.K. Schenk, A. Lussi, et al., J Biomed Mater Res, 40,1-11 (1998).

Coe09 P.G. Coelho, G. Cardaropoli, M. Suzuki, JE Lemons, Clin Implant Dent Rel Res., 11, 4, 292-302 (2009).

Cox92 P.A Cox, Transition Metal Oxides, Oxford University Press,Oxford, ISBN 0-19-855925-9 (1992).

Cro12 K. Li, K. Crosby, M. Sawicki, L.L. Shaw, Y. Wang,J. Biotechnol. Biomaterials 2 (2012).

Dad07 M.Dadfar, et. al, Mater Lett., 61, 11, 2343-2346 (2007).

Dav03 Davis JR. ASM International. Handbook of materials for medical devices. Materials Park, OH: ASM International, (2003).

Dep05 H. Deppe, Warmuths,A. Heinrich, T. Kroner, Lasers Med Sci 19, 229-33 (2005).

Die01 A. Dietrich, A. Neubrand, J. Am. Ceram. Soc., 84, 4, 806–12 (2001).

Dob83 Dobbs HS, Robertson JLM. J Mater Sci 18, 391–401 (1983).

Dud12 D. Duddeck, S. Iranpour, M.A. Derman, J. Neugebauer, J. E. Zöller, EDI Clinical Science 48-58 (2012).

Eli08 C.N. Elias, J.H.C. Lima, R. Valiev, M.A. Meyers,JOM Biol. Mater. Sci. 60, 46–49 (2008).

Eli10 C.N. Elias, L. Meirelles, Expert review of medical devices, 7, 241-256 (2010).

Esp10 F.A.Espana, et. al, Mater. Sci. E.C, 30, 1, 50-57 (2010).

Euc05 B. Eugeniu, M.M. Jan, T. Luciano, S. Patrik, Electrochemistry Communications 7, 10, 1066 (2005).

Fin07 M. P. Finnegan, H. Zhang, and J. F. Banfield,J. Phys. Chem. C, 111, 1962–8 (2007).

Fio15 J. Fiorellini, K. Wada, P.Stathopoulou, P. R. Klokkevold, Periimplant Anatomy, Biology, and Function, Chapter 71 (2015).

Gag00 A. Gaggl, G. Shultes, W.D. Muller, H. Karcher, Biomaterials 21,1067-73 (2000).

Gal05 C. Galli, S. Guizzardi, G. Passeri, D. Martini, A. Tinti, G. Mauro, G.M. Macaluso, Journal of periodontology, 76, 364-372 (2005).

Gar12 H. Garg, G. Bedi, A.Garg, Journal of Clinical and Diagnostic Research. 6, 2, 319-324 (2012).

Gav14 L.Gaviria, J.P. Salcido, T. Guda, J.L. Ong, J. Korean Assoc. Oral Maxillofac Surg., 40, 50-60 (2014)

Gbi13 Global Business Intelligence (GBI) research, Dental Implany Market to 2018 (2013).

Gee09 M. Geetha, A.K. Singh, R. Asokamani, A.K. Gogia, Progress in Materials Science, 54, 397-425 (2009).

Gem07 E. Gemelli, N.H.A. Camargo, Matéria (Rio J.) 12, 525–531 (2007).

Ger05 J. Geringer, B. Forest, P. Combrade, Wear, 259, 943-951 (2005).

Gli16 Glidcop, North American Hoganas, Inc. (2016).

Got97 M. Gottlander, C.B. Johansson, T. Albrektsson, Clin. Oral Imp. Res 8, 345–355 (1997)

Gul04 H. Guleryuz, H. Cimenoglu, Biomaterials 25, 3325–3333 (2004).

Gup08 A.Gupta, M. Dhanraj, G. Sivagami, the Internet journal of Dental Science, 7, 1 (2008).

Gup10 A.Gupta, M. Dhanraj, G. Sivagami, Indian J. Dent. Res., 21, 433-438 (2010).

Gur08 B.C. Gurgel, P.F. Goncalves, S.P. Pimentel, F.H. Nociti, E.A. Sallum, A.W. Sallum, M.Z.Casati, Journal of periodontology, 79, 1225-1231 (2008).

Hah70 H. Hahn, W. Palich, J Biomed Mater Res 45, 71-77 (1970).

Hal03 C. Hallgren, H. Reimers, D. Chakarov, J. Gold, A.Wennerberg, Biomaterials, 24, 5, 701–710 (2003).

Has04 A.W. Hassel, Minimally Invasive Therapy & Allied Technologies, 13:4, 240-247 (2004).

He09 F.M.He, G. L. Yang,Y.N. Li, X. X. Wang, S. F. Zhao, International Journal of Oral & Maxillofacial Surgery, 38, 6, 677–681 (2009).

Hem12 G. Hemlata, B. Gaurav, G. Arvind, Journal of Clinical and Diagnostic Research 6, 2, 319-324 (2012).

Hep82 C. Hepburn, Polyurethane elastomers, London: Applied Science (1982).

Her08 Y. Herr, J. Woo, Y. Kwon, J. Park, S. Heo, S. J. Chung, Key Engineering Materials, 361, 849-852 (2008).

Her11 H. Hermawan, D. Ramdan, J.R.P. Djuansjah, Metals for Biomedical Applications, in: R. Fazel-Rezai (Ed.) Biomedical Engineering - From Theory to Applications, InTech, (2011).

Hoe94 D.W. Hoeppner, V. Chandrasekaran, Wear, 173, 189-197 (1994).

Hsu10 S.-H. Hsu, W.M. Sigmund, Langmuir 26, 3, 1504–1506 (2010).

Ila05 S. Ilango, G. Raghavan, M. Kamruddin, S. Bera, A.K. Tyagi, Appl. Phys. Lett. 87, 101911 http://dx.doi.org/10.1063/1.2042537 (2005).

Jai94 R. Jairath, M. Desai, M. Stell, R. Tolles and D. Scherber-Brewer, in Advanced Metallization for Devices and Circuits-Science, Technology and Manufacturability, Pittsburgh, PA (1994).

Jan93 J.A.Jansen, J.G.C. Wolke, S. Swann, J.P.C.M. van der Waarden, K. Groot, Clinical Oral Implants Research, 4, 28-34 (1993).

Jas93 W. Jasen, et al, Clin. Oral Imp. Res., 4, 28-34 (1993).

Jún11 J.R.S.M. Júniora, R.A. Nogueiraa, R.O. Araújoa, Mater. Res. 14, 107–112 (2011).

Kal07 S. Kalyan, B.M Moudgil, Particle technology in CMP, Kona 25 (2007).

Kar15 A. Karagoz, V.Craciun, G. B.Basim, ECS Journal of Solid State Science and Technology, 4, 2, 1-8 (2015).

Kau91 F.B. Kaufman., D.B. Thomson, R.E. Broadie, M.A. Jaso,W.L. Guthrie,M.B. Pearson,M.B. Small, J. Electrochem. Soc. 138, 3460 (1991).

Ken13 H. Kenar, E. Akman, E. Kacar, A. Demir, H. Park, H. Abdul-Khalid, C. Aktas, E. Karaoz, Colloids Surf. B: Biointerfaces 108, 305–312 (2013).

Kim08 H. Kim, S.-H. Choi, J.-J. Ryu, S.-Y. Koh, J.-H. Park, I-S.Lee, Biomed. Mater. 3 1748-6041/3/2/025011, (2008).

Koh03 M. Kohn, Y.S. Eizenberg, Diamond J. Appl. Phys. 94, 3015 (2003).

Kok90 T. Kokubo, H. Kushitani, S. Sakka, T. Kitsugi and T. Yamamuro, J. Biomed. Mater. Res., 24, 721-734 (1990).

Kum05 S.S. Kumar, B.Stucker, Proceedings of th 16th Solid Freeform Fabrication Symposium, (2005).

Kur05 A. Kurella, N.B. Dahotre, J. Biomater. Appl. 20, 4–50 (2005).

Kur14 N. Kurgan, Mater Des, 55, 235-241 (2014).

Lac98 W.R. Lacefield, Implant Dent, 7, 4, 315-22 (1998).

Lam09 A. Lambotte, Presse Med Belge, 17 321-323 (1909).

Lan95 W.A. Lane, The British Medical Journal, 1, 861-863 (1895).

Lee12 M.-J. Lee, B.-O. Kim, S-J.Yu, J. Periodontal. Implant. Sci. 42, 127–135 (2012).

LeG07 L. Le Guehennec, A. Soueidan, P. Layrolle, Y. Amouriq, Dental matrials: official publication of the academy of ental Materials, 23,844-854 (2007).

Li02 D. Li, S.J. Ferguson, T. Beutler, D.L Cochrsn, C. Sitting, H.P. Hirt, D. Buser, Journal of Biomedical and Material Research, 60, 325-332 (2002).

Li04 L.H. Li, Y.M. Kong, H.W. Kim, et al., Biomaterials 25, 2867-75 (2004).

Li12 K. Li, K. Crosby, M. Sawicki, L.L. Shaw, Y. Wang, J. Biotechnol. Biomaterials, 2 (2012).

Li94 P. Li,I. Kangasniemi, K. De Groot, Journal of the Ceramic Society, 77, 5, 1307-1312 (1994).

Li99 D.-H. Li, B.-L. Liu, J.-C. Zou, K.-W. Xu, Implant. Dent. 8, 289–294 (1999).

Lin98 J. Lincks, B.D. Boyan,et al., Biomaterials 19, 2219-2232 (1998).

Lon98 M. Long, H.J. Rack, Biomaterials, 19, 1621-1639 (1998).

Lua02 H. Lua, B. Fookesa, Y. Obeng, S. Machinskia, K.A. R,chardsona, Materials Characterization, 49,35 (2002).

Lum01 N. Lumbikanonda, R. Sammons, Int. J. Oral Maxillofac. Implants 16, 627–636 (2001).

Ma12 T. Ma, P. Wan, Y. Cui, G. Zhang, J. Li, J. Liu, Y. Ren, K. Yang, L. Lu, Journal of Materials Science & Technology, 28, 647-653 (2012).

Man10 G. Manivasagam, D. Dhinasekaran, A. Rajamanickam, Recent Patents on Corrosion Science, 2, 40-54 (2010).

Man17 N.S. Manam, W.S.W. Harun, D.NA. Shri, S.A.C. Ghani, T. Kurniawan, M.. Ismail, M.H.I. Ibrahim, Journal of Alloy and Compounds, 701, 698-715 (2017).

Mas02 C. Massaro, et al , J.Mater Sci Mater Med, 13, 6, 535-48 (2002).

Mat01 L.F. Matthew, C. Miroslav, P.R. Masa, F. F. Lange, J. Am. Ceram. Soc., 84, 4, 713–18 (2001) .

Mat11 M.T. Mathew, M.J. Runa, M. Laurent, J.J. Jacobs, L.A. Rocha, M.A. Wimmer, Wear, 271, 1210-1219 (2011).

Mdo04 D. MacDonald, B. Rapuano, N. Deo, M. Stranick, P. Somasundaran, A. Boskey, Biomaterials, 25, 3135-3146 (2004) .

Mir07 N. Mirhosseini, P.L. Crouse, M.J.J. Schmidth, D. Garrod, Appl. Surf. Sci. 253, 7738–7743 (2007).

Mis13 S. Mischler, A.I. Munoz, Wear, 297, 1081-1094 (2013).

Mob09 I. Mobasherpour, M.S. Hashjin, S.S.T. Razavi, R.D. Kamachali, J. Ceram. Int. 351569–1574 (2009).

Mom12 A. Mombelli, N. Muller, N. Cionca, Clin Oral Implants Res, 23 ,6, 67-76 (2012).

Nat10 A.J. Nathananel, D. Mangalaraj, N. Ponpandian, Compos. Sci. Technol. 70, 1645–1651 (2010).

Nay10 A.K. Nayak, Int. J. ChemTech Res. 2, 903–907 (2010).

Ngu01 V. H. Nguyen, A.J. Hof, H. van Kranenburg, P. H. Woerlee and F. Weimar, Microelectronic Engineering, 55, 305 (2001).

Noo87 R.Van Noort,Journal of Material Science, 22,3801-3811 (1987).

Obe13 M. Oberringer, E. Akman, et al., Mater. Sci. Eng. C 33, 901–908 (2013).

Oka09 S. Okawa, K. Watanabe, Dent. Mater. J. 28, 68–74 (2009).

Ori00 G. Orsini, B. Assenza, A. Scarano, M. Piattelli, M., A. Piattelli, The International journal of oral & maxillofacial implants, 15, 779-784 (2000).

Ors00 G. Orsini, B. Assenza, A. Scarano,M. Piatteli, A. Piatteli, Int J Oral Maxillofac Implants 15, 6, 779-784 (2000).

Ors00 G. Orsini, B.Assenza, Int J. Oral Maxillofac Implants, 15, 779-784 (2000).

Ozd16 Z. Ozdemir, A. Ozdemir, G.B. Basim, Materials Science and Engineering C 68, 383–396 (2016).

Pan82 P.J. Pan, C.H. Ting, IEEE Trans. Ind. Electron. IE-29,154 (1982).

Pan96 J. Pan, D. Thierry, C. Leygraf, Electrochimica Acta, 41, 1143-1153, (1996).

Paq06 D.W. Paquette, N. Brodal, R.C. Williams, Dent. Clin. North Am. 50, 361-374 (2006).

Par12 P. Parida, A. Behera, S. Mishra, International Journal of Advances in Applied Science, 1, 31-35 (2012).

Pat16 Pranav S Patil, M. L. Bhongade, IOSR Journal of Dental and Medical Sciences (IOSR-JDMS), 15, 10, 132-141, (2016).

Poh02 Pohl M. Heβing C., Fenzel J. Mater Corros 53, 673, (2002).

Pon03 L. Ponsonnet, K. Reybeir, et al.,, Materials Science and Engineering C, 23, 551-560 (2003)

Por04 A.E. Porter, S.M. Rea, M. Galtrey, S.M. Best, Z.H., J Mater Sci 39, 1895–1898 (2004).

Pos03 L. Postiglione, G.D. Domenico, et al., J. Dent. Res. 82, 9, 692-696 (2003).

Rat04 B.D. Ratner, A.S. Hoffman, F.J. Schoen, J.E. Lemons JE. Biomaterials science. Amsterdam: Elsevier; (2004).

Rec01 L.Reclaru, et. al, Biomaterials, 22, 3, 269-279 (2001).

Reo02 S. Roessler, R. Zimmermann, D. Scharnweber, C. Werner, H. Worch, Colloids and Surfaces B: Biointerface 26, 387-395 (2002).

Rol11 A. Rolando, T. McLachlan, et al., Biomaterials, 32, 3395-3403 (2011).

Ros91 E.S. Rosenberg, J.P. Torosian, J. Slots, Clin. Oral Implants Res, 2, 135-144, (1991).

Run96 S. R. Runnels, J. Electron. Mater., 25, 1574 (1996).

Sam05 R.L. Sammons, N. Lumbikanonda, M. Gross, P. Cantzler, Clinical oral implants research, 16, 657-666 (2005).

Sam09 B. Sameer, D. Steve, J. Bruce, M. Jitka, P. Simon, Applied Surface Science, 255, 4873-4879 (2009).

SaM99 E. SaMcCafferty, J.P. Wightman, Appl. Surf. Sci. 143, 92–100 (1999).

SaM99 E. SaMcCafferty, J.P. Wightman, An X-ray photoelectron spectroscopy sputter profile study of the native air-formed oxide film on titanium, Appl. Surf. Sci. 143 (1999) 92–100.

San05 A. S. Santiago, E. A. dos Santos, M. S. Sader, M. F. Santiago, and G. de Almeida Soares, Brazilian Oral Research, 19,3, 203–208, (2005).

Sch03 L. Scheideler, F. Rupp, W. Lindemann, D. Axmann, G. Gomez-Roman, J. Geis-Gerstorfer, H. Weber, J Dent Res, 82, B241-B241 (2003).

Sch08 P. Schmutz, N.-C. Quach-Vu, I. Gerber, Electrochem. Soc. Interface 1, 35–40 (2008).

Sha06 A.G. Shard, P.E. Tomlins, Regan Med. 1, 789-800 (2006).

Sho13 M. dat-Shojai, M.-T. Khorasani, E. Dinpanah-Khoshdargi, A. Jamshidi, Acta Biomater. 9, 7591–7621 (2013).

Sin12 R.G. Singh, J. Dent. Implant, 2, 15–18 (2012).

Sit99 C. Sitting, M. Textor, N.D. Spencer, J.Mater. Sci. Mater. Med. 10, 35–46 (1999).

Ste97 J.M. Steigerwald, S.P. Murarka and R.J. Gutmann, Chemical Mechanical Planarization of Microelectronic Materials, John Wiley and Sons, New York, NY (1997).

Suc07 M. Suchea, S. Christoulakis,et al., Materials Science and Engineering B 144, 54 (2007).

Sul02 Y.T. Sul, C.B. Johansson, S. Petronis, et al. Biomaterials 23, 491-501 (2002).

Sul03 Y-T. Sul, Biomaterials, 24, 22, 3893–3907 (2003).

Sul05 Y.T. Sul, et al., Int J Oral Maxillofac Implants, 20, 3, 349-59 (2005).

Syk04 N. Sykaras, D. Woody Ronald, M. Lacopino Anthony, R. Triplett Gilbert, E. Nunn Martha, Int J Oral Maxillofac Implants, 19, 5, 667-78 (2004).

Tak03 M. Takeuchi, Y. Abe, Y. Yoshida, Y. Nakayama, M. Okazaki, and Y. Akagawa, Biomaterials, 24, 10, 1821–1827 (2003).

Tan07 Y. Tanaka, E. Kobayashi, S. Hirotomo, K. Asami, H. İmai, T. Hanawa, J. Mater. Sci. Mater. Med. 18, 797–806 (2007).

Tar98 Tari, G., Ferreira, J. M. F. and Lyckfeldt, O., J. Eur. Ceram.Soc., 18, 5, 479–486 (1998).

Tho97 P. Thomsen, C. Larsson, L.E. Ericson, L. Sennerby, J. Lausma, B. Kasemo, Journal of Material Science: Materials in Medicine, 8, 653-665 (1997).

Tri99 J. Trice, T.D. Fletcher, L.C. Hardy and J. Kollodge, 3-M Company, CAMP 3rd Annual International Symposium on CMP, Lake Placid, NY (1999).

Utt91 R. R. Uttecht and R. M. Geffken, Proc. 8th VMIC, Santa Clara, CA, 20 (1991).

Van04 P. Vanzillotta, G. A. Soares, I. N. Bastos, R. A. Sim˜ao, and N. K. Kuromoto, Materials Research, 7, 3, 437–444 (2004).

Var08 F. Variola, Y.-H. Yi, L. Richert, J.D. Wuest, F. Rosei, A. Nanci, Biomaterials 29, 1285–1298 (2008).

Vas11 C. Vasilescu, P. Drob, E. Vasilescu, I. Demetrescu, D. Ionita, M. Prodana, S.I. Drob, Corrosion Science, 53, 992-999 (2011).

Vel00 P. Velden, Microelectron. Eng., 50, 41 (2000).

Ver93 C.C. Verheyen, W.J. Dhert, P.L. Petit, P.M Rozing, K. Groot, J. Biomed Mater Res., 104-112 (1993).

Vog98 E.A. Vogler, Adv. Colloid. Interf. Sci. 74, 1, 69 (1998).

VSa76 Vander Sande JB, Coke JR, Wulff J. Metall Trans A, 7, 389–97 (1976).

Wen95 A. Wenerberg, T. Albrektsson, B. Andersson, J.J. Krol, Clin. Oral Implants Res., 6, 24-30 (1995).

Wen96 A.Wennerberg, T. Albrektsson, B. Andersson, Int. J. Oral Maxillofac. Implants, 11, 38–45 (1996).

Wen97 A. Wenerberg, A. Ektessabi, T. Albrektsson, C. Johansson, B. Andersson,. Int. J. Oral Maxillofac Implants, 12, 486-494 (1997).

Wen98 A. Wennerberg, International Journal of Machine and Tools Manufacturing, 38-657-662 (1998).

Wil81 Williams DF. Biocompatibility of clinical implant materials. Boca Raton, Fla: CRC Press; (1981).

Wil97 G. Willmann, Bioceramics, 10, 353-356 (1997).

Won95 M. Wong, J. Eulenberger, R. Schenk, E. Hunziker, Journal of biomedical materials research, 29, 1567-1575 (1995).

Xu15 S. Xu, Y. Xiaoyu, S. Yuan, T. Minhua, L. Jian, N. Aidi, L. Xing, Rare Metal Mater. Eng. 44, 67–72 (2015).

Yan05 Y. Yang, K.H. Kim, J.L. Ong, Biomaterials 26, 327–37 (2005).

Yan06 Y. Yan, A. Neville, D. Dowson, S. Williams, Tribol Int, 39, 1509-1517 (2006).

Yan14 Y. Yang. Engineering Sciences [physics]. Ecole Centrale Paris, (2014).

Zan04 P.B. Zantye, A. Kumar, A.K. Sikder, Materials Science and Engineering R, 45, 89-220 (2004).

Zha06 G. Zhao, O. Zinger, Z. Schwartz, M. Wieland, D. Landolt, B.D. Boyan, Clinical oral implants research, 17, 258-264 (2006).

Zha10 Z. Zhang, L. Weili, Z. Jingkang, S. Zhitanng, Applied Surface Science, 257, 1750-1755 (2010).

Zhu04 X. Zhu, J. Chen, L., Scheideler , et al., Biomaterials 25, 4087-4103 (2004).

Zhu89 Zhuang LZ, Langer EW. J Mater Sci 24, 381–388 (1989).

Zur13 A.S. Zuruzi, Y.H. Yeo, A.J.Monkowski, C.S. Ding, N.C. MacDonald,Nanotechnology 24 245304 (2013).

VITA

Zeynep Özdemir Guler was born on February 7, 1987, in Istanbul, Turkey. She graduated first in the graduating class in 2005 from Prof. Faik Somer High Scholl in İstanbul, Turkey. She then enrolled at Istanbul University in Istanbul, Turkey. In July 2009 she graduated first in the graduating class with a Bachelor of Science degree in chemistry with a specialization in semi-conductive materials. After that, she continued her studies in the interdisciplinary area and gained her M.Sc. in the polymer science from the Bioengineering Department at Yildiz Technical University, Turkey in 2012. Her master's thesis work was supported by the Yildiz Technical University under the advisory of Assoc. Professor Sevil Dinçer. In 2012, she has started her Ph.D. with Assoc.Proffessor G.Bahar Basim at the Ozyegin University, where she is working as a Research and Teaching Assistant in the Engineering Faculty.

Her dissertation research concentrated on biomaterials surface nanostructuring through chemical machnaical polishing. She graduated from Ozyegin University with a doctorate degree in mechanical engineering with materials surface structuring specialties in May 2017.